ALERT Geomaterials

Alliance of laboratories in Europe for Research and Technology
Aussois, September 25 – 27, 2023

34th ALERT Workshop / POSTER SESSION

Booklet of abstracts

Editors: Nadia Benahmed
Antoine Wautier

(INRAE, France)

ALERT Geomaterials

The Alliance of Laboratories in Europe for Education, Research and Technology

34th ALERT Workshop

Poster Session

Aussois 2023

Editors:

Nadia Benahmed
Antoine Wautier

(INRAE, Aix-en-Provence – France)

Dear colleagues,

We are pleased to welcome you to Aussois and to our 34ᵗʰ ALERT Workshop and School.

As always, it is an exciting time for us to continue to meet and bring together inspired people for fruitful days with interesting, stimulating discussions, exchange of knowledge and experience on Geomechanics. Presentations of recent advances offer the chance to get up-to-date and to remain at the cutting edge.

We would like to express our thanks to all of you who contributed to the success of this poster session! This year, this session included a poster prize. Congratulations for the two winners of this first edition:

**Rana EL NEMER (GeM, France) and Maxime PIERRE (ENPC, France)**

The number of posters is rather stable compared with previous editions with 38 contributions gathering contributors from 16 countries (France, Czech Republic, Spain, Italie, The Netherlands, Germany, Austria, Belgium, Luxembourg, UK, Japan, Columbia, Australia, India, Canada) and belonging from 34 different research institutions and 7 agencies/private companies. They are summarized in the histogram below together with the corresponding number of posters.
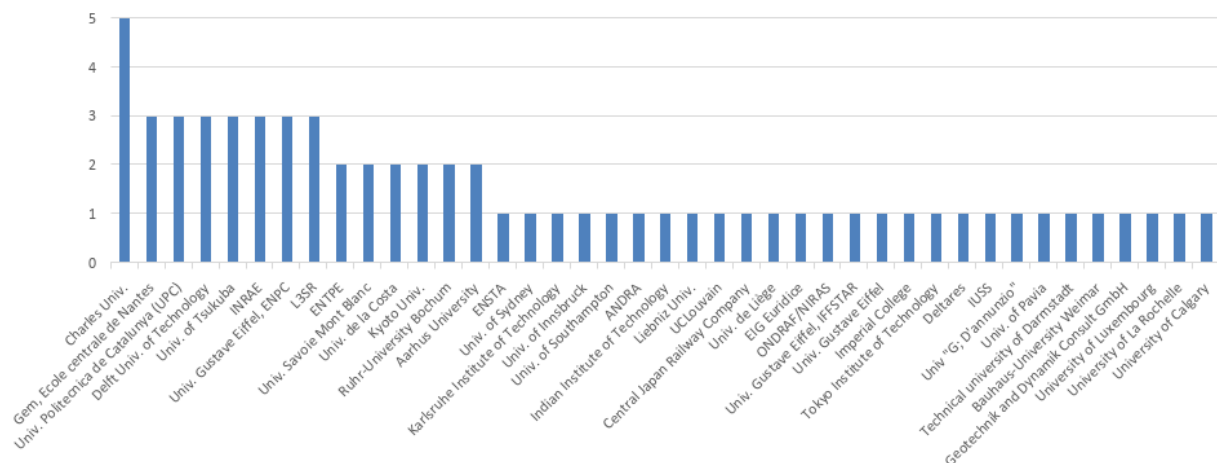

The posters cover numerical, experimental and analytical approaches with the following repartition. A small majority of the posters deal with numerical work.
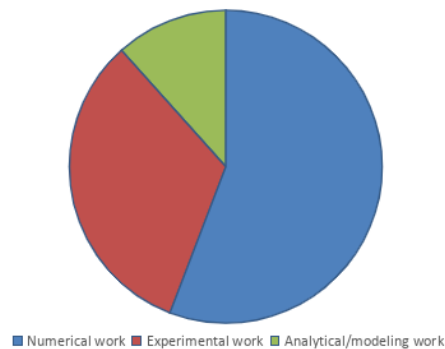
In terms of keywords, the analysis of the word frequency in the abstracts reveal the following cloud of words.
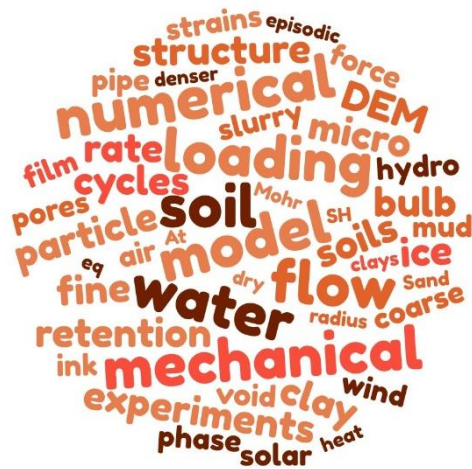
From the reading of the abstracts, we can also propose the following analysis, counting the number of abstracts dealing with different types of materials, numerical tools, specific loadings, experimental techniques, types of loading and fields of application. This gives an idea of the current hot topics in geomechanics.
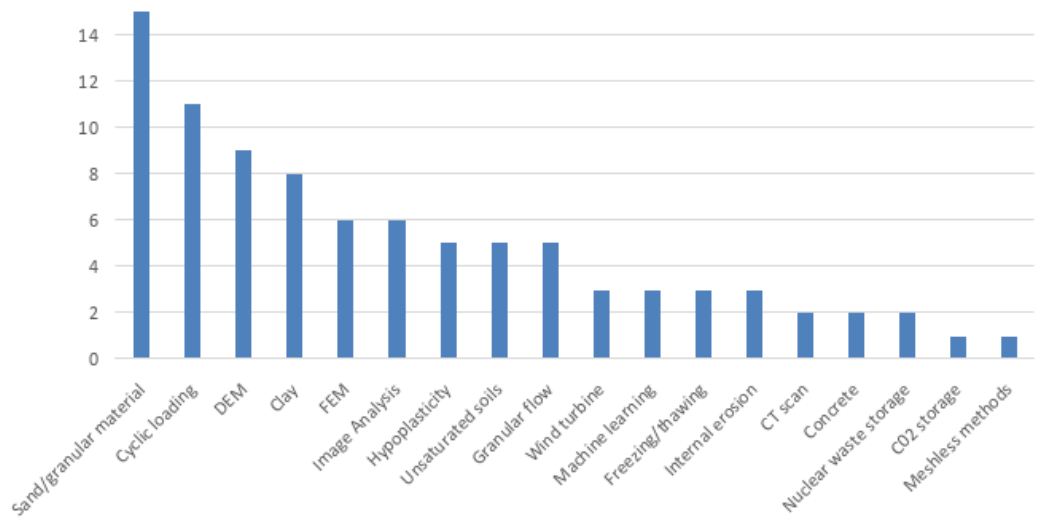
We wish you a good workshop and school experience and a pleasant stay in Aussois!

Kind regards,

Nadia Benahmed and Antoine Wautier.

Table of contents

Design of new earthquake control experiment

Abdallah Aoude[1], Ioannis Stefanou[1], Jean-Francois Semblat[2], Vito Rubino[1]

[1]Institut de Recherche en Génie Civil et Mécanique (GeM), École Centrale de Nantes, 1 Rue de la Noë, Nantes 44321, France

[2]ENSTA-Paris, Institute of Mechanical Sciences and Industrial Applications

abdallah.aoude@ec-nantes.fr, ioannis.stefanou@ec-nantes.fr, jean-francois.semblat@ensta-paris.fr, vito.rubino@ec-nantes.fr

Keywords: mathematical theory of control, laboratory earthquake mechanical apparatus, deformation, digital image correlation.

Abstract

In this work, we introduce a novel laboratory earthquake mechanical apparatus currently under design to implement established mathematical principles for earthquake control (Stefanou, 2019a; Stefanou & Tzortzopoulos, 2022; Tzortzopoulos, 2021; Gutiérrez-Oribio et al., 2022). Notably, the controller has been tested and proven effective through a laboratory experiment simulating a spring-slider system (Gutiérrez-Oribio et al., 2022; Tzortzopoulos, 2021). The forthcoming apparatus, distinct from the previous one, features an analogue rock surrounded by elastic media, providing enhanced realism.

We have accurately described how the analogue rock deforms. We designed, 3D-printed, and assembled a mechanical setup to apply this deformation. We then thoroughly explored the system using the virtual work method. Finally, we experimented and analyzed the results using the digital image correlation method.

In our experiments, we designed the stress to be uniform in the analogue rock and fault before sliding. Our digital image correlation analysis showed that the resulting deformation matched the design.

References

Gutiérrez-Oribio, D., Tzortzopoulos, G., Stefanou, I., and Plestan, F. (2022). Earthquake control: An emerging application for robust control. theory and experimental tests. arXiv preprint arXiv:2203.00296.

Stefanou, I. (2019a). Controlling Anthropogenic and Natural Seismicity: Insights From Active Stabilization of the Spring-Slider Model. Journal of Geophysical Research: Solid Earth, 124(8):8786–8802.

Stefanou, I. and Tzortzopoulos, G. (2022). Preventing instabilities and inducing controlled, slow-slip in frictionally unstable systems. Journal of Geophysical Research: Solid Earth, page e2021JB023410.

Tzortzopoulos, G. (2021). Controlling earthQuakes (CoQuake) in the laboratory using pertinent fault stimulating techniques. PhD thesis, École centrale de Nantes.

Types of shearing and anisotropy in undrained CPTu

Diego Durán Caballero[1], Lluis Monforte, Marcos Arroyo, Antonio Gens

[1]Universitat Politècnica de Catalunya, Carrer de Jordi Girona, 31, 08034 Barcelona, Spain

[1]diego.duran.caballero@upc.edu

Keywords: Anisotropy, G-PFEM, CPTu, constitutive modelling, fabric

Abstract

Natural clays show inherent anisotropy due to the stress history, to the particles size and arrangement that occurs during sedimentation. Consequently, identical soils subjected to the same loading program will display different strengths depending on the testing angle employed.

Cone penetration testing (CPTu) is probably the most well stablished in situ test. During the test, the soil suffers severe deformations and principal stress rotation. For isotropic materials it is unclear which undrained shear strength is mobilized (i.e. triaxial compression strength, triaxial extension strength, …) [1]. For anisotropic materials, advice is even more uncertain [2]. With advance of numerical methods, more realistic simulations of CPTu are possible, using a couple hydromechanical formulations and appropriate constitutive models. These simulations can be used to gain new insights into the stress path that suffers the soil during the test.

In this work, CPTu in undrained anisotropic clays is simulated employing the Particle Finite Element method [3]. The constitutive response is modelled with SCLAY-1 [4], a modified version of Modified Cam-Clay that incorporates mixed isotropic and rotational hardening with associated flow rule. Inside the yield surface isotropic elasticity is assumed. The model yield surface is a rotated ellipsoid in the p-q plane, and two hardening laws are employed: the first describes the change of the size of the yield curve with plastic volumetric strains and the second describes the creation or removal of fabric with plastic straining.

Two sets of cone penetration simulations have been performed: the first set considers isotropic materials and the focus is placed on which shear strength is mobilized during cone testing. The second set of simulations considers anisotropic materials in which the orientation of the fabric is parallel to the vertical direction. This second set of simulations is used to examine the effect of the soil anisotropy on the stress path of the soil and on the cone factor values.

For isotropic materials, contours of the Lode's angle and the magnitude of plastic strains are represented on Fig. 1. For all cases these results are similar. In the plastic region the Lode's angle is equal to -30º, so the soil is loaded at triaxial undrained compression conditions.

Preliminary results of cone penetration testing in anisotropic materials show that the cone factors are in the same range of those obtained in the numerical simulations of isotropic materials if they are computed with the triaxial compression undrained shear strength with the initial fabric oriented parallel to the major principal stress.

References

[1] Baligh, M.M., 1984. Strain Path Method. Journal of Geotechnical Engineering 111, 1180–1136.

[2] Su, S.-F., 2010. Undrained shear strengths of clay around an advancing cone. Can. Geotech. J. 47, 1149–1158.

[3] Carbonell, J.M., Monforte, L, Ciantia, M., Arroyo, M. & Gens, A. (2022) The Geotechnical Particle Finite Element Method for the modelling of soil-structure interaction under large deformation conditions, Journal of Rock Mechanics and Geotechnical Engineering 14, (3), 967-983.

[4] Wheeler, S.J., Näätänen, A., Karstunen, M., Lojander, M., 2003. An anisotropic elastoplastic model for soft clays. Can. Geotech. J. 40, 403–418.

Figures
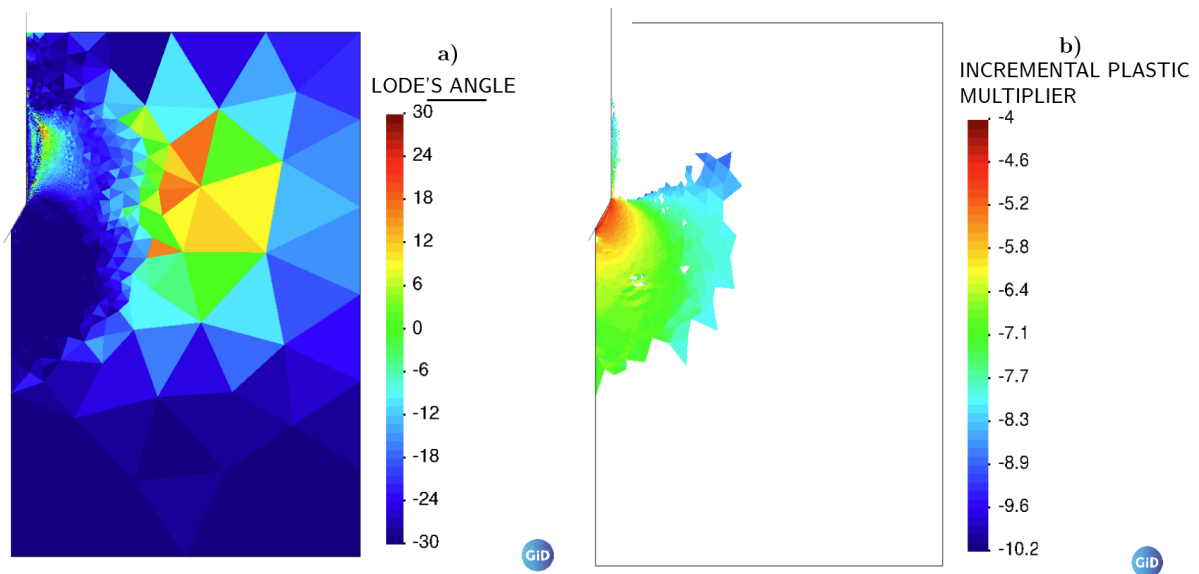
Figure 1: a) Lode's angle (a value of -30 corresponds to triaxial compression). b) Incremental plastic multiplier.

Insights on the Internal Dynamics of Bi-Disperse Granular Flows from Machine Learning

Sudip Laudari[1], Benjy Marks and Pierre Rognon

Particles and Grains Laboratory, School of Civil Engineering, The University of Sydney, Sydney, NSW 2006, Australia

[1]*slau8405@uni.sydney.edu.au*

Keywords: granular flow, machine learning, random forest, micro-mechanical

Abstract

In granular flows, differences in grain dynamics, such as force and velocity variations, are evident. To understand and predict this behaviour, the classical physicist method consists of establishing general constitutive laws supported by micro-mechanical processes. However, the ability of these models to predict full scale flows is hindered by their accuracy and their reliance on parameters which are difficult to measure precisely and obstruct in understanding micro-mechanical process taking places in flow regimes. Beyond this traditional predictive use, Machine Learning methods are a useful alternative when the primary goal is to predict the behaviour of granular materials. In this paper, we proposed a Machine Learning approach to explore the insights onto micro-mechanical processes in granular flows without depending on constitutive models.

Methodology: We model the discharge of a silo as it yields three states of granular matter: (i) a dense, liquid-like flow in the hopper (ii) a diluted, gas-like flow in the discharge jet under the silo opening, and (iii) a heap-flow including a solid-like packing underneath. Our model includes the mixture of two types of particles (r=30mm and r=20mm). Input features includes the position of the grains, {x, y, z}, their velocity {vx, vy, vz} and rotational velocities {Ωx, Ωy, Ωz}, and the total force subjected to {fx, fy, fz} at any point in time. We trained a random forest model using 80% of the grains. The ability of the model ability to classify grain size is then quantified against the remaining 20% of the grains, which we describe via the accuracy (Figure 1).

Results & Discussion: The principle of this iterative approach is to understand the micro-mechanical dynamics of flow regimes and the effect of gradually removing features that contribute the least to the grain sorting. Figure 2 shows an example of feature importance using information from the whole time series. The grains' acceleration (acc), contact force magnitude (|f|) and vertical position (z) contribute more information to the sorting and other information can therefore be removed from the sorting process without significantly affecting the predictability. Figure 2 (inset) illustrates the impact in sorting accuracy when we gradually remove less important features. We need at least two of main important features if we want to classify the mixture of bi-disperse grains in silo. Further, we analyzed the flow regimes by defining two zones (i) Collisional zone and (ii) Dense zone (see fig 1). We recorded the classification accuracy (ϵ) from overall flow, dense flow and collision flow with different features and combination of features. Further, we extended our approach to analyze granular flow in rotating drums.

Conclusion: In our research, we utilized machine learning to delve deeper into the intricacies of granular flows. By implementing a random forest classifier, we dissected the dynamic behaviors of both large and small grains within a bi-disperse flow. Our classifier successfully pinpointed not only unique feature variations but also established relationships between them, like the patterns driven by Newton's second law across various flow regimes. These findings not only enhance our understanding of granular flow but also pave the way for more precise classifications. Further, this machine learning approach can be adapted for a range of granular mixtures, underscoring its potential as an indispensable complement to conventional methods in studying granular and analogous fluid systems.

References

[1] Z. Cheng, J. Wang, Estimation of contact forces of granular materials under uniaxial compression based on a machine learning model. Granular Matter 24, 1–14 (2022).

[2] E.D. Cubuk, S.S. Schoenholz, J.M. Rieser, B.D. Malone, J. Rottler, D.J. Durian, E. Kaxiras, A.J. Liu, identifying structural flow defects in disordered solids using machine-learning methods. Physical Review Letters 114(10), 108,001 (2015).

[3] González Tejada and P. Antolin, "Use of machine learning for unravelling hidden correlations between particle size distributions and the mechanical behaviour of granular materials," Acta Geotechnical, vol. 17, no. 4, pp. 1443–1461 (2022).

[4] A. Samadani, A. Pradhan, A. Kudrolli, Size segregation of granular matter in silo discharges. Physical Review E 60(6), 7203 (1999).

Figures
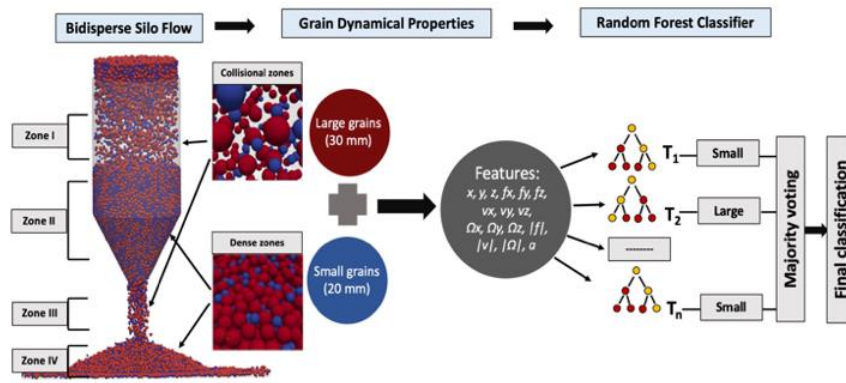
Figure 1: In a silo, a bi-disperse mixture is simulated. Grain attributes, including velocity and acceleration, train with random forest classifier to differentiate grain sizes.
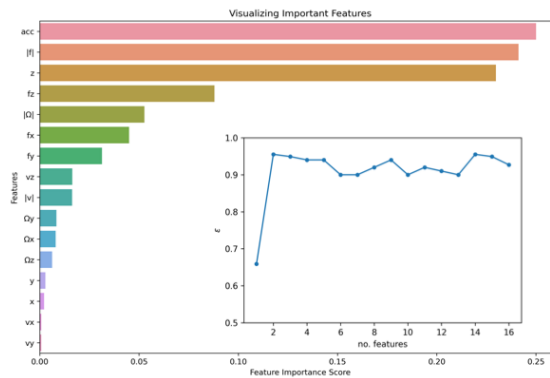
Figure 2: Feature importance in overall flow. (inset) Impact on accuracy ε while removing less important features gradually.

Neohypoplasticity for Sand: Equations and Developments

L. Mugele, A. Niemunis, H.H. Stutz

Karlsruhe Institute of Technology, Institute of Soil and Rock Mechanics, Karlsruhe, Germany

luis.mugele@kit.edu, hans.stutz@kit.edu

Keywords: neohypoplasticity, constitutive modelling, sand, parameter calibration, cyclic

Abstract

Several hypoplastic constitutive models have been developed over the last decades to model the mechanical behaviour of sand. Hypoplastic models reveal significant advantages compared to simple elastoplastic formulations. The version of von Wolffersdorff [1] with the intergranular strain extension [2] has become widely used. However, this formulation still reveals some drawbacks. These include the possibility of achieving a tensile stress state as a result of a too "elastic" behaviour caused by the intergranular strain extension and an inadequate modelling of the volumetric behaviour [3]. To fix these issues, Neohypoplasticity [4] has been developed. The constitutive equation of Neohypoplasticity

$$\dot{\boldsymbol{\sigma}} = k \cdot \overline{\mathrm{E}}(\dot{\boldsymbol{\varepsilon}} - \boldsymbol{m}Y||\dot{\boldsymbol{\varepsilon}}|| - \omega\boldsymbol{m}^z Y_z\langle -\boldsymbol{z} : \dot{\boldsymbol{\varepsilon}}\rangle - \boldsymbol{m}^d Y_d||\dot{\boldsymbol{\varepsilon}}||)$$

describes the relation between stress and strain rate. Thereby, the asymptotic hyperelastic stiffness $\overline{\mathrm{E}}$, the hypoplastic flow rule $\boldsymbol{m}$ and the degree of nonlinearity Y are explicitly defined. The current state of the soil is modelled using four state variables: stress $\boldsymbol{\sigma}$, void ratio e, structure variable $\boldsymbol{z}$ and last strain reversal $\boldsymbol{h}^r$. The structure variable $\boldsymbol{z}$ quantifies the current structure of the soil and is interpreted as the state of rolling of grains. A simple small strain stiffness approach for the increased stiffness upon a reversal of loading is proposed [3]. Therefore, the state variable called the last strain reversal $\boldsymbol{h}^r$ is introduced. This variable memorises the strain at the last reversal of the loading direction. In addition, a revised evolution equation for the structural variable $\boldsymbol{z}$ has been proposed [3].

This work summarises the current version of Neohypoplasticity. Thereby, the structural variable $\boldsymbol{z}$ and the small strain stiffness approach using the last strain reversal $\boldsymbol{h}^r$ are of particular importance. Both state variables are studied in detail. Furthermore, it is demonstrated that the user only has to calibrate 10 parameters to obtain a set of parameters for a new granular soil. For both, a fine-grained sand (Karlsruhe Fine Sand) and a medium-grained sand (Karlsruhe Sand), a parameter set have been calibrated. It is found that the number of adjustable parameters (10) in Neohypoplasticity differs significantly from the total material model parameters (28). To calibrate the two proposed parameter sets, element test simulations using *IncrementalDriver* are carried out, and the results are compared with experimental test data for Karlsruhe fine sand [5] and Karlsruhe sand [6]. Simulations of drained and undrained tests under monotonic and cyclic loading show good consistency with the test results (see Figure 1 and Figure 2).

The results show that the Neohypoplasticity in version [3] complies with two important requirements in terms of an application to geotechnical problems: the soil mechanical behaviour is reproduced remarkably in a close approximation, and it is quite easy to calibrate the necessary material model parameters.

References

[1] Von Wolffersdorff, P. A. (1996). A hypoplastic relation for granular materials with a predefined limit state surface. Mechanics of Cohesive-frictional Materials, 1(3), 251-271.

[2] Niemunis, A., & Herle, I. (1997). Hypoplastic model for cohesionless soils with elastic strain range. Mechanics of Cohesive-frictional Materials, 2(4), 279-299.

[3] Mugele, L., Niemunis, A., & Stutz, H.H. (2023). Neohypoplasticity Revisited. International Journal for Numerical and Analytical Methods in Geomechanics, (submitted).

[4] Niemunis, A., & Grandas Tavera, C. E. (2019). Essential Concepts of Neohypoplasticity. In Desiderata Geotechnica (pp. 132-142). Cham: Springer International Publishing.

[5] Wichtmann, T. (2016). Soil behaviour under cyclic loading - experimental observations, constitutive description and applications. Habilitation, Publications of the Institute of Soil Mechanics and Rock Mechanics, Karlsruhe Institute of Technology, Issue No. 181.

[6] Vogelsang, J. (2017). Untersuchungen zu den Mechanismen der Pfahlrammung. Dissertation, Publications of the Institute of Soil Mechanics and Rock Mechanics, Karlsruhe Institute of Technology, Issue No. 182.

Figures
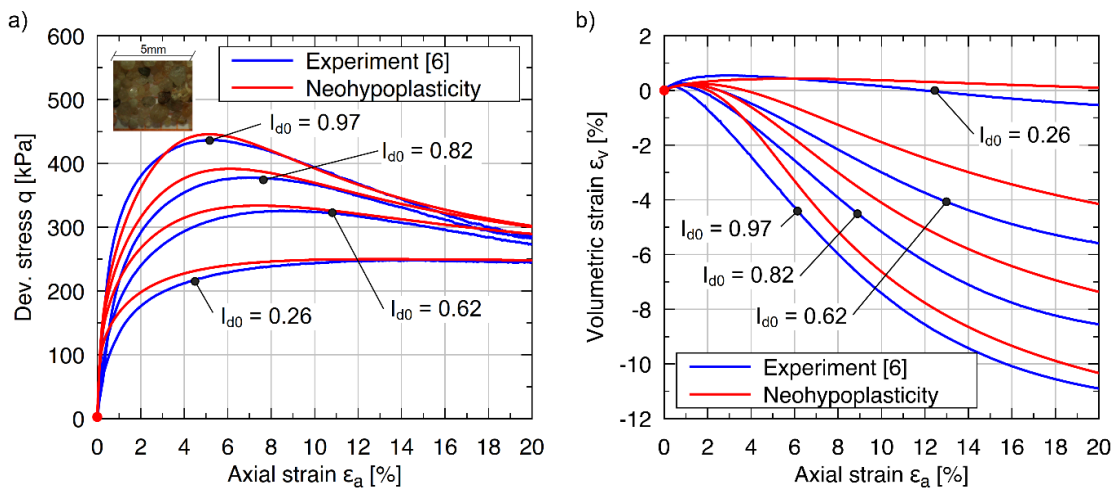
Figure 1: *Monotone drained triaxial tests on* <u>*Karlsruhe Sand (KS)*</u>*: experiments [6] and simulations.*
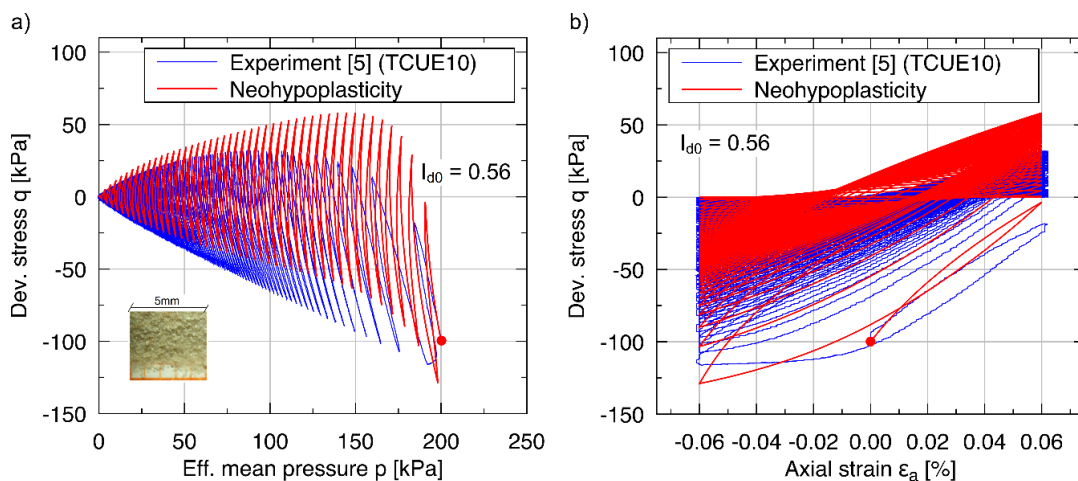
Figure 2: *Cyclic undrained triaxial tests on Karlsruhe Fine Sand (KFS): experiment [5] and simulation.*

Hypoplastic predictions of strength increase during episodic direct simple shear tests

Gertraud Medicus[1], Katherine Kwa[2]

[1]University of Innsbruck, Austria,
[2]University of Southampton, UK

Gertraud.Medicus@uibk.ac.at, K.A.Kwa@soton.ac.uk

Keywords: hypoplasticity, clays, repeated loading, stress path, offshore engineering

Abstract

Episodic loading of undrained shearing and consolidation (Figure 1) are relevant to offshore foundation whole-life applications. In related finite element simulations, the applied constitutive model then has to capture general trends of the soil response due to episodic loading. In this work, we carry out element test simulations with clay hypoplasticity with the intergranular strain concept (Mašín, 2014; Niemunis & Herle, 1997) where episodes of undrained shearing and consolidation are applied to samples of soft Kaolin clay. The simulated results are compared to experimental results from episodic direct simple shear (DSS) tests by Laham et al. (2021) and with a relation for strength increase proposed by Schofield & Wroth (1968). Clay hypoplasticity can be used to capture general trends in the evolution of void ratio and undrained strength that are observed in episodic DSS experiments (Medicus & Kwa, 2023), see also Figures 2 and 3. Therefore, hypoplasticity has potential to be more widely applied in finite element applications to explore soil strengthening responses from whole-life episodic undrained shear-consolidate loading conditions relevant to offshore foundations.

References

Laham N., Kwa K., White D. & Gourvenec S. (2021) Episodic simple shear tests to measure strength changes for whole-life geotechnical design. Géotechnique Letters.

Mašín D. (2014) Clay hypoplasticity model including stiffness anisotropy. Géotechnique.

Medicus G. & Kwa K. (submitted to: Géotechnique Letters, 2023) Hypoplastic predictions of strength increase during episodic direct simple shear tests.

Niemunis, A. & Herle, I. (1997). Hypoplastic model for cohesionless soils with elastic strain range. Mechanics of Cohesive Frictional Materials

Schofield, A. & Wroth, C. (1968). Critical state soil mechanics. McGraw-Hill.

Figures
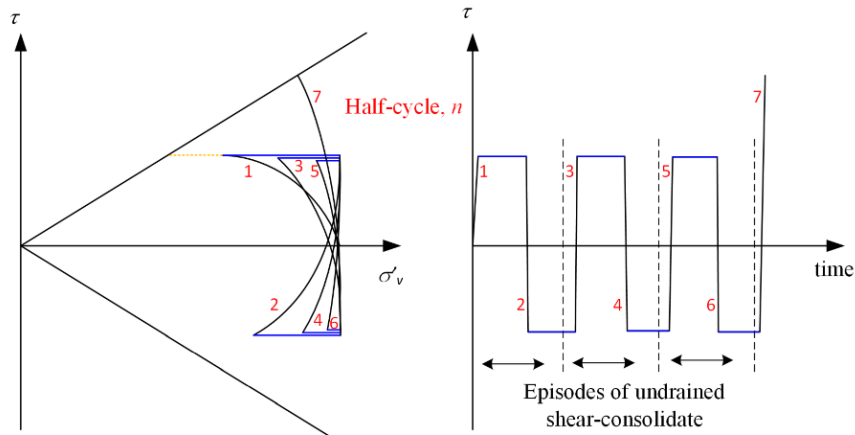
Figure 1: *Schematic description of episodes of shear-consolidate. left: τ-σ'v path. right: shear stress development over time.*
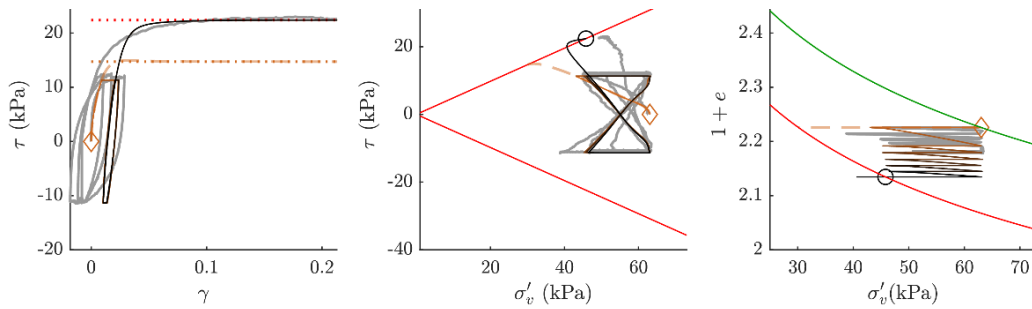
Figure 2: *Comparison between simulated and experimental results for episodic DSS test E67: The initial state ⬦ is oedometrically normally consolidated state. Experimental data from Laham et al. (2021) is shown in grey. Simulations with clay hypoplasticity (Mašín, 2014) are added with the final state marked with ∘. The dashed line indicates oedometrically normally consolidated, monotonic DSS loading with hypoplasticity.*
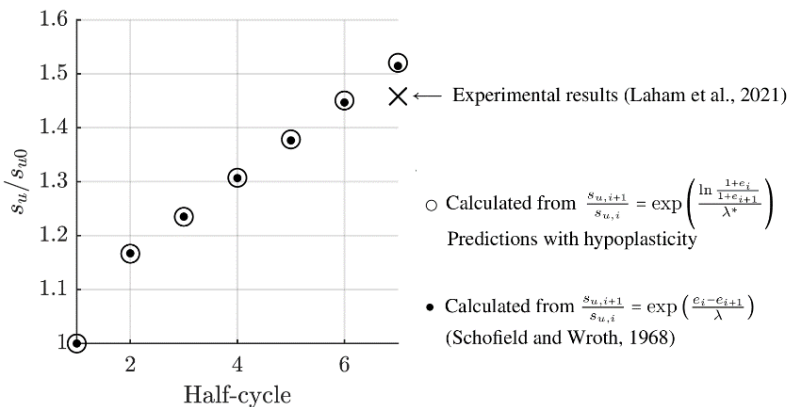
Figure 3 : *Comparison of the increase in strength per half-cycles for test E63, where su represents the undrained shear strength (τ at critical state) and su0 is the monotonic undrained shear strength. The cross (×) denotes the measured gain from the experiment (Laham et al., 2021). The dots · indicate strength gains calculated using the relation proposed by Schofield and Wroth (1968). The open circles ∘ correspond to predictions with hypoplasticity, for which an analytical relation is formulated in Medicus & Kwa (2023). It can be seen that the calculated changes in strength according to Schofield and Wroth [8] closely align with hypoplasticity. Both predictions are similar to the experimental result.*

15

3D modelling of clay rock cracking and anisotropic mechanical behaviour using a discrete element approach

Juliette Michalon [1,], Benoît Pardoen[1], Denis Branque[1], Jana Jaber[2], Gilles Armand[2]*

[1] University of Lyon, ENTPE, LTDS, UMR CNRS 5513, Vaulx-en-Velin, France

[2] French national radioactive waste management agency (ANDRA), Bure, France

*[*juliette.michalon@entpe.fr](mailto:juliette.michalon@entpe.fr)*

Keywords: 3D numerical modelling, discrete element method, Callovo-Oxfordian claystone, transverse isotropy

Abstract

The Callovo-Oxfordian (COx) clay rock is a potential host rock for deep geological nuclear waste repository in France. It is an indurated clay-rich sedimentary rock exhibiting a quasi-brittle and anisotropic mechanical behaviour. In order to reproduce the main characteristics of its mechanical behaviour under triaxial loading conditions, a 3D numerical model based on the discrete element method (Hart et al., 1988) has been developed, considering its inherent anisotropic nature. To reproduce the macroscale fracturing, localised cracking mechanisms are modelled by the possible development of various potential crack paths inside the rock matrix. To do so, the numerical sample is divided into rock matrix blocks (polyhedrons created using random Voronoi tessellations (Quey et al., 2011)) separated with damage crack model (Ghazvinian et al., 2014). Thus, the discrete model allows to describe localised damage and discrete crack development from local failure (crack initiation, growth, and propagation) to overall material specimen's failure (macroscale fracturing), either in tension or in shearing. A bilinear damageable Mohr-Coulomb failure criterion is used in the crack model (i.e. at rock block contacts) to take into account the material strength degradation (Yao et al., 2022). The degradation of shear strength properties is considered as a function of the relative displacement between the two sides of the cracks (i.e. between rock blocks) and the loss of tensile strength is considered when the crack yield criterion is reached in extension. The bilinear crack envelope allows to consider the non-linear deviatoric-confining pressure relationship typical of rock materials. In consequence, the macroscopic response of the specimen depends on the homogenisation of the elastic behaviour of the clay rock matrix (i.e. rock blocks), which is considered as deformable, and of the elastic-plastic crack behaviours, which reproduces the global macroscale non-linear material behaviour.

A series of triaxial loading tests was simulated on the COx claystone using 3DEC to calibrate the behavioural parameters of the induced cracks and of the rock matrix. First of all, the number of cracks and rock blocks as well as their morphology were determined such that the variability of the macroscopic mechanical response of the sample is low, for different random generations of possible crack paths and rock blocks. In parallel, peak and residual crack parameters of the Mohr-Coulomb bilinear failure envelopes are estimated, following a parameter calibration procedure. Secondly, in the case of this sedimentary rock, the experimental triaxial tests showed a strength dependency of COx samples on the loading direction with respect to the bedding weakness planes. Therefore, the transverse isotropy of the COx claystone was considered in the model by generating specimens with cracks oriented preferentially (and thus elongated rock

matrix blocks) (Fig. 1) along the material bedding planes. Thus, the COx claystone anisotropic strength is simulated by introducing the preferential orientation of possible induced cracks.

Furthermore, the proposed discrete element model is able to well reproduce the sample's progressive damage and the stress level (i.e. confining pressure) dependence of the rock failure mode. In fact, the transition between tensile failure under low stress level to shear failure under high stress level has been reproduced, together with the the transition from brittle to ductile rock behaviour. Lastly, the macroscopic shear strength of the samples follows a classical anisotropic U-shaped variation as a function of the bedding plane angle (Fig. 2). These results will allow to model excavation induced fractures around underground galleries, both in tensile mode in the rock close to the gallery wall and in shear mode deeper in the rock.

References

Ghazvinian, E., Diederichs, M. S., & Quey, R. (2014). Journal of Rock Mechanics and Geotechnical Engineering 3D random Voronoi grain-based models for simulation of brittle rock damage and fabric-guided micro-fracturing. Journal of Rock Mechanics and Geotechnical Engineering, 6(6), 506–521. https://doi.org/10.1016/j.jrmge.2014.09.001

Hart, R., Cundall, P. A., & Lemos, J. (1988). Formulation of a three-dimensional distinct element model-Part II. Mechanical calculations for motion and interaction of a system composed of many polyhedral blocks. International Journal of Rock Mechanics and Mining Sciences, 25(3), 117–125. https://doi.org/10.1016/0148-9062(88)92294-2

Itasca, 3DEC (3-dimensional distinct element code) version 7.00. Minneapolis, MN, USA: Itasca Consulting Group Inc.

Quey, R., Dawson, P. R., & Barbe, F. (2011). Large-scale 3D random polycrystals for the finite element method: Generation, meshing and remeshing. Computer Methods in Applied Mechanics and Engineering, 200(17–20), 1729–1745. https://doi.org/10.1016/j.cma.2011.01.002

Yao, C., He, C., Jiang, Q., Shao, J., & Zhou, C. (2022). Computers and Geotechnics A modified rigid-body-spring method for modeling damage and failure of brittle rocks subjected to triaxial compression. Computers and Geotechnics, 152(August), 105046. https://doi.org/10.1016/j.compgeo.2022.105046

Zhang, C. L., Armand, G., Conil, N., & Laurich, B. (2019). Investigation on anisotropy of mechanical properties of Callovo-Oxfordian claystone. Engineering Geology, 251(August 2018), 128–145. https://doi.org/10.1016/j.enggeo.2019.02.008
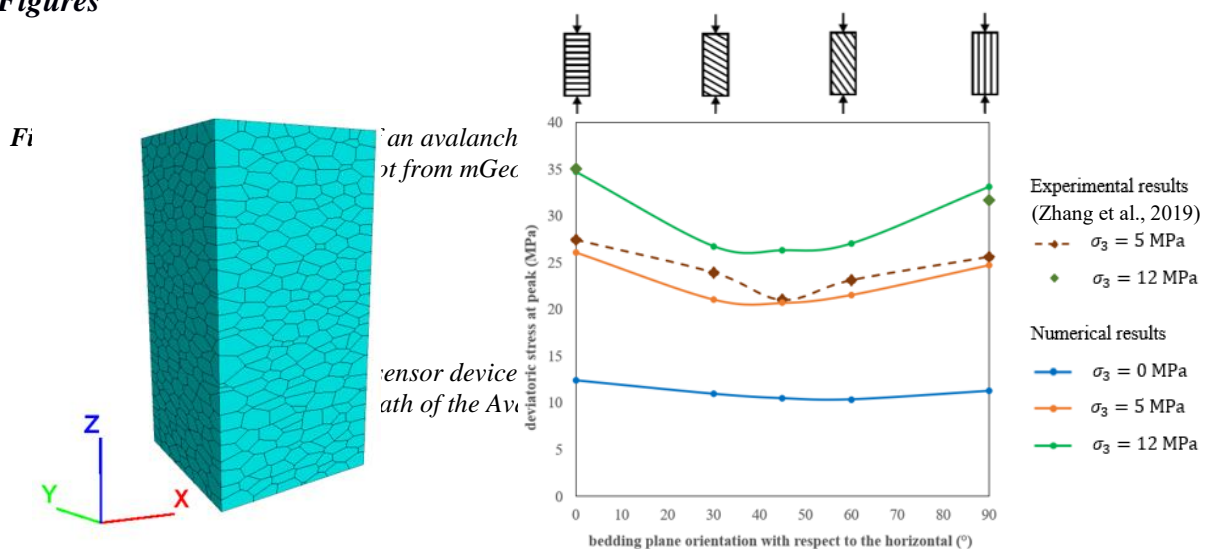
Figures

Figure 1: *A 3D numerical specimen with cracks oriented along horizontal planes.*

Figure 2: *Comparison of experimental and numerical deviatoric stress at peak as function of bedding plane (potential crack paths) orientation.*

Analysis of Offshore Wind Turbine Monopiles in Clayey Soils

Vidushi Toshniwal[1], Tanusree Chakraborty[2], Martin Achmus[3]

[1]Delft University of Technology, Delft
[2]Indian Institute of Technology, Delhi
[3]Leibniz University, Hannover

vidarya99@gmail.com

Keywords: cyclic loading, monopoles, cyclic degradation, numerical modeling, degradation equation, accumulated lateral displacement

Abstract

Renewable sources of energy like wind energy are essential to counter the adverse effects of climate change. The foundation used widely for offshore wind turbines is monopile foundation. It is important to analyse the behavior of offshore foundations as they experience the harshest environmental conditions due to cyclic wind and wave loads. In this project, FE analysis of monopile foundations in clayey soil under cyclic loading is performed. The optimisation in design would lead to cost reduction thereby ensuring the economic feasibility of future wind farms.

In design of laterally loaded offshore monopiles, the p-y approaches as per the offshore guidelines such as API (2014) and DNVGL (2016) are used majorly because of their simplicity and versatility. As shown in prior works the results of the Matlock p-y approach, the DNVGL (2016) guidelines and the linear approximation according to the API (2014) are not generally valid for arbitrary monopile geometries and soil conditions especially for cyclic loading. This is due to inadequacies in accurately modeling the behavior of the pile-soil interaction for large-diameter piles.

A new generally applicable approach for cohesive soils in cyclic loading needs to be developed in a consistent manner, based on the findings from the numerical comparative study. Hence, a constitutive model UDCAM-S is used in this thesis. It takes cyclic degradation of soil strength and stiffness into account and hence can optimize the foundation design. Back analysis of a field test and numerical validation of FE model using UDCAM-S was performed and results are compared with the API curves. Further a parametric analysis for a large monopile was done and an empirical degradation equation was developed henceforth for calculating accumulation of head displacement in pile.

References

API (2011). ISO 19901-4:2003 (Modified), Petroleum and natural gas industries – Specific requirements for offshore structures, Part 4 - Geotechnical and foundation design considerations. API Publishing Services, Washington, United States of America.

DNVGL (2016). Support structures for wind turbines - DNVGL-ST-0126. DNV GL AS, Norway.

Petrini F, Manenti S, Gkoumas K, Bontempi F. Structural Design and Analysis of Offshore Wind Turbines from a System Point of View. Wind Engineering. 2010;34(1):85-107

Jostad, H. P., Grimstad, G., Andersen, K. H., Saue, M., Shin, Y., and You, D. (2014). A FE procedure for foundation design of offshore structures - Applied to study a potential OWT monopile foundation in the Korean Western Sea. Geotechnical Engineering, 45(4):63–72.

Figures
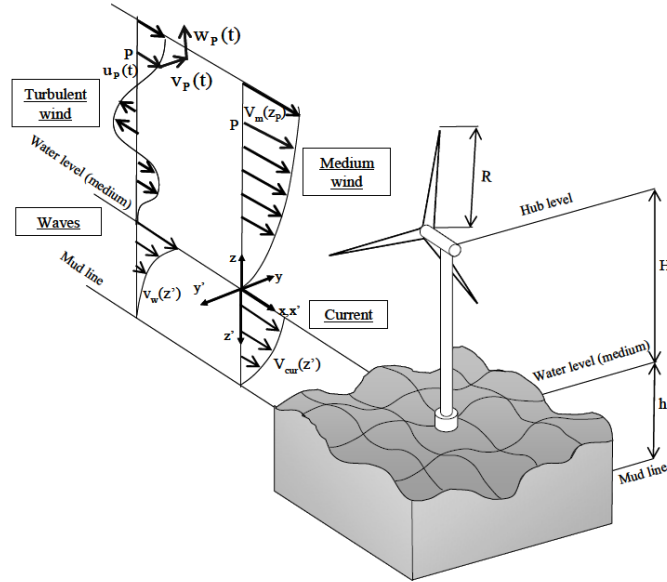
Figure 1: Offshore wind turbine experiencing wind and wave loads (Petrini F et al., 2010).
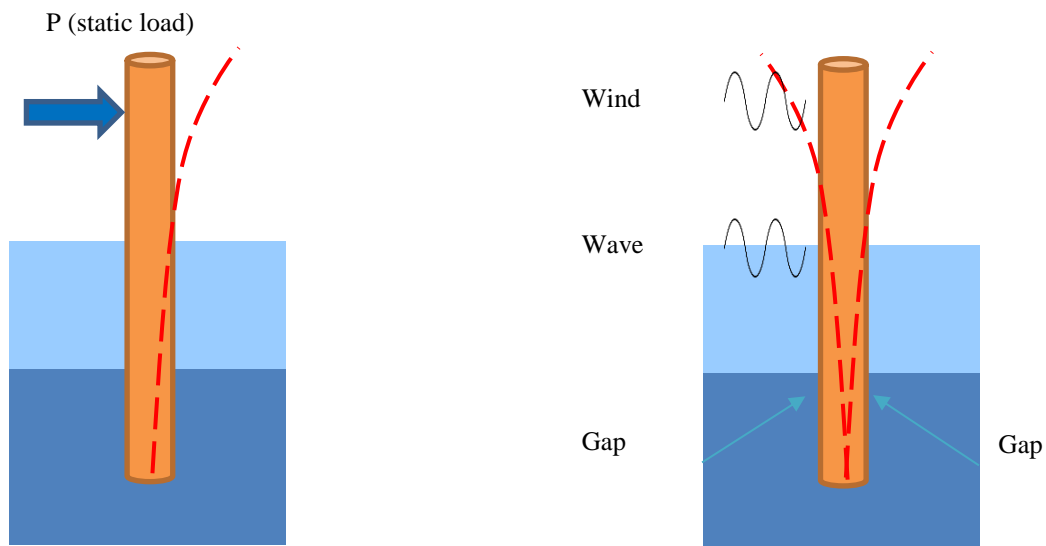
Figure 2: Monopile foundation behavior under static and cyclic loading and detrimental gap formation.

Evolution of the microstructure of altered volcanic rocks through failure: The case of Tutupaca, Peru

Jens Niclaes[1], Pierre Delmelle[2], Hadrien Rattez[1]

[1]Institute of Mechanics, Materials and Civil Engineering (IMMC), UCLouvain, Louvain-la-Neuve, Belgium

[2]Environmental Sciences, Earth and Life Institute, UCLouvain, Louvain-la-Neuve, Belgium

jens.niclaes@uclouvain.be

Keywords: volcano, landslide, hydrothermal alteration, microstructure, tomography

Abstract

The largest landslide in recorded history happened in Mount St. Helens in May 1980 and was the trigger of a major explosive eruption (Lipman & Mullineaux, 1981). This event drew attention on the instability of volcanic edifices, and their tendency to experience lateral collapse. Indeed, volcanic lateral collapses and their associated (volcanic) debris avalanche deposits are highly destructive because of their rapid onset and ability to cause destruction across large areas.

The growing structure of active volcanoes due to material addition can lead to oversteepening and overloading (McGuire, 2003). This situation can be worsened by seismic activity as most volcanoes are located in seismically active areas. Moreover, the materials forming volcanic edifices are subjected to extreme conditions in terms of temperature, pore pressure (consequence of several combined factors) and chemically aggressive fluids (very low pH for example) which can all destabilize volcanoes' flanks. Among these factors, hydrothermal activity is of particular interest as it enhances rock dissolution (and thus, increases rock porosity), promotes high pore pressures and leads to the creation of mechanically weaker materials (like clay-rich rocks) and promote the instability (Rattez and Veveakis, 2020). However, the effects that these processes have on volcano stability have been barely quantified (Heap and Violay, 2021).

To better understand the influence of different types of hydrothermal alteration on the hydraulic and mechanical properties of volcanic rocks, permeameter, and triaxial experiments have been performed on samples retrieved by Detienne et al. (2016) from the Tutupaca volcano (17° 01′ S, 70° 21′ W). This volcano is a dacitic dome complex located at the southern end of the Peruvian arc. The study focuses on a remarkably well-preserved debris avalanche deposit placed to the northeast of the volcano (Figure 1). The debris avalanche is sourced to Eastern Tutupaca; it left a horseshoe-shaped crater open to the northeast and was accompanied by a pyroclastic flow (volume: 6.5-7.5 x 10^7 m^3) (Samaniego et al., 2015). An extensive microstructural investigation was done thanks to micro-computed tomography before and after the mechanical test of the samples. This allows the assessment of the evolution of the microstructure through breakage. Preliminary results exhibit a fracture-type dependency on the kind of alteration and its intensity. This dataset could be further used in numerical models of flank collapses to constrain better the role of hydrothermal alteration on the nucleation of those events.

References

Detienne M. (2016) "Unravelling the role of hydrothermal alteration in volcanic flank and sector collapses using combined mineralogical, experimental, and numerical modelling studies". PhD thesis, UCLouvain.

Heap M. and Violay M. (2021) "The mechanical behaviour and failure modes of volcanic rocks: a review", Bulletin of Volcanology, 83:33.

Lipman PW, Mullineaux DR (eds) (1981) "The 1980 eruptions of Mount St Helens, Washington." U.S. Geological Survey, Professional Paper 1250, 844 pp.

McGuire WJ (2003) Volcano instability and lateral collapse. Revista 1:33–45.

Rattez H, Veveakis M (2020). "Weak phases production and heat generation control fault friction during seismic slip", Nature Communications, doi: 10.31223/osf.io/xupr8

Samaniego, P., Valderrama, P., Mariño, J., De Vries, B. V. W., Roche, O., Manrique, N., Chédeville, C., Liorzou, C., Fidel, L. & Malnati, J. (2015). "The historical (218±14 aBP) explosive eruption of Tutupaca volcano (Southern Peru) ». Bulletin of Volcanology, 77, 1-18.

Figures
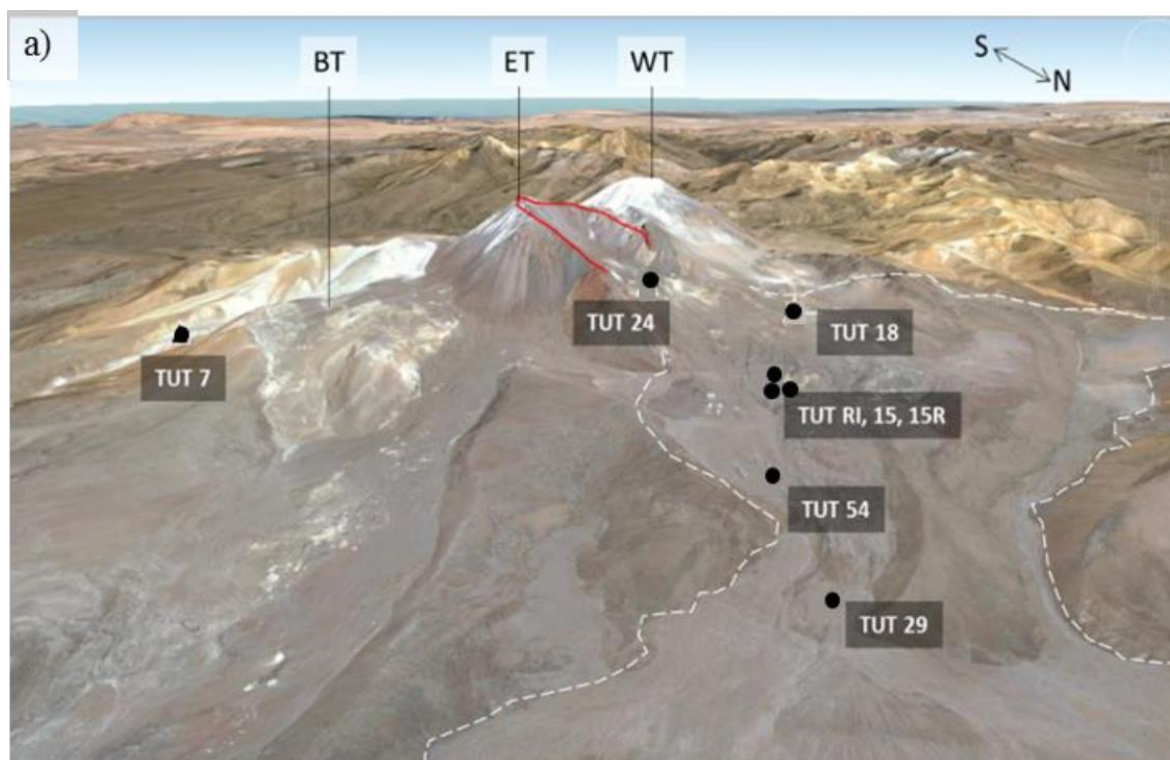
Figure 1: Google Earth image showing Tutupaca volcano, its debris avalanche deposits and the rock sample locations (From Detienne, 2016). The dotted lines delimit the debris avalanche deposit that resulted from collapse of Eastern Tutupaca ~200 years ago. The red contour indicates the scar left by the collapse.

Cell-based microscopic insights into granular packings: Combined effects of particle shape and inter-particle friction

Haoran Jiang[1], Reid Kawamoto[2], Takashi Matsushima[1]

[1]Department of Engineering Mechanics and Energy, University of Tsukuba, Tsukuba 305-8573, Japan

[2]Independent Scholar, Tsukuba 305-8573, Japan

kyokouzen9711@gmail.com

Keywords: granular packings, Level Set Discrete Element Method (LS-DEM), cell structure, shape effect, stress-structure co-organization

Abstract

There is a growing realization [1–2] that local structure and stress self-organize cooperatively during quasi-static dynamics of granular systems, but the mechanisms of this self-organization are not fully understood. To gain a better understanding on such kind of phenomenon, we explored the structure of numerically generated and mechanically equilibrated superdisk packings using a cell-based structural description [3-5]. We prepared several different systems by compressing samples quasi-statically through the level set discrete element method (LS-DEM) [6]. We then investigated the statistics of the cells, which are the irreducible, enclosed loops surrounded by particles in contact, in prepared samples and analyzed the relation between these cell stresses and cell structures. We find the following. (1) The features of resulting cell structures, including the cell order and shape, are significantly affected by both particle shape and inter-particle friction. (2) The distribution of cell stress ratios h significantly depends on both the shape and inter-particle friction. However, the probability density functions (PDFs) of normalized stress ratios $\hat{h} = h/\bar{h}$ surprisingly collapse onto a single curve, which can be fitted well by a Weibull distribution. (3) In all explored systems, the PDFs of the cell orientations θ^c, quantified by the directions of the major axes of their equivalent ellipses, and the major principal cell stress directions θ^σ are found to be almost constant. However, and significantly, we observe that θ^c aligns along θ^σ locally, except 3-order cells with stability allowing large orientational deviations. (4) For any given inter-particle friction μ_p, the cell stress-structure correlation weakens as the shape deviates from a disk. Our results provide robust evidence supporting the idea that cell structure and the stress field self-organize together and present a way to quantitatively measure the correlations between the two.

References

 [1] Tordesillas, A., & Muthuswamy, M. (2009). On the modeling of confined buckling of force chains. Journal of the Mechanics and Physics of Solids, 57(4), 706-727.

[2] Terentjev, E. M., & Weitz, D. A. (Eds.). (2015). The Oxford handbook of soft condensed matter. Oxford Handbooks.

[3] Matsushima, T., & Blumenfeld, R. (2014). Universal structural characteristics of planar granular packs. Physical review letters, 112(9), 098003.

[4] Matsushima, T., & Blumenfeld, R. (2017). Fundamental structural characteristics of planar granular assemblies: Self-organization and scaling away friction and initial state. Physical review E, 95(3), 032905.

[5] Matsushima, T., & Blumenfeld, R. (2021). Statistical properties of cell stresses in 2D granular solids. In *EPJ Web of Conferences* (Vol. 249, p. 02006). EDP Sciences.

[6] Kawamoto, R., Andò, E., Viggiani, G., & Andrade, J. E. (2016). Level set discrete element method for three-dimensional computations with triaxial case study. Journal of the Mechanics and Physics of Solids, 91, 1-13.

Figures
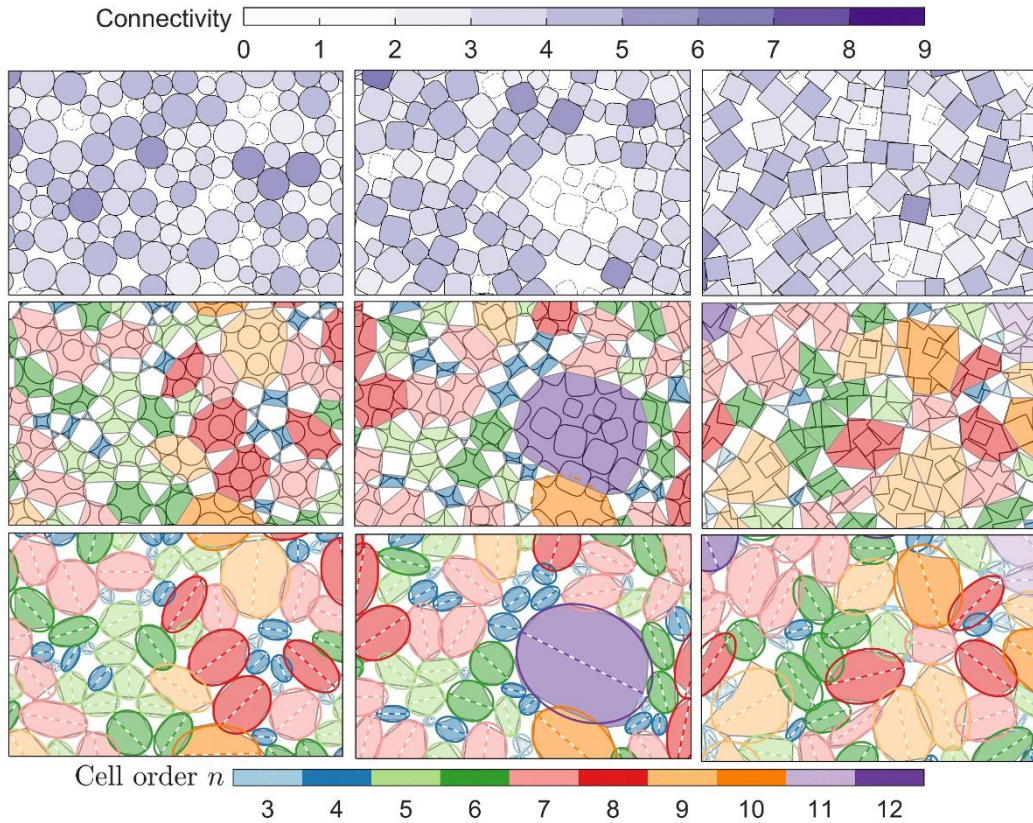
Figure 1: *Example of final packings of samples with three shapes and* $\mu_p = 1$ *(top), together with the corresponding cell structures (middle) and best-fitted ellipses for those cells (bottom).*
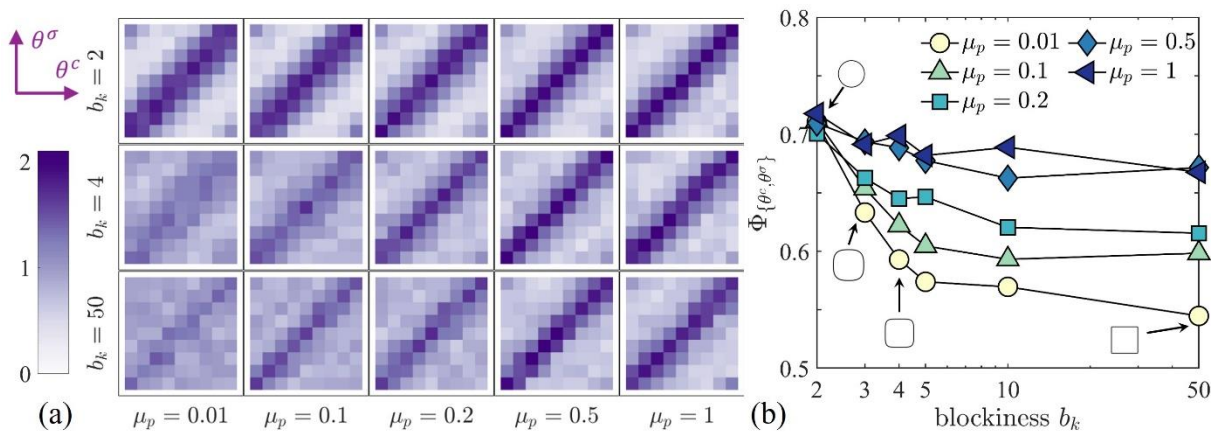
Figure 2: *(a) The conditional joint PDF of cell orientations* θ^c *and principal cell stress direction* θ^σ *for samples with various particle blockiness* b_k *and inter-particle frictions* μ_p. *(b) The correlation coefficients between* θ^c *and* θ^σ *as a function of* b_k *for various values of* μ_p.

Evaluating the accuracy of debris flow simulation by the depth-integrated particle method (DIPM)

Fazlul Habib Chowdhury, Takashi Matsushima

Geotechnical Engineering Laboratory, University of Tsukuba, Tsukuba, 305-8573, Japan

fhchy@yahoo.com

Keywords: Depth-Integrated Particle Method, debris flow, USGS debris flow-flume, accuracy evaluation

Abstract

This study presents the validation of the Depth-Integrated Particle Method (DIPM) for simulating sediment-related disasters, focusing on slope failure and subsequent debris flow/mudflow. DIPM treats the flowing mass as discrete soil columns, solving their equations of motion as two-dimensional particles in complex topography. The method incorporates bottom shear stress computed using a modified Manning's formula and considers yield stress and particle interactions based on hydraulic gradient. Flow simulations are performed to replicate the US Geological Survey debris flow flume experiments to validate the method. A quantitative evaluation is conducted to reproduce similar flow behavior and identify appropriate material parameters, including Manning's coefficient (n) and critical deposition angle (i_{cr}). Additionally, the study applied DIPM to simulate debris flow resulting from slope failures during the Hokkaido Eastern Iburi Earthquake in specific case study areas. Visual and statistical comparisons are performed to assess the agreement between simulated and actual flow characteristics, where the critical success index for accuracy evaluation is 0.69. The estimated material parameters through the flow simulation are consistent with the USGS experiment and the previous studies; the optimal values of material parameters n and i_{cr} are 0.075 to 0.15 and 3° to 6°, respectively. These findings provide valuable insights into the accuracy and reliability of DIPM in capturing the complex flow behavior of sediment-related disasters.

References

[1] Hoang GQ, Matsushima T, Yamada Y. (2009) Debris flow simulation by particle method using PRISM-DSM. In: Proceedings of 6th Geo-Kanto Conference (in Japanese)

[2] Zhang N, Matsushima T (2016) Simulation of rainfall-induced debris flow considering material entrainment. Engineering Geology 214:107–115.https://doi.org/10.1016/j.enggeo.2016.10.005

[3] Pastor M, Haddad B, Sorbino G, Cuomo S, Drempetic V (2009) A depth-integrated, coupled SPH model for flow-like landslides and related phenomena. International Journal of Numerical and Analytical Methods in Geomechanics 33:143–172. https://doi.org/10.1002/nag.705

[4] Logan M, Iverson RM, Obryk MK (2018) Video Documentation of Experiments at the USGS Debris-Flow Flume 1992–2017. https://doi.org/10.3133/ofr20071315

[5] Iverson RM, Reid ME, Logan M, LaHusen RG, Godt JW, Griswold JP (2011) Positive feedback and momentum growth during debris-flow entrainment of wet bed sediment. Nature Geoscience 4:116–121. https://doi.org/10.1038/ngeo1040

[6] Ho JY, Liu CH, Chen WB, Chang CH, Lee KT (2022) Using ensemble quantitative precipitation forecast for rainfall-induced shallow landslide predictions. Geoscience Letters 9. https://doi.org/10.1186/s40562-022-00231-0
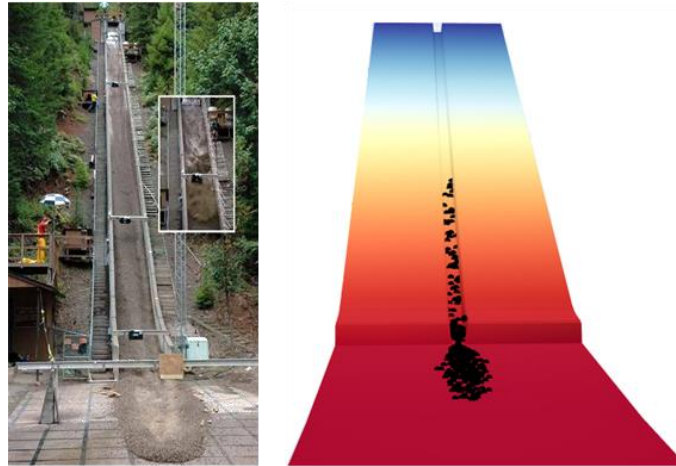
Figures

Figure 1: *USGS debris flow flume [5] and snapshot of the geometric model in simulation.*
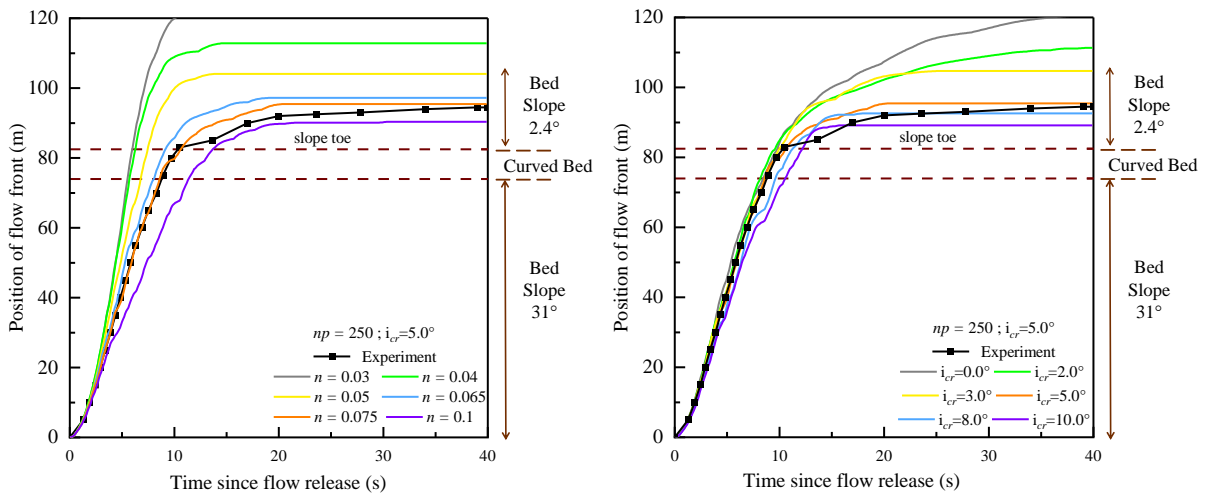
Figure 2: *Position of flow fronts as a function of time when the material parameters are varied.*
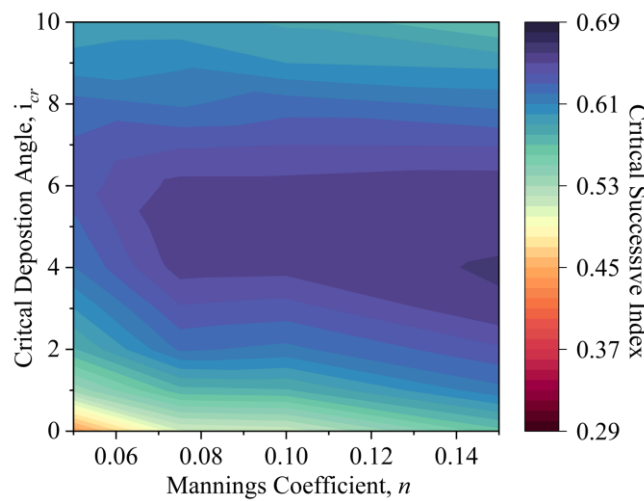
Figure 3: *Co-relation between the accuracy index and material parameter (n and i_{cr}).*

Exploring the role of contact conditions on interparticle friction of railway ballast under cyclic shear test

Opu Chandra Debanath[1], Takashi Matsushima[1], Shuichi Adachi[2], Masahiro Miwa[2]

[1]Geotechnical Engineering Laboratory, University of Tsukuba, Tsukuba, 305-8573, Japan

[2]Central Japan Railway Company, Komaki, 485-0801, Japan

debnathopu@cuet.ac.bd

Keywords: railway ballast, coefficient of friction, surface roughness

Abstract

Particle friction of granular materials significantly influences the behavior of the overall assembly [1,2], especially in the context of DEM analysis of railway ballast; the coefficient of inter-particle friction (μ) is a key parameter that can depend on various physical factors of contact [3]. This study focuses on estimating the interparticle friction coefficient of andesite ballast particles under different contact conditions using cyclic shear test. Additionally, 3D surface scanning of ballast specimens was employed for better understating on a microscopic scale. The cyclic test was extended up to 400 cycles with an increment of normal load at every 100 cycles, including both dry and flooded contact scenarios. To investigate the influence of surface topography, two test series were conducted. In test series-1, ballast tip specimens were sheared over a smooth rock surface, while in test series-2, specimens were sheared over real ballast faces with varying roughness levels. Higher friction coefficients were observed in tests conducted on ballast surfaces compared to flat rock surfaces, and the μ value exhibited a gradual increase under dry contact conditions, while wet tests significantly altered the contact behavior. Notably, water intrusion in the contact region displayed a lubrication effect, substantially reducing interparticle friction. A reduction in the roughness of tip specimens was observed throughout the shear cycles, while concurrently, the roughness of flat faces exhibited an increase along the shear direction. These findings have profound implications for the field performance of ballast subject to alternate wetting and drying scenarios.

References

[1] Cole, D.M., Mathisen, L.U., Hopkins, M.A. et al. Normal and sliding contact experiments on gneiss. Granular Matter 12, 69–86 (2010).

[2] Cole, D.M., Peters, J.F. Grain-scale mechanics of geologic materials and lunar simulants under normal loading. Granular Matter 10, 171–185 (2008).

[3] Uthus L., Tutumluer E., Horvli I., Hoff I.: Influence of grain shape and surface texture on the deformation properties of unbound aggregates in pavements. Int. J. Pavements Eng. 6(1)

Figures
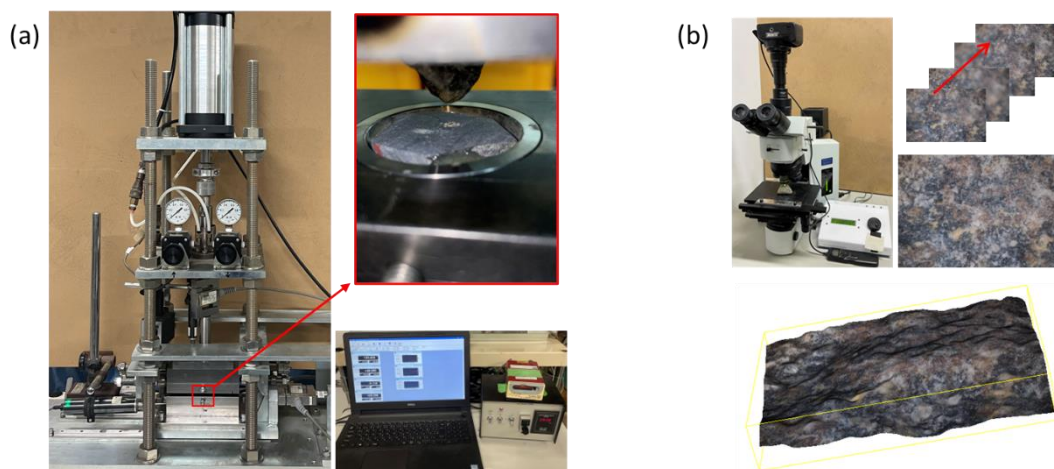
Figure 1: *(a) Shear test setup (b) 3D surface scanning by microscope.*
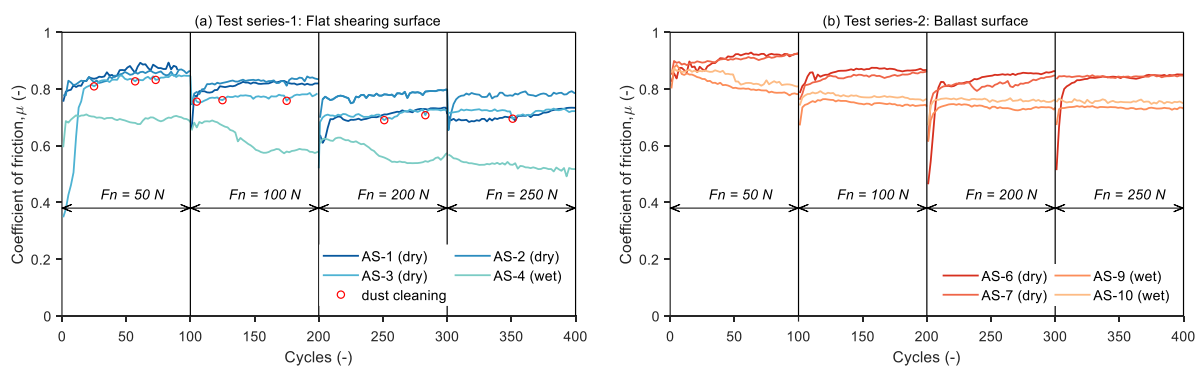
Figure 2: *Evolution of Coefficient of friction with loading cycles.*
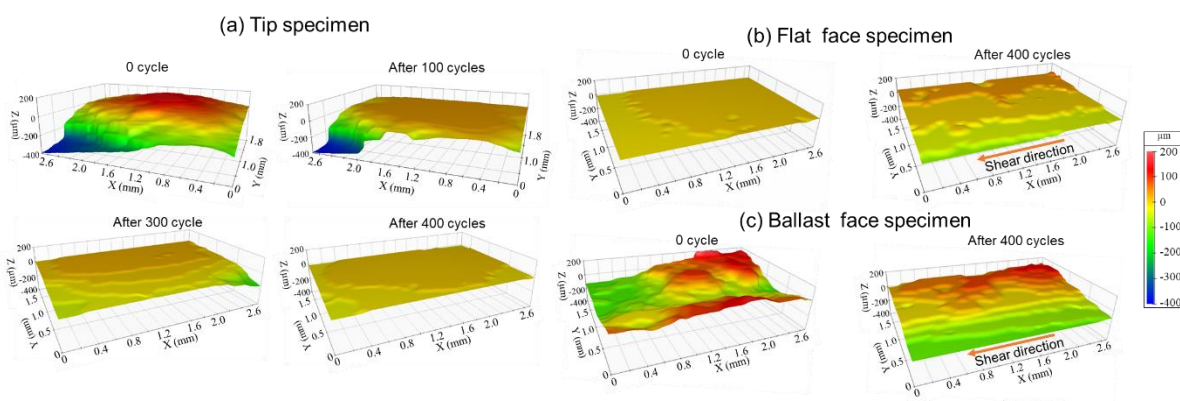
Figure 3: *3D surface topography of tip and face specimen during the shear test.*

A micromechanics-based classification of gap-graded materials

Peter Adesina, Antoine Wautier, Nadia Benahmed

INRAE, Aix Marseille Univ., RECOVER 3275 Route de Cézanne, CS 40061, 13182 Aix-en-Provence Cedex 5, France

peter.adesina@inrae.fr; antoine.wautier@inrae.fr; nadia.benahmed@inrae.fr

Keywords: gap-graded materials, regimes, drained shearing, finer fraction, coarser fraction

Abstract

It well known that the mechanical behaviour gap-graded granular materials depends on the proportion of the fines present within the materials [1–5]. However, the specific fines content delineating different families of behaviour is yet disputed in the literature. In this study, we conduct a micromechanical evaluation of the regimes delineating the behaviour of bimodal gap-graded granular assemblies of fines contents varying from 10% to 70%, using discrete element method (DEM) simulations. While two regimes delineated by the threshold fines content were identified based on the analysis of the macroscale characteristics (void ratio, peak strength and maximum dilatancy) (Figs. 1-2), up to four regimes were identified based on our analysis of the micromechanical characteristics of the assemblies (Figs. 3-7). Against the suggestion made in earlier studies that the fines control the mechanical behaviour of gap-graded materials from the threshold fines content, f_c^{th}, our analysis show that the fines did not contribute primarily to stress transfer until beyond $f_c = f_c^{eq} > f_c^{th}$, where the mean stress is equally shared by the finer and the coarser fractions (Fig. 3). A transitional regime is highlighted for $f_c \in [f_c^{th} \, f_c^{eq}]$ in which the activation of fines is very sensitive to the material density (Fig. 4). In addition, stress transmission in the transitional regime may be dominated either by c-c or c-f contacts. The conclusions of this study will be of primary interest for developing advanced micromechanical models of widely graded materials in which the fines content may evolve when subjected to internal erosion.

References

1. Thevanayagam S, Shenthan T, Mohan S, Liang J. Undrained Fragility of Clean Sands, Silty Sands, and Sandy Silts. J Geotech Geoenvironmental Eng. 2002;128(10):849–59.

2. Skempton AW, Brogan JM. Experiments on piping in sandy gravels. Geotechnique. 1994;44(3):449–60.

3. Vallejo LE. Interpretation of the limits in shear strength in binary granular mixtures. Can Geotech J. 2001;38(5):1097–104.

4. Shire T, O'Sullivan C, Hanley KJ, Fannin RJ. Fabric and Effective Stress Distribution in Internally Unstable Soils. J Geotech Geoenvironmental Eng [Internet]. 2014;140(12):04014072.

5. Li W, Chu Y, Deng G, Cai H, Xie D, Lee Lee M. Study of shear induced stress redistribution in gap-graded soils by discrete element method. Comput Geotech [Internet]. 2023;156(June 2022).

Figures
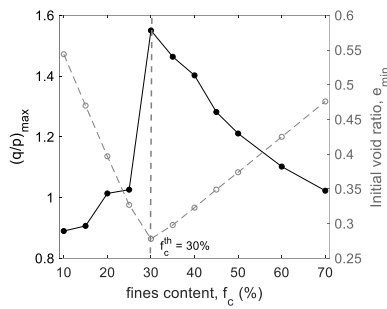
Figure 1: *Peak strength,* $(q/p)_{max}$ *vs* f_c
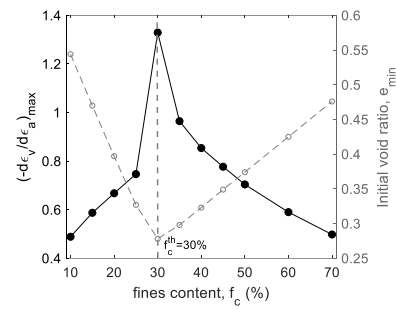
Figure 2: *Peak dilatancy vs* f_c
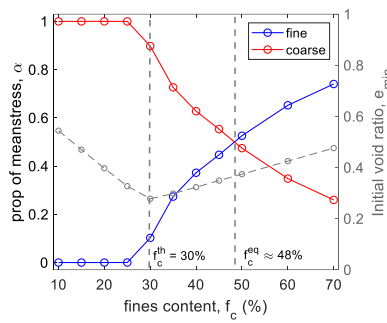
Figure 3: *Contribution of particle type to mean stress,* α
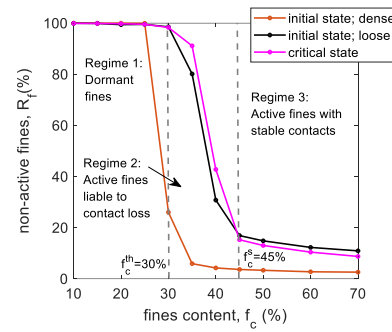
Figure 4: *Change in the non-active fines during shearing*
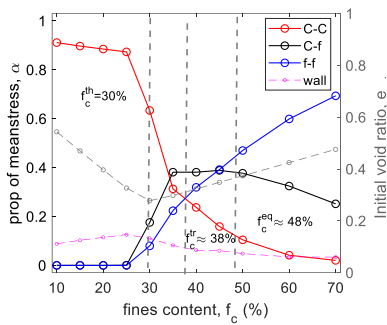
Figure 5: *Contribution of contact types to mean stress, α, dense, initial state*
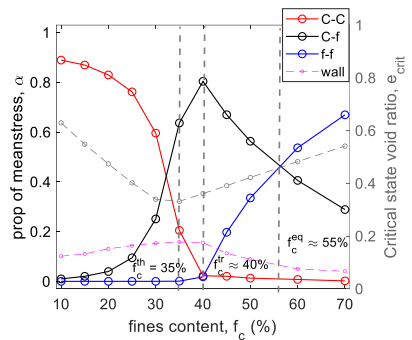
Figure 6: *Contribution of contact types to mean stress, α, critical state*

Macroscale	Underfilled	Overfilled		
Particle scale	Dormant fines	Active fines liable to contact loss	Active fines with stable contacts	
Contact scale	$\alpha_{c-c} > \alpha_{c-f} > \alpha_{f-f}$ Coarse-dominated	$\alpha_{c-f} > \alpha_{c-c} > \alpha_{f-f}$ Transitional coarse-dominated	$\alpha_{c-f} > \alpha_{f-f} > \alpha_{c-c}$ Transitional fines-dominated	$\alpha_{f-f} > \alpha_{c-f} > \alpha_{c-c}$ Fines-dominated

f_c^{th} f_c^{tr} f_c^{eq}

f_c

Figure 7: *Regime identification by macroscale, particle scale and contact scale characteristics*

Numerical investigations of fine grain diffusion behavior in 3D spherical packing

Fan Chen[1], Abhijit Hegde[1], Antoine Wautier[1], Nadia Benahmed[1], Pierre Philippe[1], François Nicot[2]

[1]INRAE, Aix Marseille Univ., RECOVER 3275 Route de Cézanne, CS 40061, 13182 Aix-en-Provence Cedex 5, France

[2]University of Savoie Mont-Blanc, ISTerre, Chambéry, France

fan.chen@inrae.fr; abhijit.hedge@inrae.fr; antoine.wautier@inrae.fr; nadia.benahmed@inrae.fr; pierre.philippe@inrae.fr; francois.nicot@univ-smb.fr

Keywords: fine infiltration, PFV-DEM, granular flow.

Abstract

Suffusion is a phenomenon commonly observed in gap-graded soils that involves the detachment and transport of the finest grains under the action of an internal fluid flow. This can have detrimental effects, as the significant loss of fines may trigger mechanical instabilities in the material, posing a potential risk of catastrophic failure for hydraulic structures, possibly in the form of static liquefaction.

To address this risk, an innovative approach is being considered – the injection of fines back into the remaining granular skeleton, primarily comprised of coarse sand grains. This remediation technique draws inspiration from recent numerical findings, which indicate that the inclusion of weakly loaded grains can substantially enhance the mechanical stability of granular materials [1, 2]. In this work we aim to study the infiltration behavior using numerical and analytical methods to assess the potential of this mitigation method against adverse impacts of suffusion.

In this work, we propose to use the discrete element method (DEM) to analyze the fine infiltration process into the suffused coarse material. Both dry and flow driven infiltration are considered with the simultaneous release of a small number of fine grains above a gravity-deposited coarse sand column following the grading of the Hostun sand used in the laboratory. For the flow case we use the Pore scale Finite Volume (PFV) scheme introduced by Chareyre et al. ([3]). Besides, different fine/coarse size ratios (D50/d from 5 to 12) and different void ratios (from loose to dense) of sand column are considered. Both the lateral and vertical displacements of fine grains are analyzed to understand the infiltration behaviors of injected fines in term of infiltration depth and lateral diffusion. Similarly to previous experiments, the distribution of fine grains penetration depth in both dry and immersed cases are fitted by exponential decay curves to determine characteristic length of infiltrations.

References

[1] Antoine Wautier, Stephane Bonelli, and François Nicot, Rattlers' contribution to granular plasticity and mechanical stability, International Journal of Plasticity,112 :172–193,(2019).

[2] Tao Wang, AntoineWautier, Sihong Liu, and François Nicot, How fines content affects granular plasticity of under-filled binary mixtures, Acta Geotechnica,1–15,(2021).

[3] Chareyre, B., Cortis, A., Catalano, E. et al. Pore-Scale Modeling of Viscous Flow and Induced Forces in Dense Sphere Packings.Transp Porous Med, 92, 473–493 (2012).

[4] Wautier, A, Bonelli, S, Nicot, F. DEM investigations of internal erosion : Grain transport in the light of micromechanics.Int J Numer Anal Methods Geomech, 43 : 339– 352, (2019).

[5] Wautier, A., Bonelli, S. & Nicot, F. Scale separation between grain detachment and grain transport in granular media subjected to an internal flow. Granular Matter 19, 22 (2017).

Figures
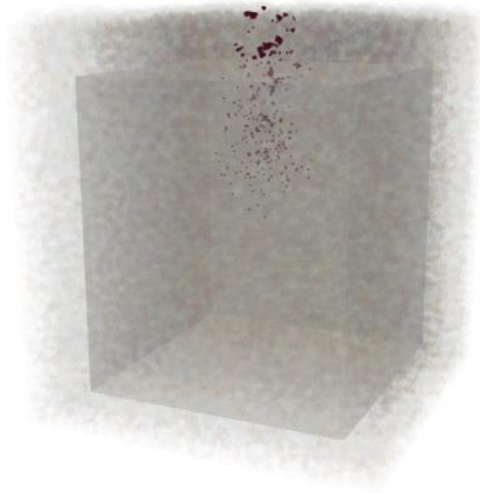
Figure 1: *Infiltration process using coupled PFV-DEM.*
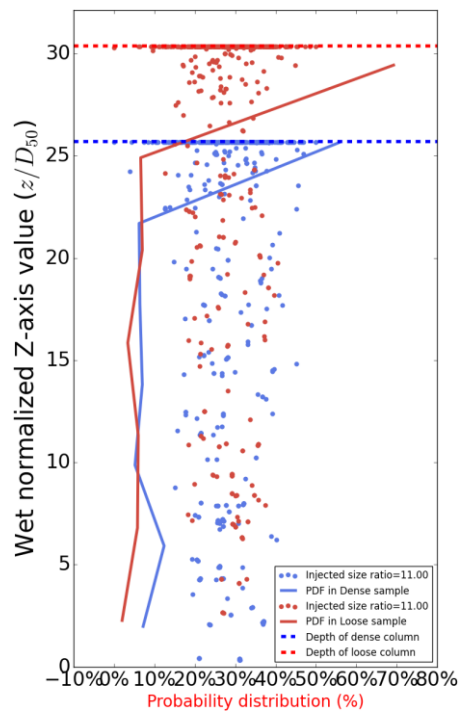
Figure 2: *Profile of the injected fines inside the column*

Experimental and numerical investigation of the hydro-mechanical behaviour of Boom Clay

Sophie De Kock[1]*, Bertrand François[1], Arnaud Dizier[2], Séverine Levasseur[3]

[1]Université de Liège, Dépt. ArGEnCo, allée de la Découverte 9, 4000 Liège, Belgium

[2]EIG Euridice, Mol, Belgium

[3]ONDRAF/NIRAS, Avenue des Arts 14, 1210 Brussels, Belgium

[*s.dekock@uliege.be](mailto:s.dekock@uliege.be)

Keywords: Boom Clay, hydro-mechanical coupling, anisotropy, compression test.

Abstract

Boom Clay is one of the potential rocks that is studied in Belgium in order to implement an underground repository for high- and intermediate-level of radioactive waste. It has been more than 40 years that Boom Clay formation is studied (Li et al., 2023), but mainly at the depth of 0 and 223 m. This last depth corresponds to the level of the underground laboratory HADES. It is now considered that the repository would be implemented at a depth between 350 and 400 m.

The end purpose of this research is to characterize Boom Clay at a depth of ± 400 m and to evaluate the transferability of the data gained at HADES URL level towards greater depth.

In order to do that, drained triaxial and isotropic compression tests are planned for samples taken at 0, 223 and 400 m.

The first step however was to look at what was already done in the literature. Many triaxial tests have already been performed on Boom Clay sample from 223 m depth (Baldi, 1991, Coll, 2005, Lê, 2008, Sultan et al., 2010, Lima, 2011). The results from these tests display a lot of disparities partly due to the fact that these triaxial tests were performed under different conditions. This show the importance of establishing one unique protocol for all the triaxial tests planned during this research.

In addition to the planned triaxial tests, eight uniaxial compression tests were performed, in order to quickly investigate the mechanical properties of Boom Clay as well as the influence of the cross anisotropy of the material (Figure 1 and Figure 2). From Figure 1 and Figure 2, it was concluded that the loading direction does not affect significantly the uniaxial compression strength of the material but it affects its stiffness.

In parallel to the experimental study, numerical simulations are run with the FEM software LAGAMINE in order to reproduce the hydro-mechanical behaviour of Boom Clay under triaxial and uniaxial compression via a hardening/softening Drucker-Prager law.

References

Baldi, G. (1991) *Developments in modelling of thermo-hydro-geomechanical behaviour of Boom clay and clay-based buffer materials*. Luxembourg: Commission of the European Communities, Directorate-General Science, Research and Development.

Coll, C. (2005) *Endommagement des roches argileuses et perméabilité induite au voisinage d'ouvrages souterrains*. Université Joseph Fourier.

Lê, T. (2008) *Thermo-hydro-mechanical- behaviour of Boom clay*. Ecole des Ponts ParisTech.

Li, X. *et al.* (2023) 'Forty years of investigation into the thermo-hydromechanical behaviour of Boom Clay in the HADES URL', *Geological Society, London, Special Publications*, 536(1), pp. 33–49. Available at: https://doi.org/10.1144/SP536-2022-103.

Lima, A. (2011) *Thermo-Hydro-Mechanical Behaviour of two deep Belgian clay formations: Boom and Ypresian clays*. Universitat Politècnica de Catlunya.

Sultan, N., Cui, Y.-J. and Delage, P. (2010) 'Yielding and plastic behaviour of Boom clay', *Géotechnique*, 60(9), pp. 657–666. Available at: https://doi.org/10.1680/geot.7.00142.
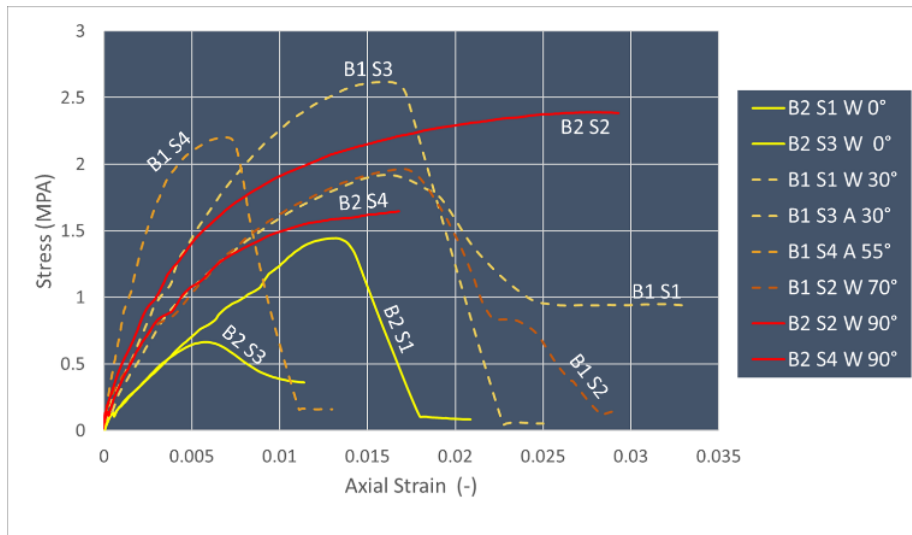
Figures

Figure 1: *Uniaxial compression strength of Boom clay under various loading directions (B#S# = name of sample, A/W = drilled with Air or Water, #°= loading direction)*
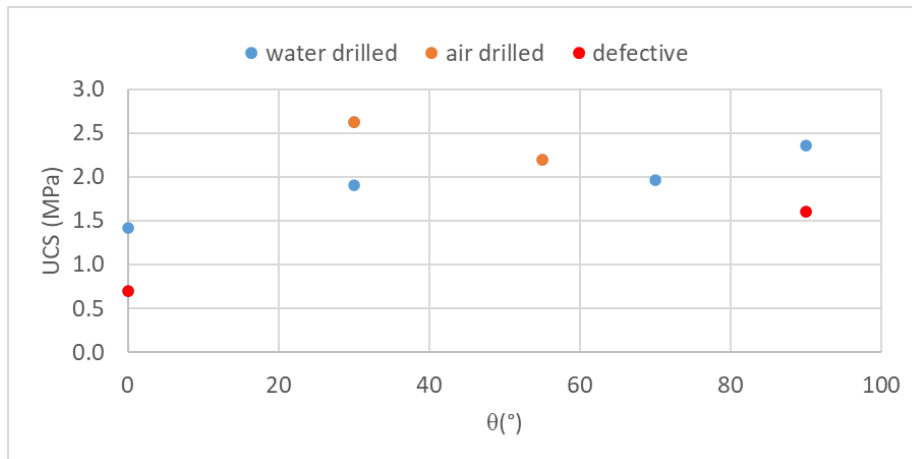
Figure 2: *Uniaxial compression strength of Boom Clay function of the loading direction (θ). Red points are considered defective because of a default that appeared during coring.*

Optimisation of particle transport in polydisperse dense granular flows: Towards sustainable processes

Santiago Caro[1,2], Patrick Richard[1], Riccardo Artoni[1] and Michele Larcher[2]

[1]*MAST-GPEM, Univ Gustave Eiffel, IFSTTAR, F-44344 Bouguenais, France*
[2]*Free University of Bozen-Bolzano, I-39100 Bozen-Bolzano, Italy*
santiago.caro-alba@univ-eiffel.fr

Abstract

This is a starting research project focused on understanding particle transport in polydisperse systems, paying special attention to segregation and diffusion phenomena. The main scientific objective is to study the coupling between particle transport and flow rheology. This is done by experiments and numerical simulations that will allow us to construct models for the spatial transport of polydisperse granular materials, with potential applications in the optimization of some industrial processes.

Granular materials are present in industrial processes but often problematic to handle as they are intrinsically polydisperse in size and composition. During polydisperse granular flows, two phenomena may take place. The first one takes place when transporting mixed polydisperse granular material and polydispersity may induce segregation or selective spatial transport according to particle size. The second one is diffusion, which is how the transport of initially segregated granular material leads to mixing. These processes are very problematic for process control and quality of granular mixing due to the competition between diffusion and segregation, leading to an excessive energy and resources demand. The goal is to carry out a theoretical and experimental study of the particle diffusion and segregation in various geometries, from simple shearing to industrial processes, in order to control these phenomena and therefore maximize the efficiency of processes involving polydisperse granular transport (e.g. biomass gasification, recycling of construction and demolition waste).

For investigating the particle scale phenomena, the project profits from the use of the discrete element method (DEM) [1] for the numerical simulation of steady, inhomogeneous, and collisional shearing flows of nearly identical, frictional, and inelastic spheres (Figure 1). This is necessary for tracking the micro-macro relation, due to the possibility of obtaining particle-level information, which can be coarse grained to obtain continuum like constitutive laws, and quantifying diffusive and segregating fluxes as a function of shear, pressure, and particle size. For investigating process scale phenomena, we use an annular shear cell (Figure 2) where glass beads are sheared for different confining and velocity configurations, while motor current and particles motion are recorded. This is useful for studying the link between shear-driven segregation, flow configuration (e.g. shear rate, bead size, confining load), and motor current measurements.

The first approach to simulations, employing the open source LAMMPS platform, was a triperiodic cell to study the self-diffusion of a bidisperse system under simple shear. Here, by reconstructing particle trajectories, the mean squared displacement (MSD) was estimated for the two sizes of spheres (Figure 3). It was found that small particles diffuse more than the big particles at least in vertical and traversal directions with respect to the flow direction. For the experiments with the shear cell, it is possible to measure the motor current, the velocity profile by a PIV analysis, and segregation by imaging. However, before starting experiments with

polydisperse systems in the annular shear cell, it was necessary to validate the setup with a monodisperse flow to determine whether the torque could be a proxy for the analysis of segregation. Initial experiments were performed with glass beads in a combination of four variables: beads diameter, shear rate, confining load, and bed height. Figure 4 shows an example of the current measurements for the glass beads of a diameter equal to 8 mm. Until now, it is evident the direct relation between the confining load or bed high with current. On the other hand, the relation remains not clear with bead size. Finally, it seems that the shear velocity does not affect current records since the curves try to flatten when increasing rotation speed, however, at low speeds current measurements show a pick independently of the grain size.

The first year of the project was useful to validate and calibrate both the experimental setup and the simulation cells with the more simple granular flow configurations. Now, the plan is to start using polydisperse systems both in simulations and experiments. Concerning simulations, the starting point will be a confined 3D cell that will recreate the flow conditions during the experiments. The main idea is to run simulations for different shearing configurations and sphere size combinations. Simultaneously, the shear cell will be set in motion to perform the first exploration campaigns with glass beads of two and then three different sizes under a non-homogeneous shearing system. For both approaches, diffusive and segregating fluxes will be quantified as a function of shear, pressure, and particle size, comparing results between experiments and simulations.

References

[1] Cundall P, Strack O. A Discrete Numerical Model for Granular Assemblies. Geotechnique. 1979.

[2] Artoni R, Soligo A, Paul JM, Richard P. Shear localization and wall friction in confined dense granular flows. Journal of Fluid Mechanics. 2018.

Figures
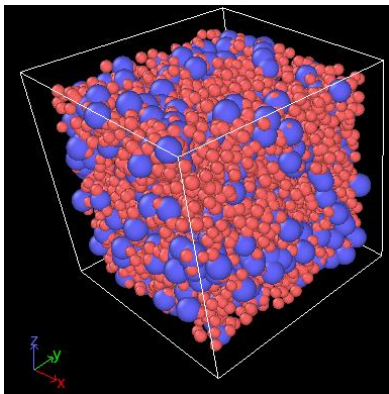
Figure 1: *Snapshot triperiodic homogeneous shearing simulation LAMMPS.*
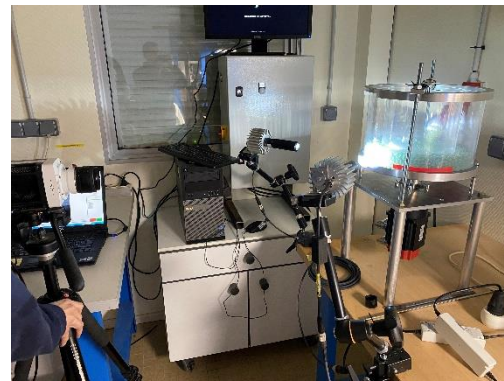
Figure 2: *Annular shear cell experimental setup including instrumentation, lights, and high-speed camera.*
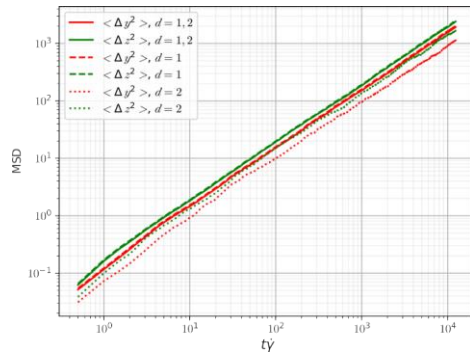
Figure 3: *Self-diffusion for a simulated bidisperse granular flow estimated as Mean Square Displacement (MSD). Colors refers to studied diffusion direction, continuous line represent the MSD for the whole system, big dashed lines for small particles only and small dashed lines for big particles only.*
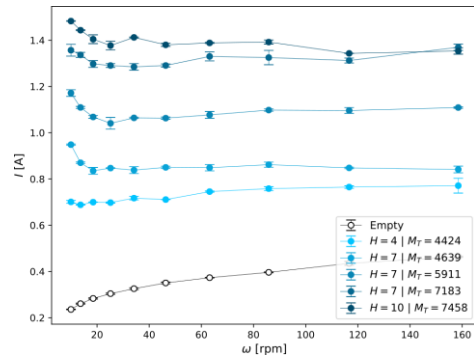
Figure 4: *Example of the current measurements for the shear cell experiments with the glass beads of diameter equal to 8 mm. H represents the bed high in cm, and Mt the total confining load in gr at the bottom plate. Note that the empty cell current (black line) was subtracted from all the data curves (blue lines).*

Modelling claystone degradation due to freezing and thawing cycles

Andrés. Macías, Jean Vaunat & Kateřina Bočková

Department of Civil and Environmental Engineering Technical University of Catalonia (UPC) Campus Nord UPC, 08034 Barcelona, Spain

andres.macias@estudiantat.upc.edu

Abstract

Claystone degradation under the effect of freezing and thawing cycles represents a key aspect in the production of erodible material in mountain ranges. Zones with a high amount of erodible materials are prone for erosion processes with numerous potential consequences such as dam filling, slope instabilities, badlands production, among others. In such regions, evaluation and management of the risk associated to erosion is of upmost importance. When quantitative evaluation is necessary, numerical models represent a useful tool to analyze the state of the soil regarding erodibility.

The modelling of effects of freezing and thawing cycles in porous media requires an understanding of the phenomenon kinetics. In general, free water experiments liquid-to-solid phase change when temperature reaches the freezing point for a given pressure and the chemical potential of ice and liquid water become equilibrated. In case of pore water, due to the presence of grain/water interfaces, the chemical potential of liquid water is higher (increasing while pore radius decreases), therefore lower temperatures are needed for enclosed water freezing.

According to the Young-Laplace equation in presence of ice phase, the relationship between water surface tension ($\sigma_{T_{\alpha L}}$) and ice/water pressure difference can be defined as: $P_i - P_L = S_{cr} = \frac{2\sigma_{T_{\alpha L}}}{R}$. where R is the pore radius, P_L is the liquid pressure and Pi the ice pressure. The difference between P_i and P_L corresponds to the cryogenic suction s_{cr}. Water/ice pressures are related to temperature through the Clausius-Clapeyron equation: $P_i = \frac{\rho_i}{\rho_L}P_L - \rho_i L ln\left(\frac{T}{273.15}\right)$. By reworking and combining the former expressions, it is possible to compute the radius of the pore experimenting freezing for a given temperature (Eqn. 1).

$$R_f = \frac{2\sigma_{T_{\alpha L}}}{1 - \left(1 - \frac{\rho_i}{\rho_l}\right)P_l - \rho_i L ln\left(\frac{T}{273.15}\right)} \tag{1}$$

Equation indicates that the water freezing point is different in pores with different size. For a given temperature, specific pores will experiment freezing while the smaller ones remain unfrozen. The effect of cryogenic suction results in water mass migration from the unfrozen pores towards the frozen ones, increasing the total water mass of the frozen pores and, thus, its volume while reducing the unfrozen pore volume. Similar processes take place during the thawing phase and leads to changes in microfabric. As such, significant microfabric strains are

expected after the end of the freezing and thawing cycle hinting mechanical degradation of the material and increasing its erodibility.

Following (Nishimura et al. 2003), when ice/water potential equilibrium is reached during freezing and thawing, the degree of saturation of the liquid phase is related to temperature by the soil freezing characteristic function (SFCF) combined with the Clausius-Clapeyron. To provide a more general expression, a extension of the one-mode freezing function has been developed considering a double porosity water retention curve based on the Van Genuchten (1980) expression, resulting in Eqn 2.

$$S_L = 1 - S_i = (1 - w)\left[\frac{1}{1 + \left(\frac{S_{cr}}{P_M}\right)^{\frac{1}{1-M}}}\right]^M + w\left[\frac{1}{1 + \left(\frac{S_{cr}}{P_m}\right)^{\frac{1}{1-m}}}\right]^m \tag{2}$$

Where S_L and S_i are the liquid and ice saturations respectively, w is a weight parameter that defined the microporosity/macroporosity ratio, P_M and P_m are the air entry values for the macropores and micropores respectively. M and m accounts for the water retention curve shape factors for the macropores and the micropores respectively.

Equation 2 evidences the strong effect of the shape of the retention curve on liquid and ice saturation during freezing/melting. This is a consequence of the close relationship that exists between soil microfabric and its water retention properties (Casini et al 2012). Since soil microfabric can be described by the pore size distribution (PSD) as a statistical representation of the volume proportion of each pore family in the soil mass, the proposed numerical model will use changes in retention curve to evaluate the changes in PSD ,and thus in soil microfabric, during freezing and thawing cycles.

In this work, a calibration and validation of the proposed numerical model is carried out by comparison with one experimental freezing/thawing test with temperature measurements. Test has been carried out on a saturated sample in undrained conditions. 4 cycles have been applied. An optimization procedure have been considered to evaluate the retention curve that allow for the best fit of temperature variations during each stage of the test. Freezing and thawing were analyzed separately.

Through the existing relationship between water retention curves and PSD, the model is able to represent the microfabric state for each freezing/thawing cycle from the calibrated retention curves. Results shown in Figure 1 reflect the increase in macroporosity and existence of pore family gaps that indicates microfabric degradation that may signify an increase in erodibility.

References

1. Casini, F., Vaunat, J., Romero, E., & Desideri, A. (2012). Consequences on water retention properties of double-porosity features in a compacted silt. Acta Geotechnica, 7, 139-150.

2. Nishimura, S., Gens, A., Olivella, S., & Jardine, R. J. (2009). THM-coupled finite element analysis of frozen soil: formulation and application. Géotechnique, 59(3), 159-171.

3. Van Genuchten, M. T. T. (1980). A closed-form equation for predicting the hydraulic conductivity of unsaturated soils. Soil Science Society of America Journal, 44(5):892.

Figures
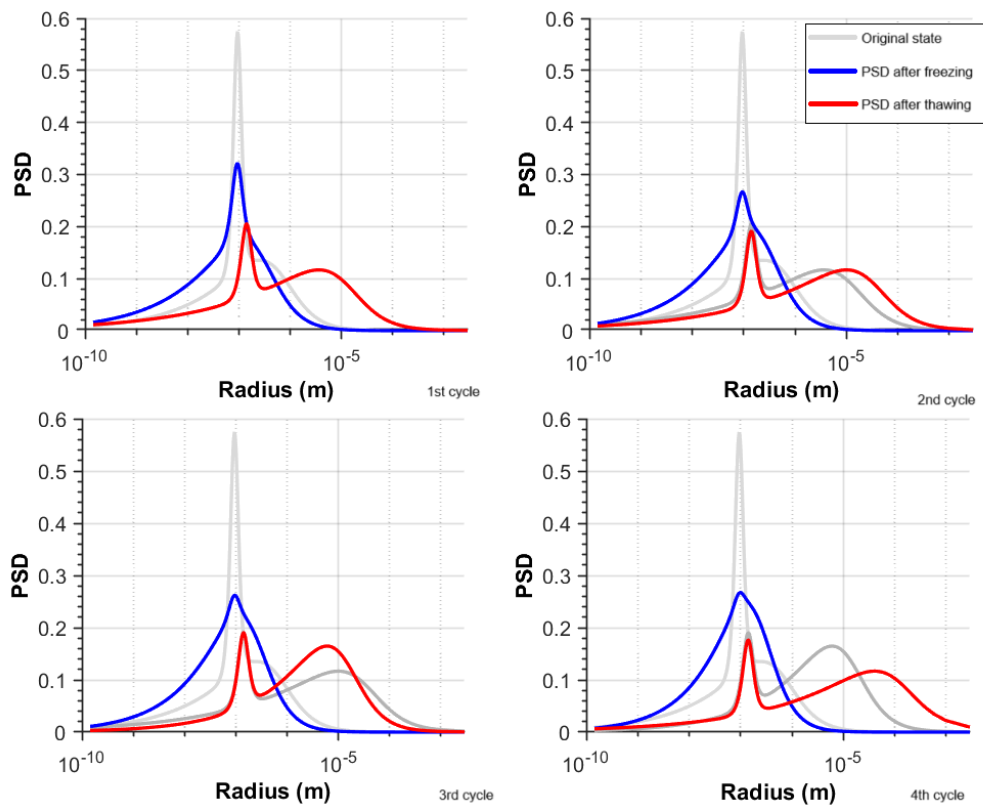
Figure1: *PSD change progression through the freezing and thawing cycles*

Using machine learning to predict stress and displacement at the wall of a tunnel

Alec Tristani, Lina-María Guayacán-Carrillo, Jean Sulem, Sebastián Ariel Donzis

Laboratoire Navier/CERMES, Ecole des Ponts ParisTech, Université Gustave Eiffel, CNRS, 77455 Marne la Vallée, France

alec.tristani@enpc.fr

Abstract

Context

Preliminary stage of tunnel design is generally performed using a plane-strain approach based on the confinement-convergence (cv-cf) method. However, this method relies on strong geotechnical and geometrical assumptions whose relevance is to be checked for each application (Panet & Sulem, 2022). In particular, when the ground exhibits large deformation and/or when the support is very stiff and installed close to the tunnel face, the classical cv-cf method appears to be inaccurate. Three-dimensional numerical modelling may then be carried out, but at rather high computational efforts and costs. As an alternative, emerging artificial intelligence techniques begin to be the more and more used in the fields of tunneling and underground construction (Jong et al. 2021) and many machine learning techniques have been tested for example to predict ground settlements based on scarce datasets (Liu L. et al. 2021).

Scope of study

Using synthetic data produced by previous work (de la Fuente et al. 2019), a machine learning model is developed to predict the maximum displacements and maximum stresses occurring at equilibrium state. A Mohr-Coulomb elastic perfectly plastic model is used to describe the constitutive behavior of the ground and a linear elastic model is assumed for the support. This analysis takes into account a large range of ground conditions, support characteristics and tunnel radius. To improve the generalization of the model, the bagging method (Breiman 1996) was coupled with neural networks. It is based on the bootstrapping sampling method and the aggregation of multiple machine learning model predictions. Bagging is mostly used to reduce the variance of a unique model. Each neural network (weak learner) is trained on a specific bootstrap sample and gives a single prediction. Eventually, the final prediction is the mean of each weak learner prediction.

Results

The results show that the model performs well with the small dataset used in this study and can capture the complex behavior of the ground. The ensemble method is able to make accurate and reliable predictions of both the maximum hoop stress and displacement that occur in the tunnel. Both variance and bias are reduced compared to a unique model. ANNs can therefore be considered as useful surrogate models to be used as a complement to numerical modelling. However, high prediction errors could be obtained if the input parameters do not belong to the

range used during training. Furthermore, since it is based on a synthetic dataset, the model can only be as good as the numerical model.

References

Breiman, L. 1996. Bagging predictors. *Mach Learn* 24 (2), pp. 123–40. DOI: 10.1007/BF00058655

De La Fuente, M., Taherzadeh, R., Sulem, J., Nguyen, X.S. & Subrin, D. 2019. Applicability of the convergence-confinement method to full-face excavation of circular tunnels with stiff support system. *Rock Mech and Rock Eng* 52 (7) pp 2361–2376. DOI: 10.1007/s00603-018-1694-8

Jong, S.C., Ong D.E.L. & Oh, E. 2021. State-of-the-art review of geotechnical-driven artificial intelligence techniques in underground soil-structure interaction. *Tunn and Undergr Space Technol* 113, pp. 103946. DOI: 10.1016/j.tust.2021.103946

Liu, L., Zhou, W. & Gutierrez, M. 2022. Effectiveness of predicting tunneling-induced ground settlements using machine learning methods with small datasets. *Journal of Rock Mech and Geotech Eng* 14 (4), pp. 1028–41. DOI: 10.1016/j.jrmge.2021.08.018

Panet, M. & Sulem, J. 2022. Convergence-Confinement Method for Tunnel Design. *Cham: Springer International Publishing (Springer Tracts in Civil Engineering).* DOI: 10.1007/978-3-030-93193-3

Tristani A, Guayacán-Carrillo L, Sulem J, Ariel Donzis S, Applicability of Artificial Neural Networks (ANN) for equilibrium state prediction in tunnel excavation, 15th ISRM Congress 2023 & 72nd Geomechanics Colloquium. (Accepted).

Figures
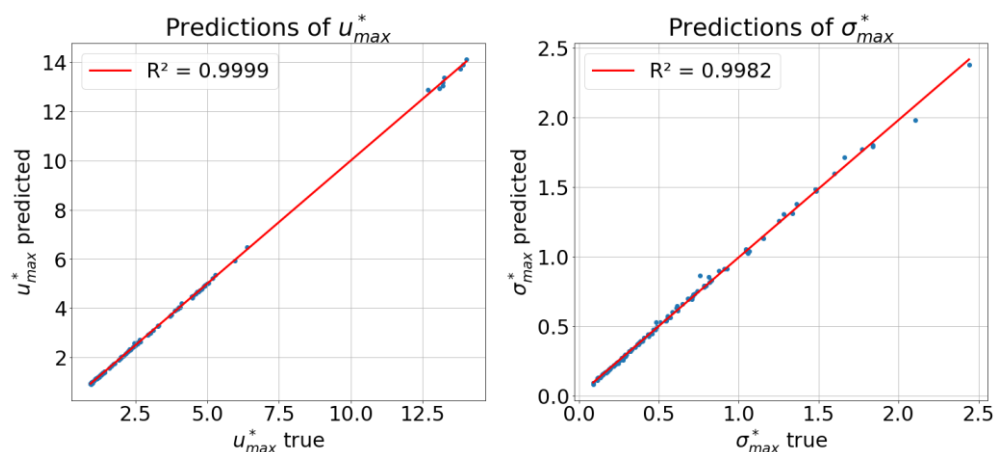
Figure 1: Model performance using the bagging technique.
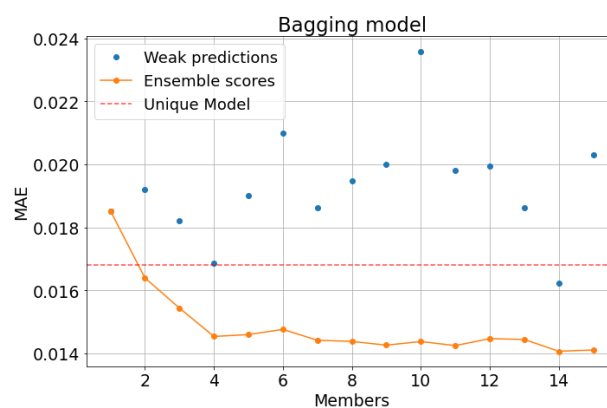
Figure 2: Ensemble predictions in regards of the number of members versus each weak learner prediction.

Hydration-based multi-physics modelling of cementitious materials for 3D printing: from simulation to process and mix design optimization

Maxime Pierre*, Siavash Ghabezloo, Patrick Dangla, Romain Mesnil, Matthieu Vandamme, Jean-François Caron

Navier, École des Ponts, Univ Gustave Eiffel, CNRS, Marne-la-Vallée, France

maxime.pierre@enpc.fr

Keywords: 3D concrete printing, numerical simulation, constitutive modelling, poromechanics, thermo-hydro-mechanical couplings

Abstract

The necessary reduction of greenhouse gas emissions in order to limit the consequences of climate change pause many challenges to the construction industry, among which the reduction of cement-based materials' use which are responsible for 8% of global CO_2 emissions. 3D printing with cementitious materials could contribute to solving this issue through shape optimization, ultimately using less material than traditional casting methods. However, achieving quality 3D printing with cement-based materials requires fine knowledge of the fresh state behaviour as well as its evolution at the early age. This behaviour exhibits couplings between thermal, hydraulic, chemical and poromechanical processes which need to be taken into account in order to assess the buildability of 3D printed objects.

Modelling of cement-based 3D printing has so far been mainly focused on the mechanical aspect. Herein, the authors propose a new simulation framework for 3D printing based on a coupled multiphysics material model for chemically solidifying porous media. It constitutes an extension of classical unsaturated THM poromechanics in the scope of elastoplasticity, with chemically-dependent parameters. This model is used in conjunction with a FEM-based program aiming at reproducing conditions during printing by simulating a sequential deposition of the material and incorporating environmental actions on the object being printed.

Using an axisymmetric corolla geometry, plastic collapse during printing is studied by numerical simulation at different printing speeds. Two main failure mechanisms are exhibited: yielding of the bottommost layer and yielding at an intermediary layer with bottom layers remaining intact, which has been observed experimentally.

Temperature also plays a crucial role in stability during printing, in that it greatly affects the hydration kinetics. Through a parametric study, it is shown that even in a non-linear geometry, a difference in temperature can be corrected by adjusting the printing speed by using a relationship taking into account the hydration's activation energy. This could be used on the field as a rule of thumb to print in varying environmental conditions.

Furthermore, water consumption in cement hydration reactions along with the use of low water to cement ratios in 3D printing mortar formulations leads to a progressive desaturation of the medium. As in classical poroplasticity, the yield criterion is believed to depend on an effective stress, resulting in a role of suction pressure in plasticity. As is shown from simulations, the water retention curve of the material and its evolution throughout the hydration process can be

a determining factor in the stability during printing, effectively acting as an isotropic prestress to the mortar paste. Adequate mix designs focusing on improving granular packing to maximize suction could then allow for lower cement content in 3D printing mixes.

References

i. Samudio, M. (2017). *Modélisation d'un ciment pétrolier depuis le jeune âge jusqu'à l'état durci: cinétique d'hydratation et comportement poromécanique* (Doctoral dissertation, Paris Est, in french).

ii. N. Agofack, S. Ghabezloo, J. Sulem, Chemo-poro-elastoplastic modelling of an oilwell cement paste: Macroscopic shrinkage and stress-strain behaviour, Cement and Concrete Research, Volume 132, 2020

iii. Carneau, P., Mesnil, R., Baverel, O., & Roussel, N. (2022). Layer pressing in concrete extrusion-based 3D-printing: Experiments and analysis. *Cement and Concrete Research*, *155*, 106741.

iv. M. T. Van Genuchten, A closed-form equation for predicting the hydraulic conductivity of unsaturated soils, Soil science society of America journal 44 (5) (1980) 892–898.

v. O. Coussy, Mechanics and physics of porous solids, John Wiley & Sons, 2011.

Figures
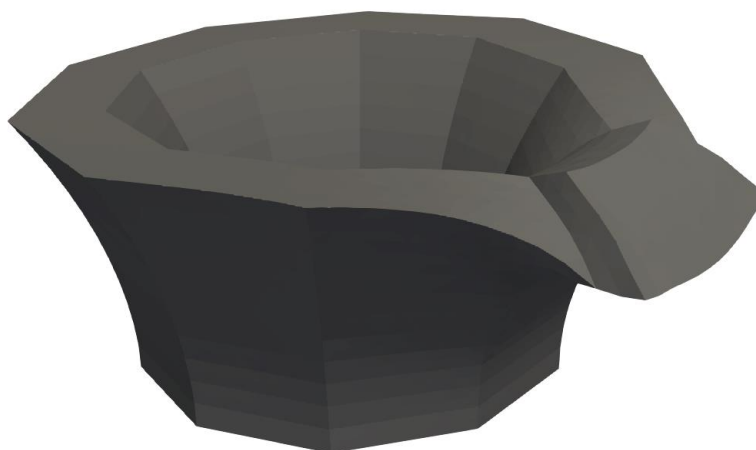
Figure 1: 3D simulation of a corolla during printing (magnified deformations).
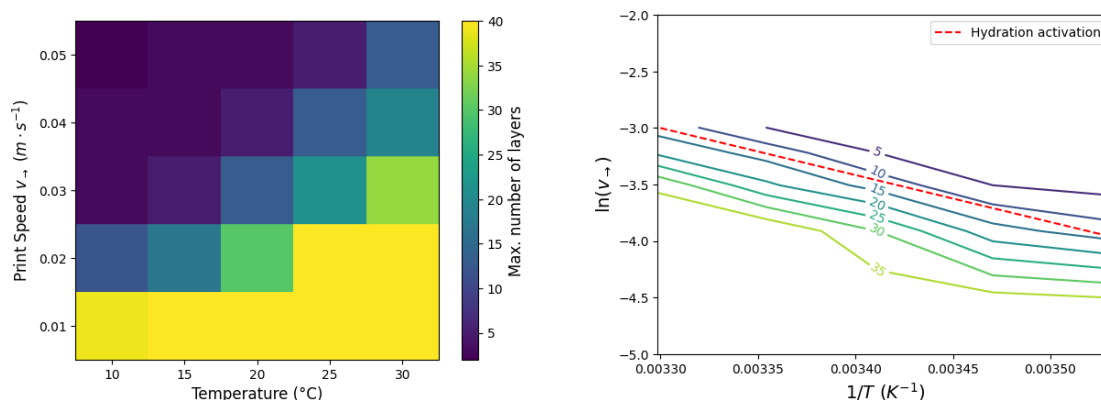
Figure 2: Parametric study of number of printable layers for different temperatures and print speeds – Comparison between activation energy of the printing process and that of hydration.

Discrete element modelling of cyclic triaxial loading on a model sand

A. Ezzeddine[1], B. Cazacliu[1], P. Richard[1], L. Thorel[2], R. Artoni[1]

[1]*Univ Gustave Eiffel, MAST-GPEM, F-44344 Bouguenais, France*
[2]*Univ Gustave Eiffel, GERS-CG, F-44344 Bouguenais, France*

alice.ezzeddine@univ-eiffel.fr

Keywords: cyclic triaxial loading; DEM simulations; Fontainebleau sand NE34; rolling resistance moment; micro-mechanical analysis

Abstract

This study employs the discrete element method (DEM) (Cundall and Strack (1979)) to comprehensively analyze the response of Fontainebleau sand NE34 to a drained cyclic loading path. Yade, an open-source DEM software developed by Kozicki and Donze (2009), enables introducing a linear contact model and accounting for anisotropic particle shapes through a rolling resistance moment. The work begins by preparing a numerical sample with periodic boundary conditions and calibrating the model parameters to match experimental behavior obtained from drained monotonic triaxial tests conducted on NE34 sand samples at different confining pressure and initial index density (I_D) (Andria-Ntoanina and al., (2010)).

Subsequently, a series of drained cyclic triaxial tests is conducted on elementary volume samples, varying the cyclic stress ratio (CSR) and I_D across various tests. These tests enable the assessment of small-strain properties, specifically the shear modulus (G) and damping ratio (D), with strain amplitude and the comparison with experimental values from the literature.

The study proceeds with a micro-mechanical analysis, investigating the evolution of fabric and contact force orientation within the samples when loaded. This analysis establishes a link between observed microscopic and macroscopic behavior. This relationship shows an effect of the initially set I_D particularly on the levels of damping in a sample. In conclusion, this work provides important understandings of the behavior of Fontainebleau Sand NE34 under cyclic loading and how micro-scale interactions combine with macro-scale responses.

References

Andria-Ntoanina, I., Canou, J., & Dupla, J. (2010). Caractérisation mécanique du sable de fontainebleau ne34 à l'appareil triaxial sous cisaillement monotone. PROJET DE RECHERCHE SOLCYP (ANR + PN), Comportement des pieux sous sollicitations cycliques (juillet 2008 - juin 2012) Groupe de travail GT1, EXPERIMENTATIONS SUR LES SOLS ET LES INTERFACES,Internal report.

Cundall, P. A., & Strack, O. D. (1979). A discrete numerical model for granular assemblies. geotechnique, 29 (1), 47–65. https://doi.org/10.1680/geot.1979.29.1.47

Kozicki, J., & Donze, F. V. (2009). Yade-open dem: An open-source software using a discrete element method to simulate granular material. Engineering Computations. https://doi.org/10.1108/02644400910985170

Figures

Figure 1: *a) Sample of 10,000 particles with PBC highlighted by virtual spheres represented in wireframe style b) Hysteresis loop used to evaluate G and D.*

Figure 2: *a) Modulus reduction curves (b) Damping ratio with increasing deviatoric strain amplitude at I_D = 46, 66, 83 %.*

Experimental verification of Miner's rule on Zbraslav sand and Malaysian kaolin under one-dimensional conditions
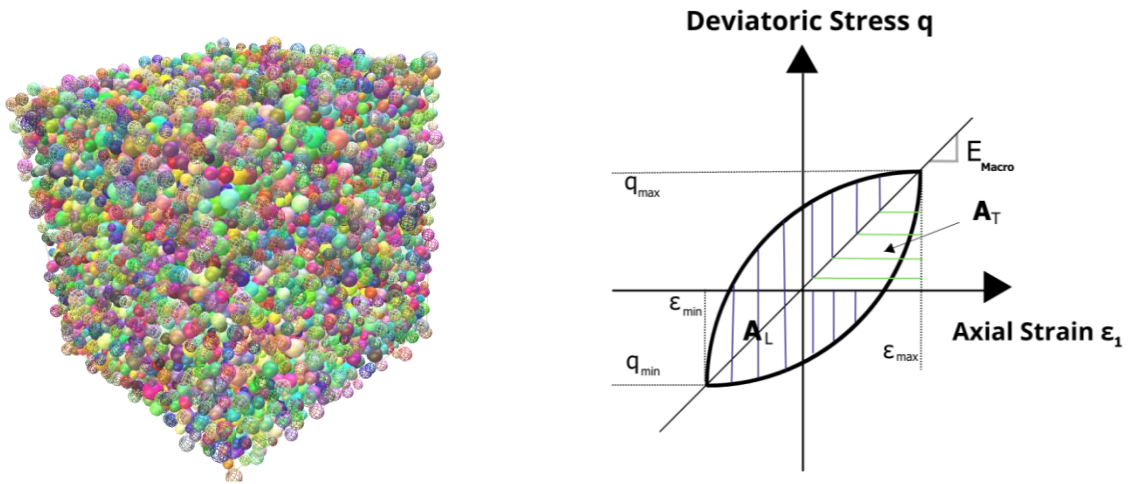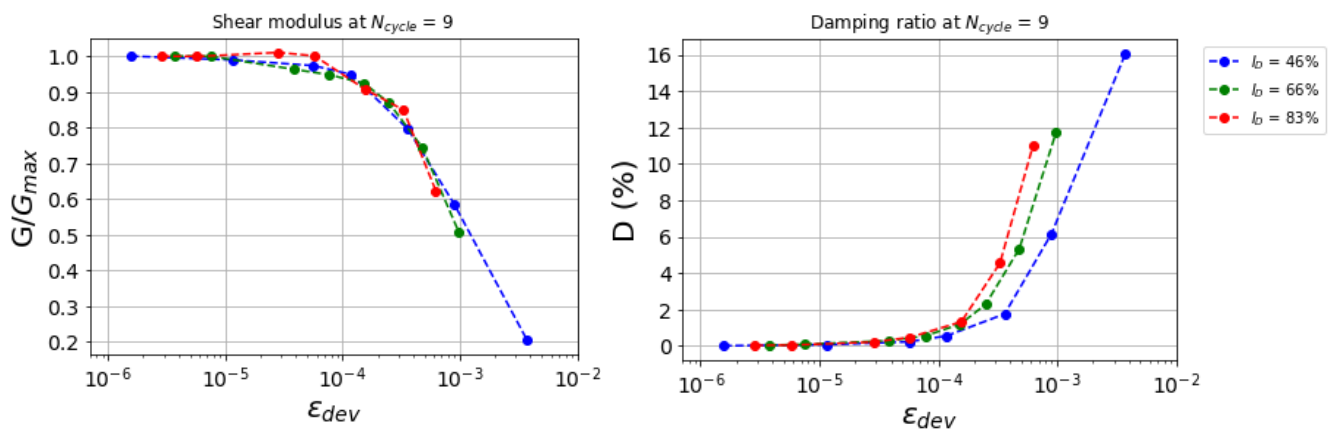
Rodrigo Polo-Mendoza[1] , David Mašín[1] , Jose Duque[1,2] , Jan Najser[1]

[1]Faculty of Science, Charles University, Prague, Czech Republic.

[2]Department of Civil & Environmental Engineering, Universidad de la Costa, Barranquilla, Colombia.

polomenr@natur.cuni.cz , david.masin@natur.cuni.cz , duquefej@natur.cuni.cz, jan.najser@natur.cuni.cz

Keywords: coarse-grained soils, fine-grained soils, Miner's rule, oedometer test

Abstract

Many geotechnical structures are subjected to cyclic loading scenarios of variable magnitude due to the stochastic nature of the loads (e.g., winds, waves, flooding, vehicles). Such irregular loading scenarios are commonly simplified into packages of cycles with constant amplitudes, which are afterwards treated sequentially. Such simplification assumes that Miner's rule is valid, i.e., that the sequence of the packages of cycles with different amplitudes do not affect the final accumulation [1]. However, Miner's rule was only validated on coarse-grained soils under drained cyclic triaxial conditions [2]. It is not valid on fine-grained soils under undrained cyclic triaxial conditions [3]. However, no attempts have been performed to investigate whether Miner's rule holds under one-dimensional conditions.

In this work, a series of stress-controlled oedometric tests were performed to investigate the validity of Miner's rule under one-dimensional conditions. Two different types of soils were considered for that purpose: Zbraslav sand and Malaysian kaolin. Both soils were subjected to the same experimental protocol, i.e., an initial preloading episode followed by the loading sequence. In the initial preloading, the axial stress (σ_1) is raised to 1600 kPa and then unloaded to 100 kPa. This preloading episode is mainly employed to limit the deformation obtained in the subsequent cyclic stages. Meanwhile, the subsequent loading sequence is described in **Table 1**. According to **Table 1**, each soil sample was subjected to 6 different loading sequences. In turn, each loading sequence is comprised of 30 load cycles. Notably, three types of load cycles were considered: (i) from 200 kPa to 100 kPa (x10), (ii) from 400 kPa to 100 kPa (x10), and (iii) from 800 kPa to 100 kPa (x10).

Figure 1 and **Figure 2** present the laboratory results on accumulated axial strains for Zbraslav sand and Malaysian kaolin, respectively. These graphs show that both types of soils yield similar final values of accumulated axial strain regardless of the order of the loading sequence. The Zbraslav sand exhibits a minimum value of 0.4200%, a maximum of 0.4428%, and a standard deviation of 0.0079%. The Malaysian kaolin presents minimum, maximum, and standard deviation values of 1.7234%, 1.8454%, and 0.0454%, respectively. Accordingly, under the adopted experimental conditions, the sequence of the load cycles does not significant influence the magnitude of the final accumulated axial strain. In light of the above, it is feasible to conclude that Miner's rule is valid for the coarse-grained and fine-grained soils under one-dimensional conditions.

Table 1. Experimental protocol proposed for this investigation.

Test name	Soil sample	Loading sequence, σ_1 [kPa]		
OED1		200-100 (x10)	400-100 (x10)	800-100 (x10)
OED2		200-100 (x10)	800-100 (x10)	400-100 (x10)
OED3	Zbraslav	400-100 (x10)	200-100 (x10)	800-100 (x10)
OED4	sand	400-100 (x10)	800-100 (x10)	200-100 (x10)
OED5		800-100 (x10)	200-100 (x10)	400-100 (x10)
OED6		800-100 (x10)	400-100 (x10)	200-100 (x10)
OED7		200-100 (x10)	400-100 (x10)	800-100 (x10)
OED8		200-100 (x10)	800-100 (x10)	400-100 (x10)
OED9	Malaysian	400-100 (x10)	200-100 (x10)	800-100 (x10)
OED10	kaolin	400-100 (x10)	800-100 (x10)	200-100 (x10)
OED11		800-100 (x10)	200-100 (x10)	400-100 (x10)
OED12		800-100 (x10)	400-100 (x10)	200-100 (x10)

Acknowledgements

References

[1] M. A. Miner, "Cumulative Damage in Fatigue," *J. Appl. Mech.*, vol. 12, no. 3, pp. A159–A164, 1945, doi: 10.1115/1.4009458.

[2] J. Duque, J. Roháč, D. Mašín, and J. Najser, "Experimental investigation on Malaysian kaolin under monotonic and cyclic loading: inspection of undrained Miner's rule and drained cyclic preloading," *Acta Geotech.*, vol. 17, no. 11, pp. 4953–4975, 2022, doi: 10.1007/s11440-022-01643-0.

[3] M. Tafili, J. Duque, M. Ochmański, D. Mašín, and T. Wichtmann, "Numerical inspection of Miner's rule and drained cyclic preloading effects on fine-grained soils," *Comput. Geotech.*, vol. 156, no. 105310, pp. 1–15, 2023, doi: 10.1016/j.compgeo.2023.105310.
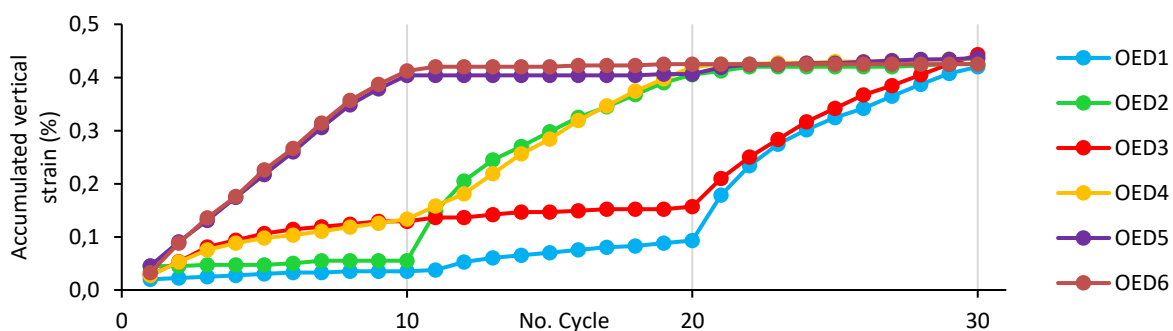
Figures

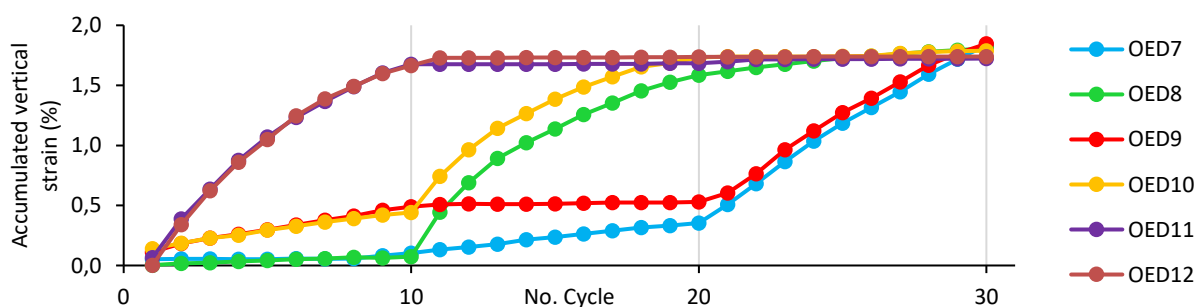*Figure 1: Results on accumulated axial strains for the Zbraslav sand.*

Figure 2: Results on accumulated axial strains for the Malaysian kaolin.

Pore-scale investigations on mud film formation during infiltration of bentonite slurry solution

Ryunosuke Kido[1,2], Hijiri Ueda[1]

[1]*Civil and Earth Resources Engineering, Kyoto University, Japan*

[2]*Laboratoire 3SR, Université Grenoble Alpes, France*

Kido.ryunosuke.2m@kyoto-u.ac.jp

Abstract

When cast-in place pile foundations are constructed using an earth drilling technique, ground excavation is conducted using stabilizing solution made by bentonite slurry. As shown in Figure. 1, a thin mud film is formed on the excavated wall, and then the slurry solution pressure works well to resist to lateral earth pressure and groundwater pressure, resulting in a stable state of the excavated wall. It is possible, however, that the excavated wall collapses because slurry pressure is reduced due to the infiltration of the solution into the excavated caused by incomplete formation of mud film. Previous studies (e.g., [1]) have investigated the effective conditions to form mud film by experiments, and they found that small grain size, low permeability of soils, large water level difference, large concentration of bentonite slurry contributes to stability of the soil wall. From microscopic viewpoint, the mud film formation probably occurs due to the clogging of cohesive clay particles included in bentonite slurry solution, transported via pore networks. On the other hand, such a micro-scale phenomenon has not been clear. This is because the previous studies have focused on whether the mud film is formed or not from macroscopic viewpoint. It is, therefore, that the mechanism of the mud film formation in soils has not been clear.

The objective of the present study is to clarify the mechanism of the mud film formation during infiltration of the bentonite slurry solution into soils from a microscopic viewpoint. An infiltration test apparatus was developed and tests using bentonite slurry were conducted for sand specimens with different levels of permeability under different levels of infiltration pressure of the solution. In the infiltration tests, the specimen was initially in water-saturated condition, and then the amount of solution flow through the specimen was measured with time. At the initial state and the last state after the infiltration of the bentonite slurry, the internal structure of the specimens was visualized using an X-ray micro CT. The region where the bentonite phase exists was extracted by making difference images between CT images at the initial and last states. After the segmentation of the bentonite phase from the difference images, a morphology analysis [2] was applied to the segmentation images of the bentonite phase, in order to identify where and how bentonite distributes in pore spaces and to calculate volume distributions of the bentonite. The test procedure is described in Figure. 2.

It was found from the infiltration tests that the amount of solution flow was increased at the beginning, and then it was kept constant after the formation of the mud film at the surface of the specimen. The mud film formation was clearly observed for the sand specimen with lower permeability and higher level of infiltration pressure, and these tendencies were consistent with the

results obtained in Nagura et al. (2004). The X-ray CT observation and image analysis successfully revealed the bentonite distributions in pore spaces. It was clearly observed that the larger number of bentonite clusters distributed in pore spaces with the larger volume in a case where the higher infiltration pressure is provided, whereas the bentonite clusters with smaller volume distributed in a wider range inside the specimen in a case where the lower infiltration pressure is provided.

References

[1] Nagura, K. and Higuchi, Y. (1992). Stability of slurry trench in sandy ground, Ground Engineering, Vol.10, No.1, pp.25-32. (in Japanese)

[2] Kido, R., Higo, Y., Takamura, F., Morishita, R., Khaddour, G. and Salager, S. (2020). Morphological transitions for pore water and pore air during drying and wetting processes in partially saturated sand, Acta Geotechnica, Vol.15, pp.1745-1761

Figures
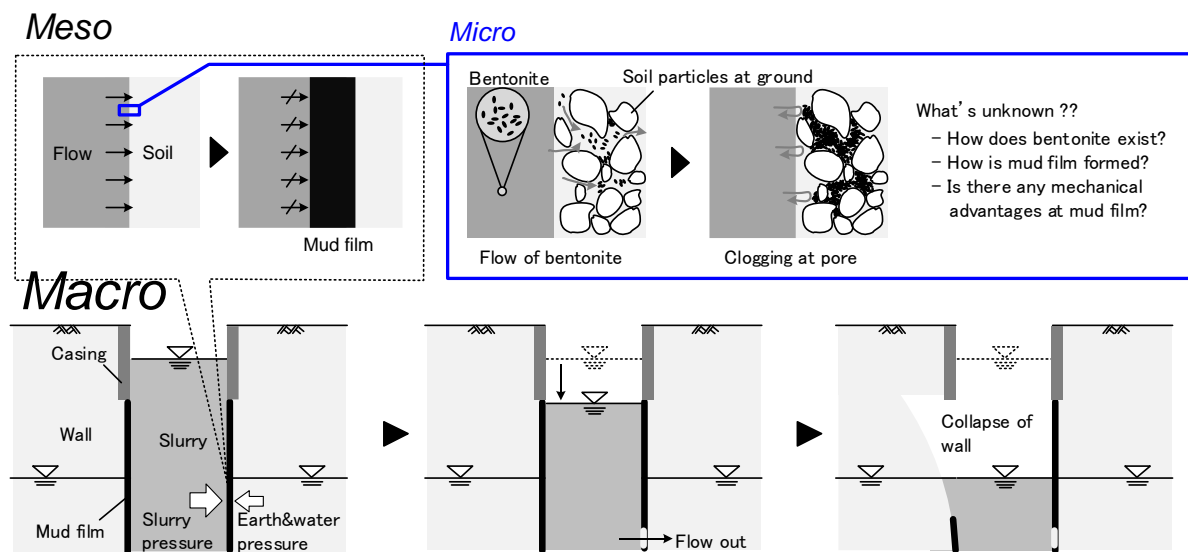
Figure 1: Multi-scale representations of stability of excavated wall using bentonite slurry solution and possible mechanism of mud film formation in pore spaces of soils. This study focuses on micro scale phenomenon.
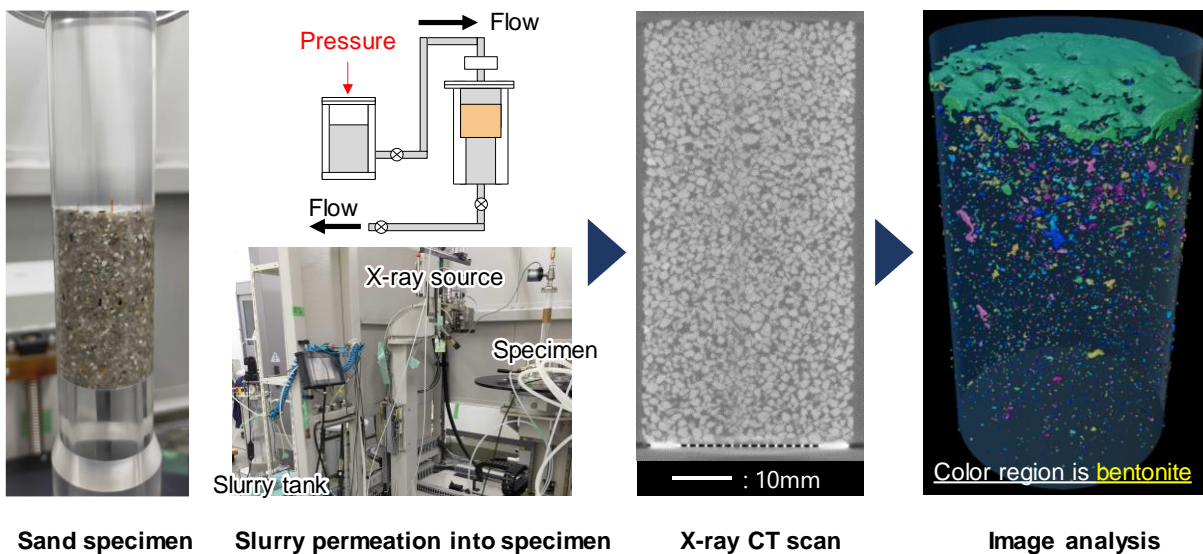
Figure 2: Procedure of infiltration test of bentonite slurry solution into sand with X-ray CT and image analysis.

Experimental investigation of the influence of soil plasticity on creep and soil mixtures compression characteristics

Manh Nguyen Duy, Jan Jerman

Institute of Hydrogeology, Engineering Geology and Applied Geophysics, Faculty of Science, Charles University, Albertov 6, 128 00, Prague, Czech Republic

nguyendma@natur.cuni.cz, jan.jerman@natur.cuni.cz

Keywords: creep, hypoplasticity, time-dependency, viscous behaviour, secondary compression

Abstract

Creep deformation is a primary aspect of long-term settlement investigation, which results in numerous geotechnical issues, especially in the case of clayey soils. The main purpose of this research is to characterize the creep behaviour of different clays. Several recent experimental studies have indicated that creep behaviour is influenced by soil plasticity, referred to [1], [2] and [3]. Nevertheless, no comprehensive description and relationship has been proposed to date. To investigate this, an extensive experimental program was prepared under well-defined conditions with reconstituted samples of kaolinite, bentonite and their mixture. Particularly, a series of standard oedometer tests were carried out to study compression characteristics, as shown in Table 1 and creep oedometer tests were conducted to investigate creep behaviour, as shown in Table 2. In the end, the dependency of soil compressibility and the coefficient of secondary compression (C_α) on soil plasticity are inferred. The results show that more compressible behaviour is achieved with higher soil plasticity, see Figure 1. In addition, the soil with higher plasticity exhibits more creep deformation demonstrated by higher values of $C\alpha$, see Figure 2.

References

[1]: OLEK, Bartłomiej Szczepan. An experimental investigation of the influence of plasticity on creep degradation rate. Acta Geotechnica, 2022, 17.3: 803-817.

[2] : WEN, Bao-Ping; JIANG, Xiu-Zi. Effect of gravel content on creep behaviour of clayey soil at residual state: implication for its role in slow-moving landslides. Landslides, 2017, 14: 559-576.behaviour

[3]: Yin JH (1999) Properties and behaviour of Hong Kong marine deposits with different clay contents. Can Geotech J 36:1085–1095. https://doi.org/10.1139/t99-068

Tables

Table 1: List of Standard Oedometer Tests

Standard Oedometric Tests			
Number	Material	Stress Increments	Date Started
S1	Kaolin	0-25-50-100-200-400-800-1600-800-400-200-100-50-25-0	23-03-23
S2	Bentonite	50-100-200-400-800-400-200-100-50-25-0	04-05-23
S3	Kaolin	25-50-100-200-400-800-1600-800-400-200-100-50-25	10-05-23
S4	Kaolin	25-50-100-200-400-800-1600-800-400-200-100-50-25	15-05-23
S5	50K/50B	0-25-50-100-200-400-200-100-50-25-0	17-05-23
S6	50K/50B	0-25-50-100-200-400-200-100-50-25-0	30-05-23
S7	Kaolin	0-25-50-100-200-400-800-1600-800-400-200-100-50-25-0	05-06-23
S8	Kaolin	0-25-50-100-200-400-800-1600-800-400-200-100-50-25-0	29-06-23
S9	Bentonite	25-50-100-200-100-50-25-0	28-06-23
S10	75K/25B	0-25-50-100-200-400-800-400-200-100-50-25-0	08-08-23
S11	25K/75B	0-25-50-100-200-400-(800)-400-200-100-50-25-0	29-06-23

Table 2: List of Creep Oedometer Tests

| Creep Oedometer Tests					
Number	Material	Multi-Stage	Creep at	Stress	Date Started
C1	Kaolin	No	200	25-50-100-200	23-03-23
C2	Bentonite	No	200	25-50-100-200	13-04-23
C3	Bentonite	No	200	25-50-100-200-0	18-04-23
C4	Kaolin	Yes	25-50-100-200-400	25-50-100-200-400-0	11-05-23
C5	Bentonite	Yes	25-50-100-200	25-50-100-200-0	11-05-23
C6	Bentonite	No	50-100	25-50-100-0	28-06-23
C7	50K/50B	Yes	25-50-100-200	25-50-100-200-0	28-06-23
C8	75K/25B	Yes	25-50-100-200	25-50-100-200-0	25-07-23

Figures
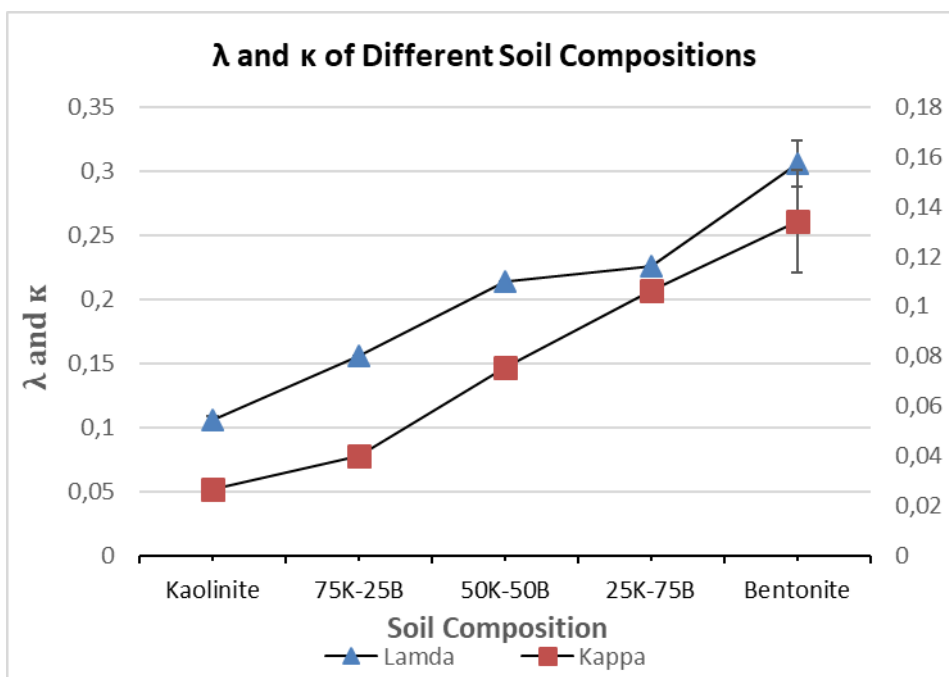
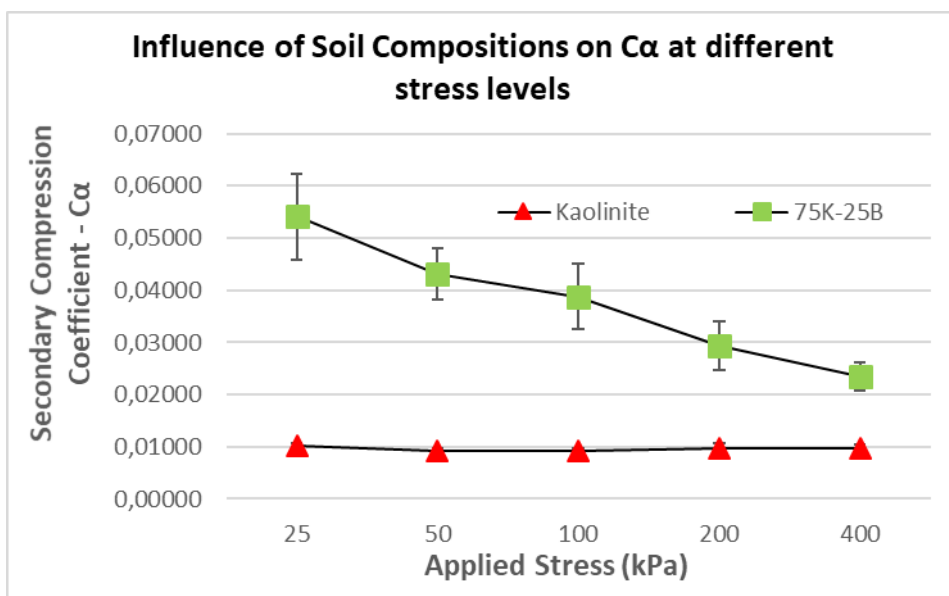***Figure 1:*** *Compression Index Affected by Soil Compositions.*

Figure 2: *Secondary Compression Coefficient (Cα) Affected by Soil Compositions at Different Stress Levels.*

Ink-bottle effect in soil water retention curves: insights from CFD analysis

Mai Sawada[1, 2], Catherine O'Sullivan[1], Aikaterini Tsiampousi[1]

[1]Imperial College London,
[2]Tokyo Institute of Technology

sawada.m.af@m.titech.ac.jp

Keywords: Computational fluid dynamics, Multiphase flow, Unsaturated soil, Capillary rise, Hysteresis

Abstract

Soil water retention curves, i.e. the relationships between water content or degree of saturation and suction, play essential roles in predicting water transfer in partially saturated soils. Water retention curves in drying and wetting processes are generally hysteretic; at a specific suction, the water content in a soil experiencing drying is higher than in the same soil experiencing wetting. The ink-bottle effect is understood to be a major cause of the hysteresis of soil water retention curves. The ink-bottle effect is a consequence of the geometry of the soil pores. Taylor (1948) explained the ink-bottle effect using a capillary tube with a bulb (Fig. 1), and this analogy to a soil pore is cited in several textbooks, including Fredlund & Rahardjo (1993). Taylor's model is useful to qualitatively explain the ink-bottle effect: however, this is not sufficient to understand the tube-bulb system completely. The effects of the presence of a bulb on the capillary height in a tube can vary depending on its geometry such as the height of the bulb.

This study numerically simulated the ink-bottle effect by simulating Taylor's model using the open-source CFD code OpenFOAM (OpenFOAM, 2023; Weller et al., 1998) to explore the effect that the height of the bulb has on the capillary height. The response of systems with bulbs placed at four different heights during both the drying and wetting processes was observed. Furthermore, the computed capillary heights were summarised in the form of water retention curves.

The diameter and height of the capillary tube were 1 mm and 30 mm, respectively. A bulb with a diameter of 2 mm and a height of 4 mm was placed at positions of 3, 13, 18, and 23 mm from the bottom (datum). Three-dimensional analyses were performed using the *interFoam* solver. A capillary force was modelled at the tube's inner walls with a contact angle of 45 degrees. Gravity and capillary forces were applied to the water column in the tube, and the steady state capillary height was recorded as a key output. The capillary height of a tube without a bulb (hereinafter referred to as the "CHWOB") was also computed to validate the model. The numerical CHWOB matched the theoretical value. Two initial water levels were applied for each bulb position to simulate both drying and wetting processes. The ink-bottle effect is well-illustrated by the representative results shown in Fig. 2. In the drying process, the water column was held at the top of the bulb, which was higher than the CHWOB (i.e. 20.4 mm). The extra capillary height is supported by the capillary force acting on the inner wall of the bulb. However, this was not the case when the bulb was placed at a higher elevation, and the mass of the water column exceeded the capillary force. In the wetting simulation, the capillary rise was limited at the bottom of the bulb when it was placed below the CHWOB. The contact angle increased to reduce the vertical component of the capillary force and balance with the mass of the short water column when the bulb was placed at lower positions. In both the drying and

wetting processes, the bulb did not affect capillary height if its position was not between the initial water level and the CHWOB.

The water retention curves for the tube-bulb systems were obtained from the computed capillary heights, as shown in Fig. 3. Suction is defined in the same manner as in the water column method. The discrepancy between the drying and wetting curves is caused by the ink-bottle effect that occurred at the bulb. The water retention curves of the single tube are simple but illustrate essential features of those of irregular-shaped real soil pores. These results suggest that the water retention curves of real soil can be numerically estimated by the CFD analysis when the geometry of the soil pores is provided.

Acknowledgments

References

Fredlund, D. G., & Rahardjo, H. (1993). Soil mechanics for unsaturated soils. John Wiley & Sons.

OpenFOAM (2023). "OpenFOAM v8". OpenFOAM Foundation. https://www.openfoam.com/. Accessed 12/9/23.

Taylor, D. W. (1948). Fundamentals of soil mechanics Vol. 66, No. 2. LWW.

Weller, H. G., Tabor, G., Jasak, H., and Fureby, C. (1998). "A tensorial approach to computational continuum mechanics using object-oriented techniques." Computers in Physics, 12(6), 620–631.
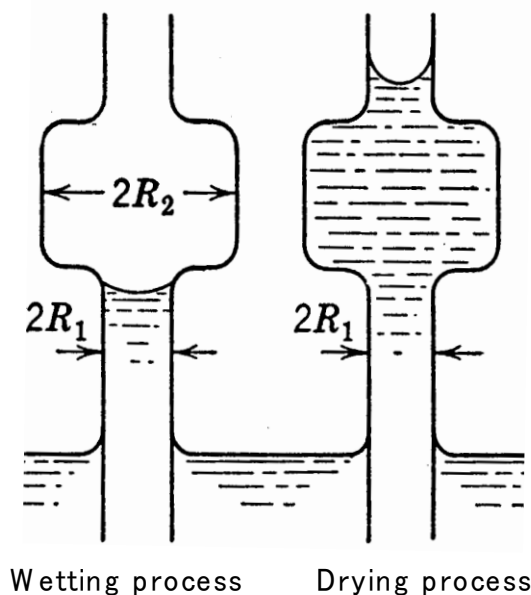
Figures

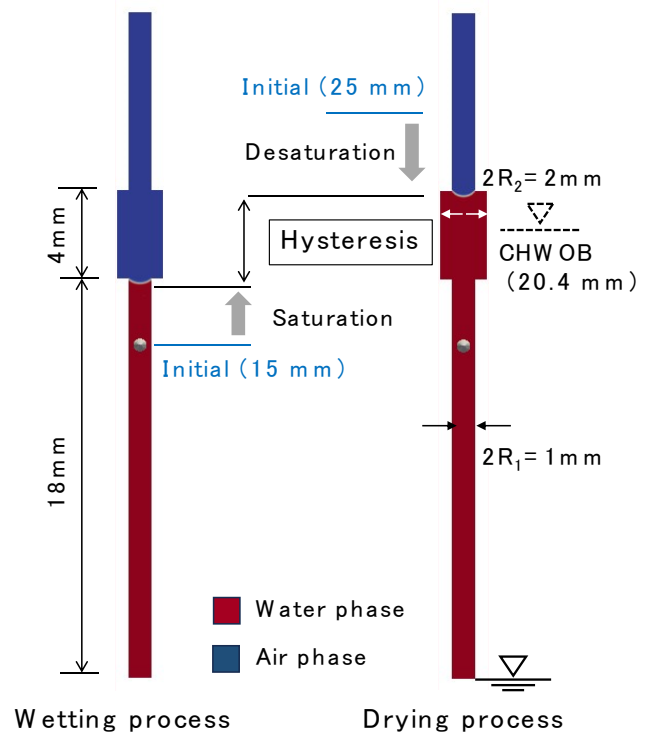**Figure 1:** *Ink-bottle effect (Taylor, 1948).*

Figure 2: *Computed capillary heights.*
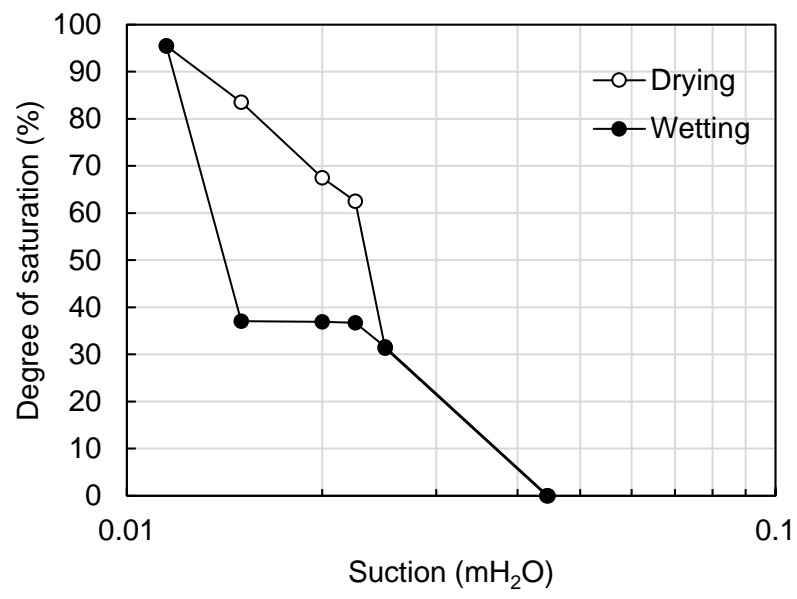
Figure 3: *Water retention curves for the tube with a bulb.*

Estimation of Frozen Layer Thickness in Field by Spectral Analysis

Kateřina Bočková, Jean Vaunat, José Moya

Department of Civil and Environmental Engineering, Universitat Politècnica de Catalunya, Barcelona, Spain

katerina.bockova@upc.edu

Keywords: soil temperature, solar radiation, spectral analysis, transfer function

Abstract

Cyclic freezing and thawing is a major factor of degradation in mountainous badlands. In order to quantify the extent of this degradation with depth and time, the knowledge of freezing propagation within the soil profile is necessary. The depth of freezing is primarily determined by air temperature, temperature history, and solar radiation. In order to estimate it, we have to understand the relationship between meteorological data and soil temperature profile. This work aims to determine this relationship using spectral analysis of extensive monitoring data.

The collection of monitoring data takes place on a small North-South oriented claystone ridge in a badland area of the Vallcebre basin (Spanish Eastern Pyrenees). Each of the two slopes of the ridge is equipped with a weather station and a 40 cm deep profile of sensors measuring (among others) temperature. The temperature data (including air temperature) is collected in a 5-minute interval. It is then supplemented by hourly solar radiation data from a nearby meteorological station.

The monitoring data provide information for building a model that estimates the relationship between meteorological data and soil temperature. In order to perform the analysis on a broader scale, the model must be able to process long time series quickly. For this reason, a Fourier transformation (passing from time to frequency domain) is used. It decomposes the temperature and solar radiation signal into modes. Using the most significant modes we define a transfer function between atmospheric and soil variables. The resulting transfer function then depends on solar radiation incidence, thus on slope inclination and orientation.

In this poster, we present the method used to predict soil temperature profiles at a regional scale for slopes with different orientations and inclinations. This profile will be further used to estimate the freezing and degradation profile, which is one of the main variables of erosion volume estimation.

Mitigating backward erosion piping by flow barriers: a nature-based solution

Lexin Li [a], Vera van Beek [b], Timo Heimovaara [a], Anne-Catherine Dieudonné [a]

[a] Faculty of Civil Engineering and Geosciences, Delft University of Technology

[b] Unit Geo-Engineering, Deltares

L.LI-10@tudelft.nl, Vera.vanBeek@deltares.nl, T.J.Heimovaara@tudelft.nl, A.A.M.Dieudonne@tudelft.nl

Keywords: backward erosion piping, nature-based solution, low-permeability barriers

Abstract

Backward erosion piping (BEP) is an internal erosion mechanism, in which a channel forms underneath dykes or structures due to the removal of soil by water. In this work, we present a nature-based solution to mitigate BEP by creating low-permeability barriers with aluminium-organic matter (Al-OM) flocs, which are the products of metal-organic complexation and subsequent flocculation. The Al-OM flocs can clog the pore space and consequently reduce soil permeability. We aim to answer the following two questions: can flow barriers inhibit pipe progression, and to which extent can these flow barriers resist internal erosion?

In this experimental work, we mix Al-OM flocs with sand to create sand-flocs barriers with a hydraulic conductivity reduction (defined as the ratio between the hydraulic conductivity of sand and that of the sand-flocs mixtures) of about 100. We impose an increasing hydraulic gradient across the sample and measure the flow rates as well as the pipe length evolution. We find that the pipe can progress through homogeneous sand at a relatively small total hydraulic gradient, while flow barriers can intercept the pipes in barrier tests. The evolution of the pipe length with the imposed hydraulic gradient demonstrates that it requires large hydraulic gradients, about 5 times the reference critical gradient, for pipes to reach barriers. After that, the pipe lengths stop increasing, indicating the barriers are sustaining erosion. When flow rates and pipe lengths surge, the pipes break through the barriers. The failure gradients are 7 to 9 times larger than the reference critical gradient. Based on experimental observations, we generalise the processes of pipe progression in the presence of flow barriers into four stages: the progression stage, the interception stage, the branching stage and the failure stage. This generalisation can guide the design of barriers in practice. Through this work, we conclude that the sand-floc barriers can inhibit pipe progression by raising the failure gradient 7 to 9 times and exhibit a higher resistance against internal erosion than sand. Large-scale laboratory tests are being carried out at TU Delft where sand-flocs barriers are created in situ by direct injection of Al-OM solution.

Strength retrogression in high-temperature oil-well cements: Microstructural origins

Math Lecomte, Siavash Ghabezloo, Axelle Alavoine

Laboratoire Navier, Ecole des Ponts, Champs-sur-Marne

math.lecomte@enpc.fr , siavash.ghabezloo@enpc.fr

Keywords: cement, maturation cells, strength retrogression, MIP, XRD, TGA

Abstract

Cementing is considered one of the most important operation performed on a well, ensuring zonal isolation between the different formations exposed to the wellbore and mechanical support. Along a given well, the temperature is increasing with depth due to geothermal gradient. This hydration temperature has a particular importance as it significantly affects the cement paste microstructure. Under temperatures higher than 110°C (typically below 4 km depth) the C-S-H undergoes a progressive metamorphosis, converting progressively to more crystalline and denser phases, e.g. Jaffeite (C_3SH) and α-C_2SH as shown by (Bresson et al., 2002), resulting in a continuous decrease of its mechanical properties and an important increase of its porosity and consequently permeability, affecting the well sealing and zonal isolation. The phenomenon is usually referred to as "strength retrogression".

In the continuity of the research work carried out by (Bahafid et al., 2017) for cement pastes cured under temperatures ranging from 7°C to 90°C, the present work aims at developing a better comprehension and characterization of the chemical and microstructural origins of the strength retrogression for cement hydrated under a temperature above 110°C.

Samples were prepared from a class G cement with a water to cement ratio of 0.44 and cured under different temperatures and pressures into special maturation cells equipped with acoustic sensors for 7, 14 and 28 days. Compressive tests were performed on a part of the extracted samples while the rest was freeze-dried prior to X-Ray Diffraction (XRD), Thermogravimetric Analyses (TGA) and Mercury Intrusion Porosimetry (MIP).

The compressive tests as well as the acoustic measurements have exhibited as expected a loss of elastic properties and compressive strength with increasing curing temperature and time, corresponding to the strength retrogression phenomenon.

Typical results from MIP tests for samples cured under temperatures ranging from 30°C to 190°C are shown in Fig 1, with a significant increase in porosity observed between 90°C and 130°C, accompanied by a major change of the pore size distribution itself. Above 90°C, the cement pastes are mainly formed by one pore family with pores that tend to be larger and more homogeneous in size with increasing temperatures, which is explainable by the formation of denser hydration products.

For samples cured at a temperature above 140°C, the formation of α-C_2SH and Jaffeite is observed in the XRD and TGA results. The Rietveld analysis exhibits a significant diminution of the general amorphicity of the cement paste with an increasing temperature, evolving from 74% for samples cured at 30°C to a rate of 40% for samples cured at 190°C, indicating a progressive crystallization of the microstructure. This observation is consistent with the MIP

results suggesting a densification of the hydrates phases. The coarsening of the microstructure is also visible on the SEM images.

The phase assemblage given Fig 2 can be established from the chemical equilibrium of the system for each oxide, with the XRD, TGA and porosity measurements. Volume fraction of crystalline hydrates with a C/S ratio over 2 (α-C$_2$SH and Jaffeite) increases with curing temperature up to 14% for the sample at 190°C. At this temperature the volume fraction of C-S-H is only 16% whereas samples cured under 20°C have a volume fraction of C-S-H equal to 41%.

The previous results have exhibited two main factors associated with the strength retrogression. The first one is the change in chemical composition with the formation of dense crystalline phases for curing temperatures above 140°C, growing at the expense of the C-S-H phase. The second one is the metamorphosis of the porosity, in total value but more specifically in the distribution of the pores size and the type of porosity. These phenomena are certainly related; the formation of denser crystalline phases at the expense of C-S-H can be correlated to the formation of porosity with specific pore sizes detrimental to the macrostructural strength.

References

i.   (2017) S. Bahafid, S. Ghabezloo, M. Duc, P. Faure, J. Sulem, „ Effect of the hydration temperature on the microstructure of Class G cement: C-S-H composition and density", Cement and Concrete Research, Volume 95.

ii. (2002) B. Bresson, F. Meducin, H. Zanni, C. Noïk. „Hydration of tricalcium silicate (C3S) at high temperature and high pressure". Journal of Materials Science, 2002, 37 (24).
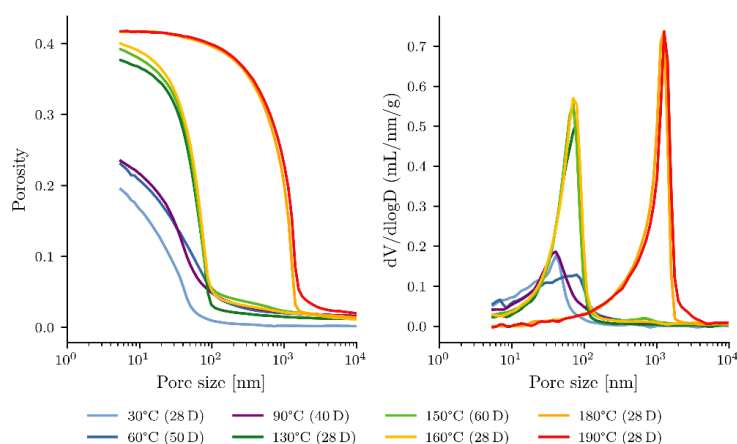
Figures

Figure 1: Evolution of the total porosity for samples cured at various temperatures.
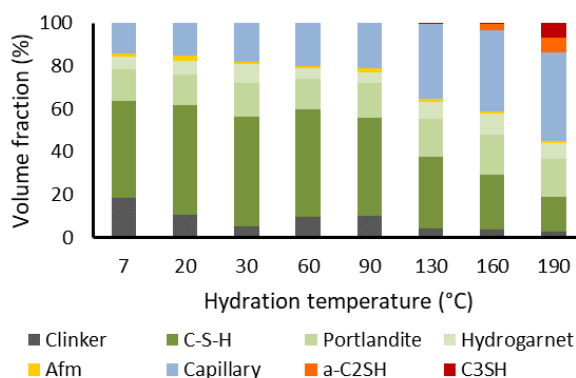

Figure 2: Phase assemblage for cement pastes hydrated for 28 days at various temperatures.

Theoretical soil water characteristic curve model with regular packing considering density heterogeneity of soil particle structure

Shizuka Eshiro[1,2], Yosuke Higo[1]

[1]Department of Urban Management, Kyoto University, Japan

[2]Laboratoire 3SR, Université Grenoble Alpes, France

eshiro.shizuka.72m@st.kyoto-u.ac.jp

Keywords: unsaturated soil, soil water characteristic curve, theoretical model, regular packing

Abstract

The soil water characteristic curve (SWCC) is a crucial index to evaluate the water retention property of unsaturated soil. Currently, frequently used SWCC models are empirical models such as the van Genuchten model[1], which require long-term water retention tests. In contrast, theoretical SWCC models [2,3] with the regular packing structure (regular packing model) have been developed based on the pore-scale water retention mechanism, which can readily estimate SWCCs using the basic soil information, e.g., the grain-size distribution. In this research, density distribution has been introduced into a theoretical model, employing the rhombohedron, whose structure and density vary with angle θ, as the unit cell of the regular packing structure (Figure 1). Assuming that θ follows some distribution, a density distribution can be introduced into this SWCC model (Figure 2(a)); the conventional SWCC model without density distribution uses uniform unit cells (Figure 2(b)).

In the present study, density heterogeneity of soil particle structure was expressed by introducing the density distribution of isospheric random packing. Aste et al. (2010)[4] showed that the Voronoi volume distribution of isospheric random packing could be described as;

$$f(V) = \frac{k^k}{\Gamma(k)} \frac{(V - V_{min})^{k-1}}{(\langle V \rangle - V_{min})^k} e^{-k\frac{V - V_{min}}{\langle V \rangle - V_{min}}} \tag{1}$$

V: Voronoi volume, V_{min}: Volume at the densest packing, $\langle V \rangle$: Average Voronoi volume, k: parameter

V is the volume of the particle-centered Voronoi cell shown in Figure 3. f(V) indicates the density distribution of the structure; by assuming that the Voronoi volume distribution of the particle center in this model follows f(V), we introduced a density distribution for isospheric random packing into the regular packing model.

Here, consider Case 1 with a narrow grain size range and Case 2 with a wide grain size range. The parameters for each case are shown in Table 1. Figure 4 shows each case's SWCC for the non-uniform model (solid line) and the uniform model (dashed line). The SWCC estimated by the non-uniform model provided a more moderate decrease in the degree of saturation than that estimated by the uniform model. This indicates that the density distribution increases the diameter variance of the pore throat, which is the pathway for air into the saturated pores of unit cells. In addition, the effect of density distribution on SWCC is more significant in Case 1, with relatively small variations in particle size distribution, than in Case 2 because the variation in the throat diameter is affected by both the particle size distribution and the density distribution.

References

1) van Genuchten, M.: *Soil Sci. Soc. Am. J.*, **44**, 892-898, 1980.

2) Likos, W. J. and Jaafar, R.: *J. Geotech. Geoenviron. Eng.*, **139**(5), 724-737, 2013.

3) Alves, R. D., Gitirana, G. D. N. and Vanapalli, S. K.: *Computers and Geotechnics*, **127**, 2020.

4) Aste, T., Delaney, G. W. and Matteo, T. D.: *AIP Conference Proceedings*, **1227**, 157-166, 2010.

Figures
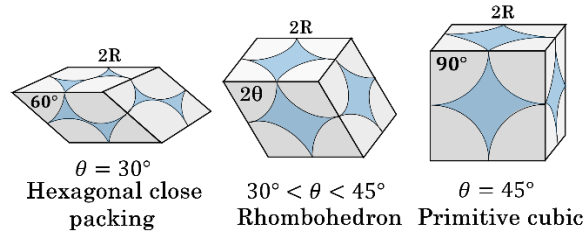
Figure 1: Rhombohedron structure employed in the proposed model.
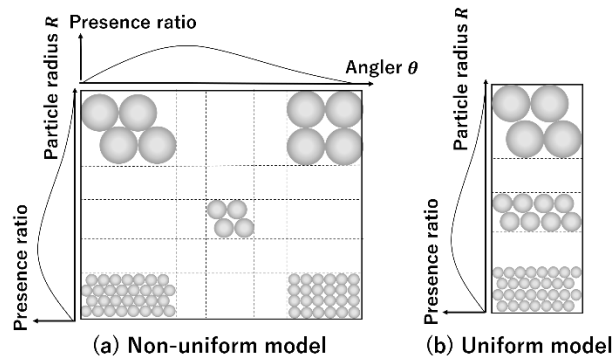
Figure 2: Soil particle structure for (a)non-uniform model and (b)uniform model.
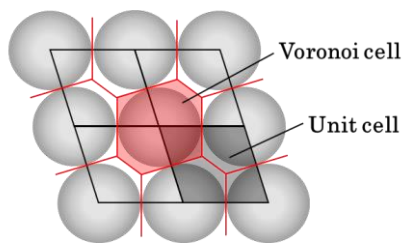
Figure 3: Voronoi cell in the regular packing.
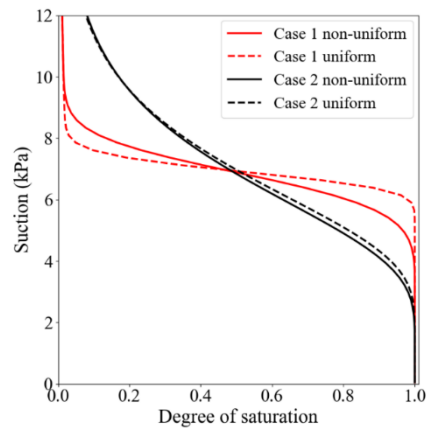
Figure 4: Comparison of the non-uniform model and the uniform model.

Table 1: The parameters for SWCCs

	e	k	D_{50} (μm)	$D_{84.13}$ (μm)
Case 1	0.637	12	187	200
Case 2	0.637	12	187	270

61

Coupled hydro-mechanical hypoplastic model for partially saturated soils under monotonic and cyclic loading

Pico Maria, Mašín David

Charles University, Prague, Czech Republic.

picoduam@natur.cuni.cz, masin@natur.cuni.cz

Keywords: unsaturated fine-grained soils, hypoplasticity, constitutive modeling, cyclic loading

Abstract

There are several scenarios in which the soil is subjected to cyclic hydro-mechanical loads, such as energy geostructures, nuclear waste disposal storage, embankments, landslides, and pavements. Additionally, the increasing effects of climate change are causing more severe seasonal variations that have a significantly influence in the performance of foundations. To analyse this type of behaviour from a geotechnical perspective, existing constitutive models and their capabilities to reproduce such behaviour must be evaluated. However, reproducing the coupling between suction and/or degree of saturation with stress rate is not a trivial task.

 This research presents the enhancement of an existing hypoplastic constitutive model for fine grained soils, proposed by Wong and Mašín [1]. The following three main features are included in the constitutive model: i) To predict the non-linear dependency of the degree of saturation on suction, the Water Retention Curve (WRC) is replaced by a smoothed hysteretical void ratio-dependent WRC proposed by Svoboda et al. [2]. ii) The Improvement to the intergranular strain (ISI) concept, as proposed by Duque et al. [3] was added into the model formulation for better capturing the effects of strain accumulation rate with increasing number of cycles. iii) A dependency of the ISI on the degree of saturation was added to predict partially saturated effects under cyclic loading. The enhanced constitutive model was thoroughly validated by comparing element tests simulations with experimental results taken from Ng et al. [4]–[6] on a completely decomposed tuff. The experimental program included monotonic and cyclic tests under several suction magnitudes. The numerical predictions using the new enhanced constitutive model were also compared with the previous formulation.

The outcomes showed that the new version of the constitutive model more accurately captures the effects of cyclic loading in partially saturated soils. First, the improved water retention curve enables more realistic predictions of the soil's hydraulic response. Second, the model is able to better capture the strain accumulation rates, thanks to the incorporation of the ISI concept. As a result, the strain accumulation rate decreases as the number of cycles increases. Third, the model qualitatively reproduces the effect of suction on the strain accumulation rate, showing a reduction in accumulated strain as suction increases. Moreover, the new features do not affect the predictive capabilities of the model under monotonic loading.

References

[1] K. S. Wong and D. Mašín, "Coupled hydro-mechanical model for partially saturated soils predicting small strain stiffness," *Comput. Geotech.*, vol. 61, pp. 355–369, 2014, doi: 10.1016/j.compgeo.2014.06.008.

[2] J. Svoboda, D. Mašín, J. Najser, R. Vašíček, I. Hanusová, and L. Hausmannová, "BCV bentonite hydromechanical behaviour and modelling," *Acta Geotech.*, vol. 18, no. 6, pp. 3193–3211, 2023, doi: 10.1007/s11440-022-01689-0.

[3] J. Duque, D. Mašín, and W. Fuentes, "Improvement to the intergranular strain model for larger numbers of repetitive cycles," *Acta Geotech.*, vol. 15, no. 12, pp. 3593–3604, 2020, doi: 10.1007/s11440-020-01073-w.

[4] C. W. W. Ng, J. Xu, and S. Y. Yung, "Effects of wetting-drying and stress ratio on anisotropic stiffness of an unsaturated soil at very small strains," *Can. Geotech. J.*, vol. 46, no. 9, pp. 1062–1076, Sep. 2009, doi: 10.1139/T09-043.

[5] C. W. W. Ng and J. Xu, "Effects of current suction ratio and recent suction history on small-strain behaviour of an unsaturated soil," *Can. Geotech. J.*, vol. 49, no. 2, pp. 226–243, Feb. 2012, doi: 10.1139/T11-097.

[6] C. W. W. Ng and C. Zhou, "Cyclic behaviour of an unsaturated silt at various suctions and temperatures," *Geotechnique*, vol. 64, no. 9, pp. 709–720, Jul. 2014, doi: 10.1680/geot.14.P.015.
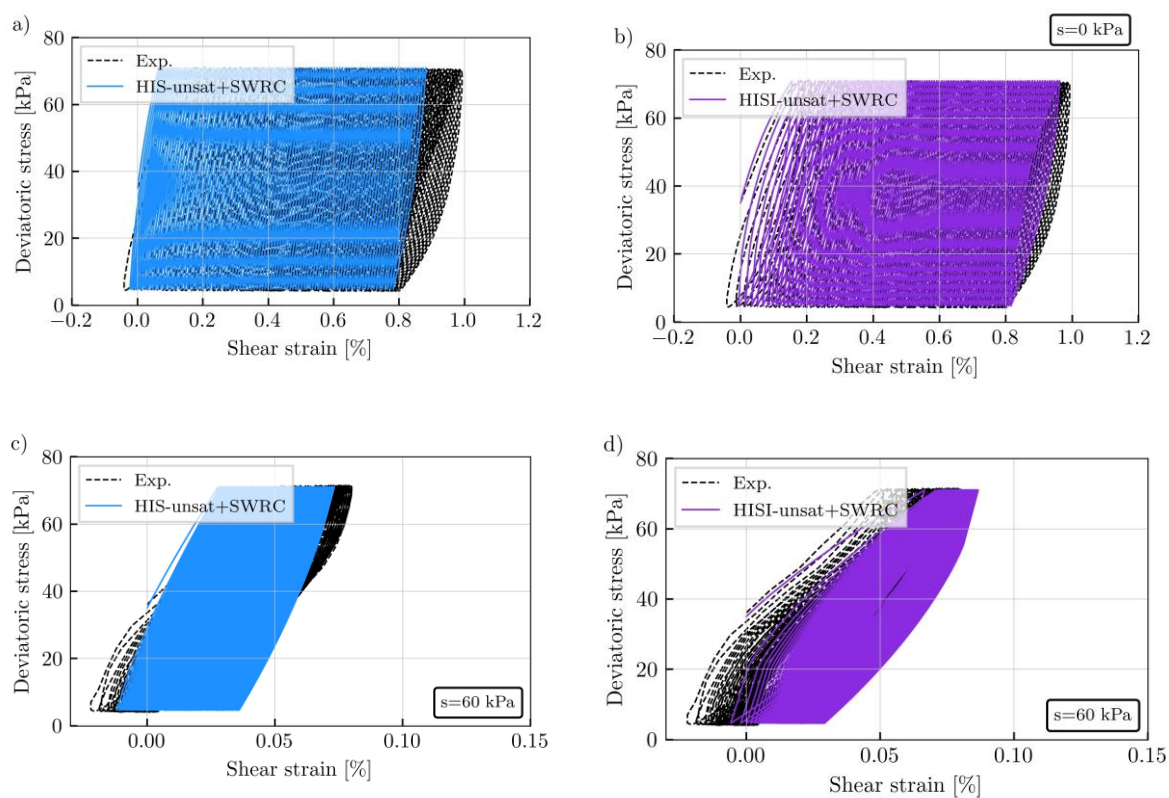
Figures

Figure 1: *Constant water cyclic triaxial test. Experimental results by Ng and Zhou [6] compared with numerical simulations using the reference model (HIS-unsat+SWRC) and the enhanced model (HISI-unsat +SWRC) at two suction magnitudes a) b) s=0 kPa c) d) s=60 kPa.*

On the influence of the shearing rate on the cyclic response of Malaysian kaolin

Elvis Covilla[1]*, David Mašín[1], Jose Duquel[1,2], Jakub Roháč[1], Jan Najser[1]

[1]Faculty of Science, Charles University in Prague, Czech Republic
[2]Universidad de la Costa, Barranquilla, Colombia

*covillae@natur.cuni.cz

Keywords: rate-dependency, cyclic loading, triaxial, kaolin, loading frequency

Abstract

An experimentally evaluation on the influence of shearing rate on the cyclic response of isotropically-consolidated samples of Malaysian kaolin is presented. A series of undrained cyclic triaxial tests were conducted considering 80 kPa deviatoric stress amplitudes and different loading frequencies. The experimental results suggest that depending on the loading frequency different shapes of mobilized effective stress loops are obtained. Larger loading frequencies lead to banana-shaped effective stress loops, while smaller frequencies reproduce eight-shaped effective stress loops. In order to further analyse the experimental results, fully coupled numerical simulations were performed considering the advanced rate-independent anisotropic hypoplastic model with intergranular strain for fine-grained soils by Mašín [2] and the software Plaxis 2D considering axisymmetric conditions. Different shapes of mobilized effective stress loops are obtained depending on the loading frequency. Higher loading frequencies result in banana-shaped effective stress loops, while lower frequencies reproduce eight-shaped effective stress loops, see Figure 1. Furthermore, the fully coupled simulations showed only minor effect of loading rate on calculated stress-strain curves and pore water pressures within the samples. We thus concluded that the observed effect of loading rate, can be attributed to the mechanical loading rate dependency of material properties rather than to the effect of ground water flow and excess pore water pressure redistribution within the sample.

References

[1] D. Mašín. Clay hypoplasticity model including stiffness anisotropy. Géotechnique, 64(3):232–238,

392 2014.

Figures

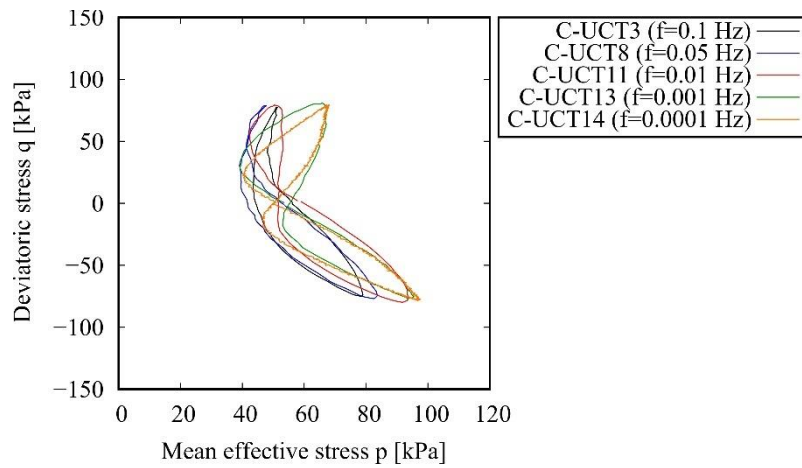***Figure 1:*** *Typical results of undrained cyclic triaxial tests with different frequencies.*
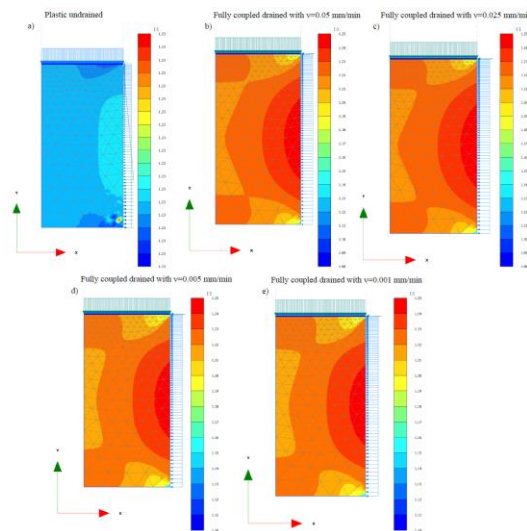

Figure 2: *Results of numerical simulations of void ratio variation in fully coupled simulations. Minimum and maximum values of void ratio: a) 1.227, 1.227; b) 1.081, 1.249; c) 1.083, 1.249; d) 1.105, 1.249; e)1.107, 1.249*
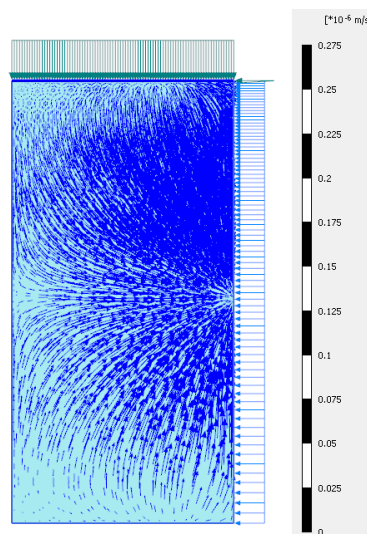

Figure 3: *Local ground water flow for a fully coupled analysis.*

Correlation analysis of the hypoplastic clay parameters based on ExCalibre database

P.C. Do , T. Kadlíček , D. Mašín, J. Najser

[1]*Institute of Hydrogeology, Engineering Geology and Applied Geophysics,*
Charles University, Czech Republic

dophu@natur.cuni.cz

Keywords: Hypoplastic clay; ExCalibre; correlation analysis

Abstract

Over the decades, researchers dedicated their effort to improve prediction of soil behaviour under various conditions by introducing more advanced constitutive models. In spite of their demonstrable advantages, practical applications of these models are far from the desired level. This state is caused not only by the lack of knowledge of advanced constitutive models but also by challenging calibration procedures, which often requires several cycles of back calculation on available laboratory experiments. Therefore, an online calibration software, the ExCalibre (Kadlíček et al., 2022a, 2022b), was developed to provide users with a tool of prompt and accessible calibration of parameters for four constitutive models: Hypoplastic Clay, Hypoplastic Sand, Modified Cam-Clay and Mohr-Coulomb. Calibration requires input data to be presented in the form of Excel file whose template is available on the website of ExCalibre software. In addition, the data must include a combination of compression (isotropic or oedometric) and shear (drained/undrained triaxial) test results. During the recent years of software operation, users have uploaded over 2,000 input files. This database was carefully inspected and it currently includes over 200 unique files which will be further analysed in order to deduce correlations between the constitutive models parameters and soils index characteristics.

In this paper, selected data from the ExCalibre database of 33 individual files are analysed after a close inspection to ensure a high level of consistency. Each file includes one to two reconstituted oedometric tests (OED-REC) and two to four undrained triaxial compression tests of reconstituted nature (CIUP-REC). Using ExCalibre, a unique set of hypoplastic clay (Mašín, D. 2013) parameters was generated for a single input file. Each parameter is then analysed using regression analysis, to determine relationships with soil properties or grain size distribution. The hypoplastic clay model defines the asymptotic state boundary surface in the space of stress and void ratio, encompassing all admissible states, and can be represented completely by five parameters: N, λ^*, κ^*, ν and φ_c, and state variables including stress and void ratio. The three compression parameters N, λ^* and κ^*, which are defined in $\ln p \times \ln(e+1)$ space, are found to have strong correlations to the Atterberg's limit, as shown in Fig.1. The Pearson's coefficients are reported to be $r = 0.944$, $r = 0.854$ and $r = 0.797$ between N and λ^*, κ^* and λ^*, λ^* and Plastic Limit W_P, respectively. Since these parameters are counterparts of the compression index C_c, swelling index C_s and initial void ratio e_0, these results are in good agreement with the literature. Moreover, Fig.2 supports an existence of the convergence point of all Critical State Lines (CSL) called Ω-point whose coordinates are defined by Schofield & Wroth, (1968) as $e_\Omega = 0.25$ and $\sigma'_\Omega = 10.342$ MPa. The hypoplastic clay model defines CSL shifted by the constant value $\lambda^* \ln 2$ beneath the Isotropic Normal Compression Line (INCL).

On the other hand, the critical state friction angle φ_c displayed a negative correlation with the Plastic Limit W_P and Liquid Limit W_L. Furthermore, strong correlations were observed with the fine and coarse particles, as discussed in literature by Simpson & Evans (2016). The correlation coefficients between φ_c and properties listed are high, in the range of 0.7-0.85.

The parameter ν, which controls the stiffness of the hypoplastic clay model, does not hold any direct correlation to other parameters or soil's properties. Using the idea of response envelope, the model's undrained shear stiffness was analysed and correlated with the parameter l^* due to its high correlation to other soil's properties.

Overall, although the parameters N, l^*, k^* and φ_c can be reasonably estimated from the derived relations, the parameter ν should be determined based on the simulation of triaxial shear tests, as none of examined relations provided a reliable approximation for this parameter.

References

Kadlíček, T., Janda, T., Šejnoha, M., Mašín, D., Najser, N., Beneš, Š. 2022a. Automated calibration of advanced soil constitutive models. Part I: Hypoplastic Sand, *Acta Geotechnica* **17**, 3421–3438.

Kadlíček, T., Janda, T., Šejnoha, M., Mašín, D., Najser, N., Beneš, Š. 2022b. Automated calibration of advanced soil constitutive models. Part II: hypoplastic clay and modified Cam-Clay, *Acta Geotechnica* **17**, 3439–3462.

Mašín, D. 2013. Clay hypoplasticity with explicitly defined asymptotic states, *Acta Geotechnica,* **8**, 481–496.

Schofield, A., Wroth, P. 1968. *Critical state soil mechanics,* London: Cambridge University.

Simpson, D. C., Evans, T. M. 2016. Behavioral Thresholds in Mixtures of Sand and Kaolinite Clay. *Journal of Geotechnical and Geoenvironmental Engineering*, **142**(2).

Figures
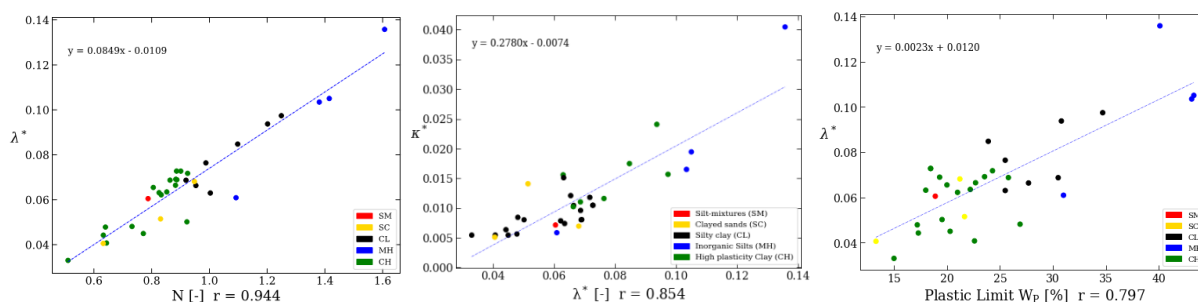

Figure1: *Correlation between N and λ^*, κ^* and λ^*, λ^* and Plastic Limit.*
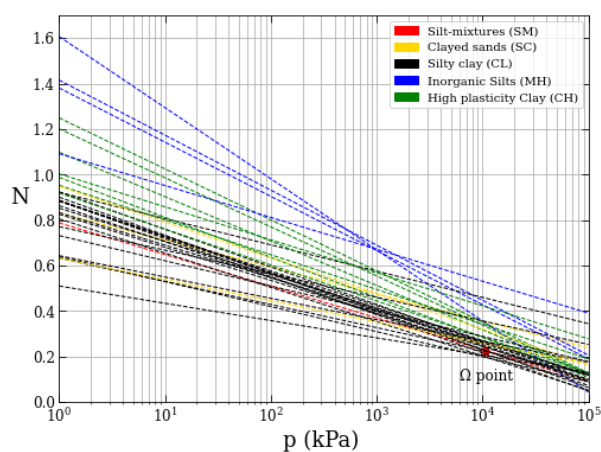

Figure 2: Convergences of INCLs in the $ln\,p \times ln(e+1)$ space for different types of soils (in USCS classification).

Reduced-scale testing of masonry structures to explosions

Ahmad Morsel[a], Filippo Masi[b], Ioannis Stefanou[a], Panagiotis Kotronis[a], Guillaume Racineux[a], Emmanuel Marche[a]

a. *Nantes Université, Ecole Centrale Nantes, CNRS, GeM, UMR 6183, France*
b. *Sydney Centre in Geomechanics and Mining Materials, The University of Sydney, Australia*

Keywords: experiments, reduced scale, explosions, exploding aluminum wires, masonry, infrastructure

Abstract

Historical and modern structures have encountered an increasing number of accidental or deliberate threats arising from blast events in recent decades. Examples include the Parthenon in Athens (1687), the Chicago Port in the United States (1944), and the Cathedral of Azerbaijan (2020).

In this work, we investigate the dynamic responses and failure mechanisms of structures subjected to dynamic loading originating from blast events at a reduced scale. To achieve this, we have developed a novel experimental setup, as shown in **Figure 1**, to study the behavior of masonry structures under blast loading (refer to **Masi et al., 2019, 2022**) within a secure laboratory environment (refer to **Figure 2**). This setup can be applied across a broad spectrum of applications in civil and environmental engineering, ranging from structural dynamics to geomechanics and underground infrastructures where explosions are a threat.

Conducting a real-scale explosion is achieved by exploding wires triggered by high-voltage discharges from a capacitor. These experiments take place within a controlled laboratory environment, guaranteeing both repeatability and safety. The resulting loads closely mimic those from real TNT explosions (cf. TNT equivalence), facilitating accurate blast effect assessments when upscaled.

References

F. Masi, I. Stefanou, P. Vannucci, and V. Maffi-Berthier. Rocking response of inverted pendulum structures under blast loading. International Journal of Mechanical Sciences, 157:833–848, 2019.
F. Masi, I. Stefanou, and V. Maffi-Berthier. Scaling laws for the rigid-body response of masonry structures under blast loads. American Society of Civil Engineers, 2022.

Figures

Figure 1: *Experimental setup of reduced scale experiments installed in the GeM research laboratory.*
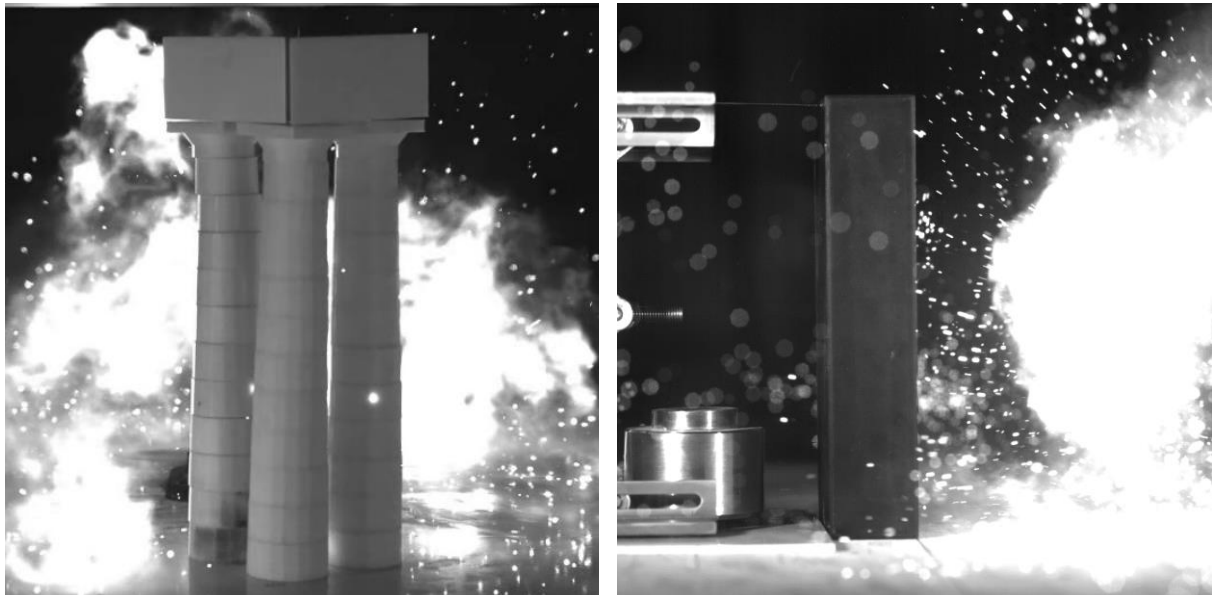

Figure 2: *Reduced-scale structures subjected to blast loads.*

Multiphase Flow through Granular Material under Hydro-Mechanical Loading

Rana Al Nemer, Giulio Sciarra, Julien Réthoré

GeM, Ecole Centrale de Nantes, Nantes Université, France

rana.al-nemer@ec-nantes.fr

Keywords: multiphase flow, hydro-mechanical loading, unstable infiltration, localized strains

Abstract

The goal of carbon neutrality relying massively on renewable energy sources can be accelerated by considering underground CO_2 sequestration and underground storage of (i) hydrogen produced by the water electrolysis from renewable electricity, and (ii) synthesised methane produced by the methanation. However, the injection of these fluids into deep saline aquifers, can succeed in infiltrating through the sealing rock via pre-existing cracks or new pathways, and can trigger local instabilities in the form of fluid fingering.

Many researchers have been interested in this complex interactions and numerous experimental and numerical studies have been conducted to investigate the various processes taking place. For instance, (Lenormand, 1990) has determined a drainage phase diagram allowing to classify the unstable fluid displacement patterns into viscous or capillary fingering domains. Then, countless experiments have been performed using the so-called Hele-Shaw cell; to cite among others, the work of (Eriksen *et al.*, 2015) where the air percolating through a monolayer of liquid saturated glass beads has been filmed then the deformation of the granular medium has been determined via Digital Image Correlation (DIC). However to our knowledge, the quantification of the full-field fluid-driven skeleton deformation under hydro-mechanical loading is still missing.

The objectives of this work are to quantify the effect of unstable gas (air) percolation on the remodeling of the granular structure on one side and to investigate the effect of mechanical loading on the skeleton response and the bi-phasic flow on the other side. For this aim, a new experimental setup constitued of a biaxial machine endowed with a high resolution optical system has been designed. The special feature of this machine is that it allows to control simultaneously the confining pressure and the pressures of three fluids and consequently to perform suction-controlled experiments. A detailed procedure for a successful drainage experiment has been established (Al Nemer et al., 2022) and two drainage experiments (with air as the injected fluid and water as the defending one) distinguished by the level of hydro-mechanical loadings are going to be discussed (see Figure 1 and Figure 2). Then, the acquired images through the lens of the high resolution camera, have been exploited to discover the hidden information, by means of DIC to extract the response of the solid skeleton upon the air infiltration and by means of robust algorithms to detect the 2D ondulated interface evolving in time.

The infiltration of air through a water saturated sand medium has shown to be impacted by the level of the applied mechanical loading: more preferential pathways are generated by the injected fluid when the applied initial effective stress is less important. Moreover, the outputs from DIC calculations based on finite element mesh generated over a region of interest

enclosing the developed finger, have also shown different responses of the skeleton with respect to the applied mechanical loadings. Combined with detected interface, the main findings can be summarized into two panels. The first panel concerns the correlation between the mechanical loading and the strain localization. We have concluded that (1) the infitration of air is accompanied by localized volumetric strains and (2) the higher the initial effective stress is the denser the distribution of volumetric strains will be and the larger the magnitude of these strains will be. The second panel concerns the correlation between the mechanical loading and the properties of the moving bi-phasic interface regarding the growth aspect and the morphological one. Among the growth properties, the evolution of cumulative invaded areas as function of time for each finger is presented; it shows that the higher the mechanical loading is, the smaller the transition zone area will be. To investigate the morphological properties of the interface, the corrugation amplitude giving a macroscopic estimation of the average depth of the bulges (irregularities) constituing the interface has been calculated for each borders on each finger. The reported values do not show any relationship between the effective stress and the ondulation of the interface but seem to be more dependant on the microstructure of the medium, since for the same experiment (test (2)), different ranges of corrugation amplitude have been obtained.

References

Al Nemer, R., G. Sciarra, and J. Réthoré (2022). Drainage instabilities in granular materials: a new biaxial apparatus for fluid fingering and solid remodeling detection. Frontiers in Physics, P. 202

Eriksen, F. K., R. Toussaint, K. J. Måløy, and E. G. Flekkøy (2015). Invasion patterns during two-phase flow in deformable porous media. Frontiers in Physics, 3:81.

Lenormand, R. (1990). Liquids in porous media. Journal of Physics: Condensed Matter, 2(S):SA79.

Figures

Figure 1: *Infiltration of air through water saturated sand under an initial effective stress $\sigma'0=40$ kPa and a capillary pressure Pcap=30 kPa.*

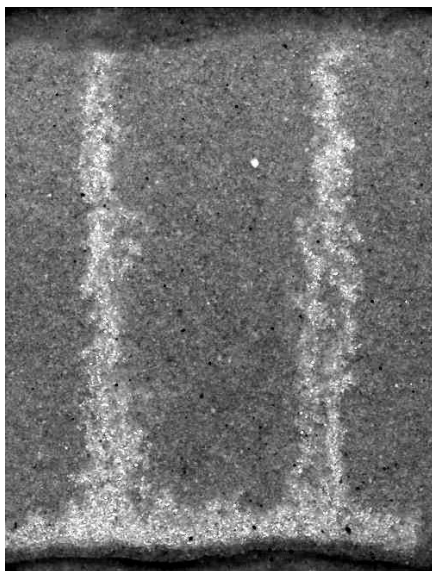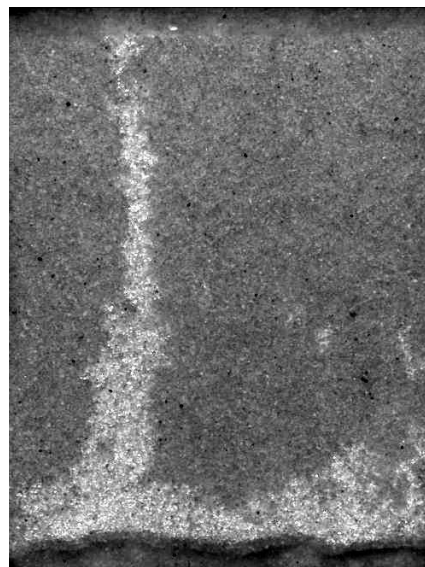**Figure 2:** *Infiltration of air through water saturated sand under an initial effective stress $\sigma'0=120$ kPa and a capillary pressure Pcap=30 kPa.*

Micro-mechanically enhanced multi-yield surface modeling of drained sand behavior in dynamic boundary value problems

Onur Deniz Akan[1], Guido Camata[2], Carlo G. Lai[3] and Enrico Spacone[2]

[1]Centre for Training and Research on Reduction of Seismic Risk, University School for Advanced Studies (IUSS) Pavia, Pavia, Italy

[2]Department of Engineering and Geology, University "G. D'Annunzio" of Chieti-Pescara, Chieti, Italy

[3]Department of Civil Engineering and Architecture, University of Pavia, Pavia, Italy

onur.akan@iusspavia.it

Keywords: constitutive model, cyclic loading, data-driven multiscale, FEMxDEM, sand response

Abstract

Soil behavior plays a crucial role in the seismic analysis of geotechnical infrastructures. The wave propagation velocity and the amplitude depend on the soil stiffness, resulting in amplified accelerations. At the same time, structural movements may be modified due to the additional soil flexibility and the energy dissipation provided by the hysteretic response. The nonlinear cyclic sand behavior is often represented by a phenomenological equation and a set of material internal variables. Relatively more straightforward models [1], [2] miss some of the most crucial soil behaviors, such as dilative-contractive transformation, strain softening, and anisotropy due to initial fabric, but enjoy numerical stability and low computational cost. In comparison, mathematically complex models [3] capture the desired behavior but may suffer from convergence issues in extreme cases, a high number of iterations for convergence, and a strenuous calibration procedure.

Alternatively, the desired mechanics may be modeled using micro or multiscale simulations. Some multiscale approaches abandon the constitutive model [4], using direct FEMxDEM bridging, whereas others keep the constitutive model and couple FEMxDEM to update the material internal variables [5]. The double-scale approaches are robust and accurate in modeling the sand response. However, they have yet to solve an engineering scale transient problem due to their computationally intensive nature. The data-driven multiscale approach can be used as a remedy, which relies on a database of low-level simulations to do the return mapping without the need for constitutive equations [6].

This study proposes a micro-mechanically enhanced constitutive model to capture the desired soil behavior at the macro scale. First, a response database is obtained by analyzing a granular unit cell under various stress paths. The homogenized stress, strain, and fabric tensors are recorded at each step. Then, the database is used to update the material internal variables of a multi-yield surface model. At each Gauss point, the strain tensor is downscaled. A "micro-scale-like" problem is solved by searching the database for the closest data point by comparing the tensor invariants or the tensor-to-tensor distance. Then, information such as the shear strength, kinematic modulus, and dilatancy is transferred to the macro scale through yield surface parameters. The return mapping is done with an implicit solution, and the stiffness and residual tensors are upscaled. The database to constitutive model communication is repeated when there is a need to define the next yield surface during the analysis. Finally, the stress

reversals are handled via a back-stress-like tensor that stores the material state at the reversal. The memory variables are reverted once the material returns to the threshold state.

The proposed approach captures the dilative-contractive transformation, strain hardening/softening, induced anisotropy, and anisotropy due to the initial fabric. Furthermore, since the model formulation results in a piece-wise linear modulus between yield surfaces, increased numerical stability and a mathematically simpler consistent tangent definition is available.

References

[1] J. H. Prevost, "A simple plasticity theory for frictional cohesionless soils," *Int. J. Soil Dyn. Earthq. Eng.*, vol. 4, no. 1, pp. 9–17, Jan. 1985, doi: 10.1016/0261-7277(85)90030-0.

[2] Q. Gu, J. P. Conte, Z. Yang, and A. Elgamal, "Consistent tangent moduli for multi-yield-surface J2 plasticity model," *Comput. Mech.*, vol. 48, no. 1, pp. 97–120, Jul. 2011, doi: 10.1007/s00466-011-0576-7.

[3] Y. F. Dafalias and M. T. Manzari, "Simple Plasticity Sand Model Accounting for Fabric Change Effects," *J. Eng. Mech.*, vol. 130, no. 6, pp. 622–634, 2004, doi: 10.1061/(asce)0733-9399(2004)130:6(622).

[4] N. Guo and J. Zhao, "A coupled FEM/DEM approach for hierarchical multiscale modelling of granular media," *Int. J. Numer. Methods Eng.*, vol. 99, no. 11, pp. 789–818, 2014, doi: 10.1002/nme.4702.

[5] J. E. Andrade, C. F. Avila, S. A. Hall, N. Lenoir, and G. Viggiani, "Multiscale modeling and characterization of granular matter: From grain kinematics to continuum mechanics," *J. Mech. Phys. Solids*, vol. 59, no. 2, pp. 237–250, Feb. 2011, doi: 10.1016/j.jmps.2010.10.009.

[6] K. Karapiperis, L. Stainier, M. Ortiz, and J. E. Andrade, "Data-Driven multiscale modeling in mechanics," *J. Mech. Phys. Solids*, vol. 147, p. 104239, Feb. 2021, doi: 10.1016/j.jmps.2020.104239.
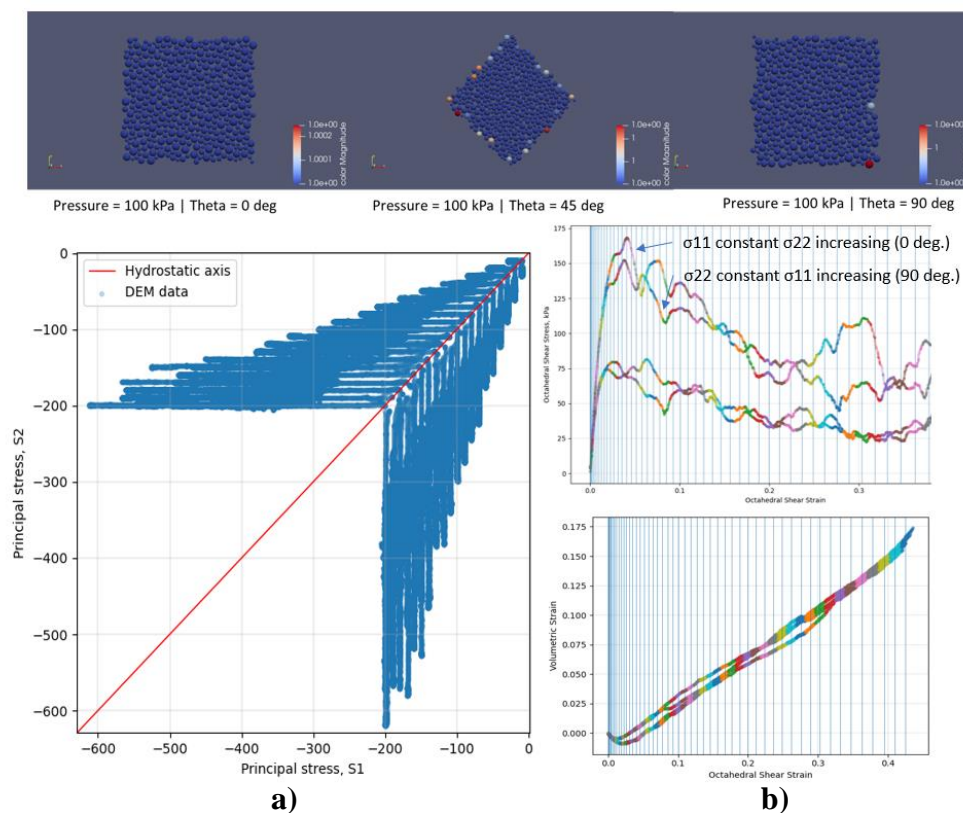
Figures

Figure 1: *The database generated based on various stress paths (a). Monotonic shearing cases for initial isotropic stresses of 100 kPa and 200 kPa with yield surfaces shown as vertical lines (b).*

Influence of the calibration procedure of HCA parameters on the predicted long-term monopile deformations

Lucian Canales Brenlla[1], Merita Tafili[1], Frederik Koch[1], Jan Machaček[1,2], Lisa Tschirschky[1,3], Luis Felipe Prada Sarmiento[4], Patrick Staubach[1,3], Torsten Wichtmann[1]

[1]Ruhr-University Bochum,
[2]Technical University of Darmstadt,
[3]Bauhaus-University Weimar,
[4]Aarhus University,

lucian.canalesbrenlla@rub.de

Keywords: drained cyclic tests, high-cycle accumulation model, calibration, offshore foundation

Abstract

Offshore wind turbines are subjected to both wave and wind loading comprising millions of cycles including small to moderate amplitudes. This high-cyclic loading may cause an accumulation of strain in the soil that can lead to a tilting of the foundations and thus a loss of the serviceability of structures. High-cycle accumulation (HCA) models can be used for the prediction of the long-term behaviour under these loading conditions common in the offshore environment. In this work, the effect on the HCA model prediction following different calibration procedures for the determination of the HCA material constants is discussed. Namely, through correlations of the model parameters with index properties, by considering the traditional "by-hand" procedure or determined by means of an automatic parameter calibration approach. The HCA model parameters have been calibrated for UWA silica sand based on drained cyclic triaxial tests with 10^5 cycles performed with different amplitudes, densities and initial stresses. To assess the influence on the long-term serviceability, finite element simulations of a monopile foundation for offshore wind turbines subjected to $4 \cdot 10^5$ lateral loading cycles are carried out with the different sets of parameters. In this regard, the finite element calculation strategy combines the HCA model with hypoplasticity as the conventional (low-cycle) model. The robustness of both parameter sets is illustrated. Furthermore, the influence of different optimized parameter sets is inspected.

References

P.-A. von Wolffersdorff (1996), "A hypoplastic relation for granular materials with a predefined limit state surface, " Mechanics of Cohesive-frictional Materials, vol. 1, pp. 251–271

A. Niemunis and I. Herle (1997), "Hypoplastic model for cohesionless soils with elastic strain range," Mechanics of Cohesive-frictional Materials, vol. 2, pp. 279–299

A. Niemunis, T. Wichtmann, and T. Triantafyllidis (2005), "A high-cycle accumulation model for sand," Computers and Geotechnics, vol. 32, no. 4, pp. 245–263

T. Wichtmann, A. Niemunis, and T. Triantafyllidis (2015), "Improved simplified calibration procedure for a high-cycle accumulation model," Soil Dynamics and Earthquake Engineering, vol. 70, pp. 118–132

J. Machaček, P. Staubach, C. E. G. Tavera, T. Wichtmann, and H. Zachert (2022), "On the automatic parameter calibration of a hypoplastic soil model," Acta Geotechnica, vol. 17, no. 11, pp. 5253–5273

T. Wichtmann (216), "Soil behaviour under cyclic loading - experimental observations, constitutive description and applications", Habilitation, Karlsruher Institut für Technologie (KIT)
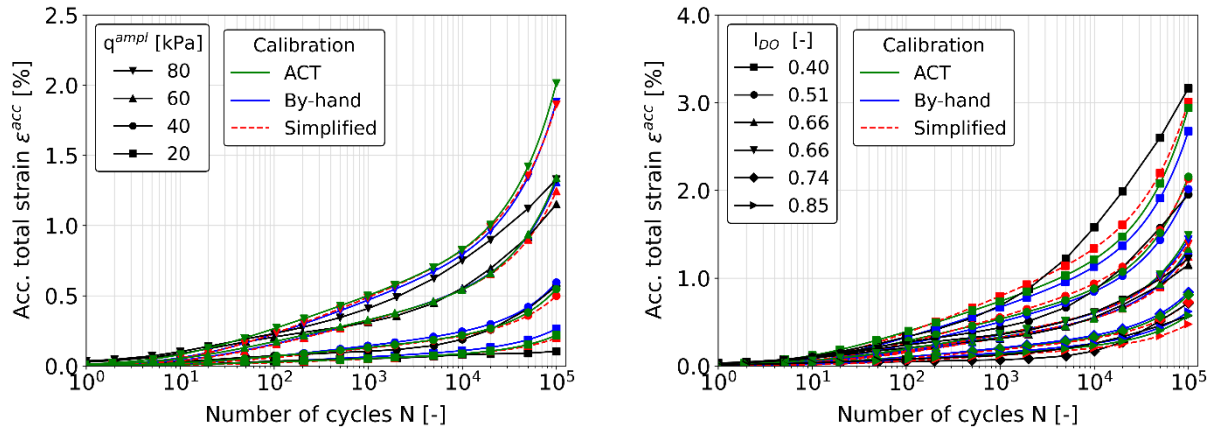
Figures

Figure 1: *Results of drained cyclic tests with different stress amplitudes q^{ampl} and initial relative densities I_{D0}.*
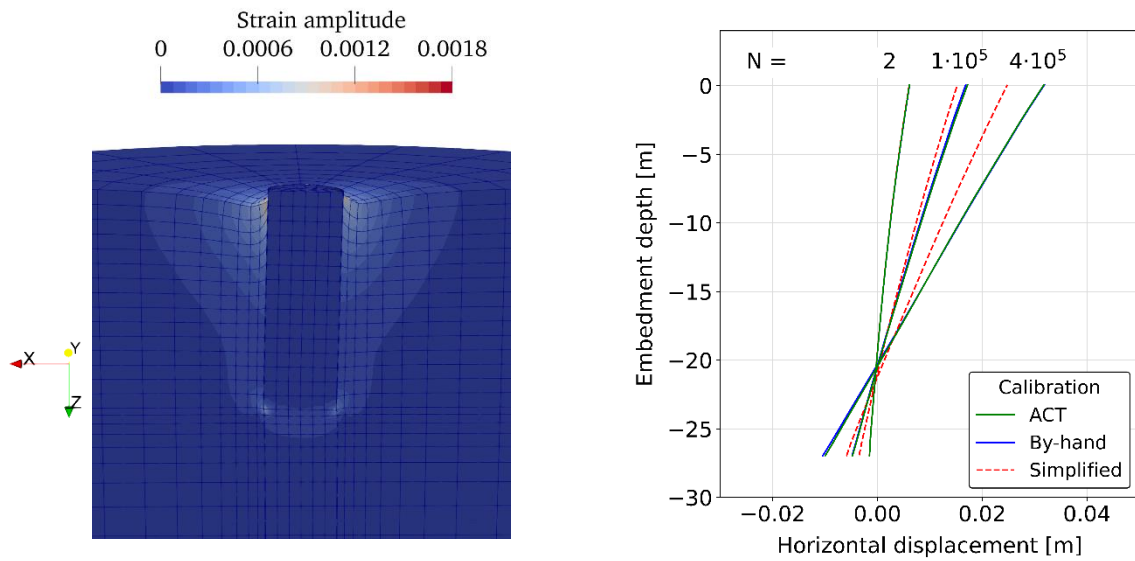

Figure 2: *Spatial distribution of the strain amplitude and deflection curves at N = 2, N = 1·10^5 and N = 4·10^5.*

The use of geothermal energy to prevent road pavement icing and damage in cold climate areas

E. Ilari[1,*], B. Pardoen[2], A. Di Donna[1]

[1]*Université Grenoble Alpes, 3SR Lab., France*
[2]*Université de Lyon, ENTPE, France*

[*]elena.ilari@hotmail.com

Keywords: geothermal system, ice formation

Abstract

The primary objective of this research is to evaluate the effectiveness of a deicing system, specifically designed for cold regions where ice on road surfaces is a frequent occurrence. In addition to causing hazardous conditions, accidents, travel disruptions, and eroding road safety perceptions, ice can also form beneath the road surface within the soil, therefore this study delves into the behavior of soil when subjected to ice, within a thermo-hydro-mechanical framework.

Central to this investigation is the assessment of the deicing system's efficiency, which relies on a geothermally activated tunnel as its core component. This innovative yet underutilized approach incorporates embedded pipes encased within concrete linings. These pipes extend just beneath the road surface, with a heat carrier fluid circulating inside. This fluid extracts heat from the tunnel and the surrounding soil, transferring it to the road surface to prevent ice formation and enhance road safety.

A numerical investigation (Di Donna and Pardoen, 2023) was performed to analyze the thermal characteristics within a three-dimensional soil domain, as depicted in the provided geometry (Figure 1(a)). Furthermore, relevant thermal boundary conditions were integrated into the study. To be specific, the lateral and bottom boundaries were modeled as adiabatic, while the top surface was exposed to convective heat flux conditions representative of Oslo's typical external temperature in Norway. Similarly, the inner surface of the concrete lining was subjected to imposed heat flux conditions resembling the typical temperature profile found within a metro tunnel.

Figure 1(b) presents the outcomes observed both before and after the activation of the geothermal system, signifying the point at which fluid circulation within the pipes commenced. In this particular scenario, the decision was made to initiate the geothermal system after a 2-year period, following an initial 2-year period during which the soil was allowed to reach a state of thermal equilibrium.

Furthermore, a numerical investigation was conducted to examine the thermo-hydro-mechanical coupling (Li et al., 2022), providing insights into the soil's behavior concerning displacement and liquid pressure. This study assumes a linear elastic soil response to describe the mechanical behaviour.

Expanding upon the prior simulation, comprehensive hydraulic and mechanical initial and boundary conditions were carefully addressed. Specifically, the analysis assumed a fully saturated soil with the water table positioned at ground level. In terms of the mechanical aspect,

the influence of gravity was duly incorporated. Furthermore, all boundaries, with the exception of the bottom boundary, were treated as impermeable, prohibiting fluid flux. Mechanically, an oedometric condition was adopted.

The soil's response to ice involves two opposing effects: thermal contractions causing soil shrinkage and an increase in capillary pressure due to water-to-ice transformation, leading to volumetric expansion. The latter effect, influenced by the water retention curve, has the potential to damage road surfaces. To mitigate these issues, it is essential to implement anti-icing systems (Li et al., 2022).

References

Li, X., Liu, Y., Wong, H., Pardoen, B., Fabbri, A., McGregor, F., and Liu, E. (2022). Analytical and numerical studies on the behavior of a freezing soil layer. *Cold Regions Science and Technology*, 198, 103538.

Di Donna and Pardoen (2023). The use of geothermal energy to prevent road pavement icing and damage in cold climate areas. P*roceedings of the Symposium on Energy Geotechnics Accelerating the energy transition (SEG23)*, 3-5 October 2023, Delft, the Netherlands.

Figures
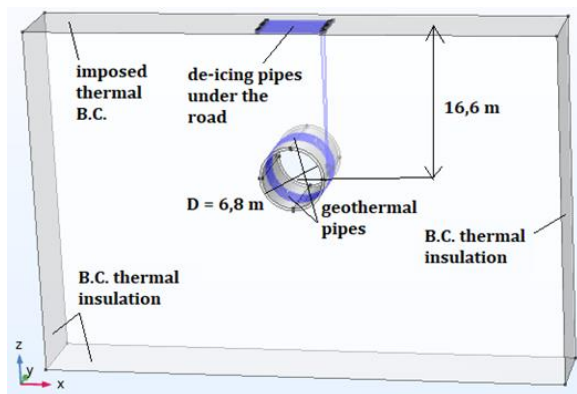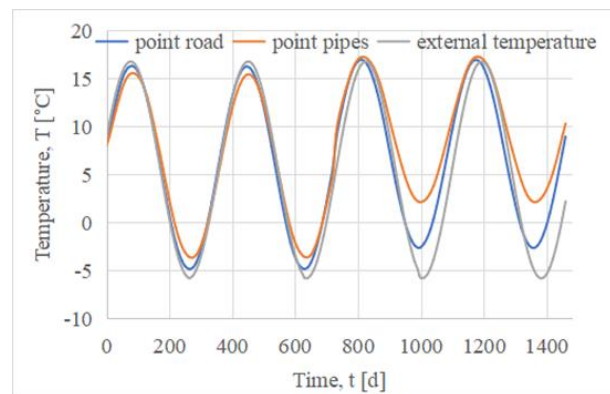

Figure 1a

Figure 1b

Automatic calibration of SANISAND parameters for a granular material using multi-objective optimization strategies

Sai Sri Harsha Vallurupalli[1], Debdeep Sarkar[2], Meisam Goudarzy[1], Luis Felipe Prada-Sarmiento[3], Arash Alimardani Lavasan[4], Torsten Wichtmann[1]

[1]Ruhr-University Bochum, Germany

[2]GuD Geotechnik und Dynamik Consult GmbH, Berlin, Germany

[3]Aarhus University, Denmark

[4]University of Luxembourg, Luxembourg

Sai.Vallurupalli@ruhr-uni-bochum.de

Keywords: automatic calibration; SANISAND model; granular materials; multi-objective optimization

Abstract

This is a template The parameter calibration of a constitutive model is a requisite to counter the uncertainty in the parameters and to approximate the simulation results effectively. Yielding a robust set of parameters for various test conditions is complicated as innumerable parameter combinations have to be investigated. In previous works, this calibration has been performed manually by trial and error without checking the robustness of the chosen parameters. Therefore, the present study introduces an automated calibration procedure using multi-objective optimization techniques. This assists in searching the parameter domain space extensively for better combinations that simulate the experiment results precisely. Though this approach is quite popular in various other engineering aspects, proposing the concept of calibrating the soil parameters and validating their efficiency has been always a challenge and interesting in this framework. In this research, SANISAND model parameters have been calibrated for crushed glass material under different triaxial conditions considering the barotropy, and pycnotropy effects. The results demonstrated that the optimized SANISAND parameters approximated the experiment results far better than manually calibrated results. This calibration approach facilitates in conserving the robust parameters besides dealing with time constraints and motivates the idea of adapting this automation platform to any constitutive model for significant approximations.

References

Dafalias, Y.F. and Manzari, M.T., 2004. Simple plasticity sand model accounting for fabric change effects. Journal of Engineering mechanics, 130(6), pp.622-634.

Wichtmann, T, 2005. Explicit accumulation model for noncohesive soils under cyclic loading. PhD thesis, Publications of the Institute of Soil Mechanics and Foundation Engineering, Ruhr-University Bochum.

Deb, K. and Jain, H., 2013. An evolutionary many-objective optimization algorithm using reference-point-based nondominated sorting approach, part I: solving problems with box constraints. IEEE transactions on Evolutionary Computation, 18(4), pp.577-601.

Sarkar, D., Goudarzy, M. and König, D., 2019. An interpretation of the influence of particle shape on the mechanical behavior of granular material. Granular Matter, 21(3), pp.1-24.

Zhao, C., Lavasan, A.A., Barciaga, T., Zarev, V., Datcheva, M. and Schanz, T., 2015. Model validation and calibration via back analysis for mechanized tunnel simulations – The Western Scheldt tunnel case. Computers and Geotechnics, 69, pp.601-614.
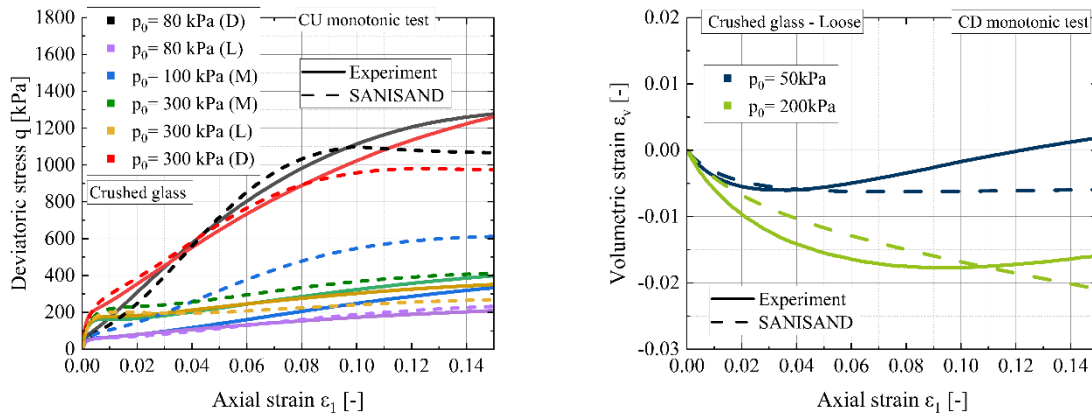
Figures

Figure 1 : *Comparison of SANISAND calibrated results with undrained (left) and drained (right) triaxial experiments. (L, M, and D represent loose, medium, and dense materials respectively).*

Figure 2 : *Comparison of SANISAND validated results with undrained (left) and drained (right) triaxial experiments. (L, M, and D represent loose, medium, and dense materials respectively).*
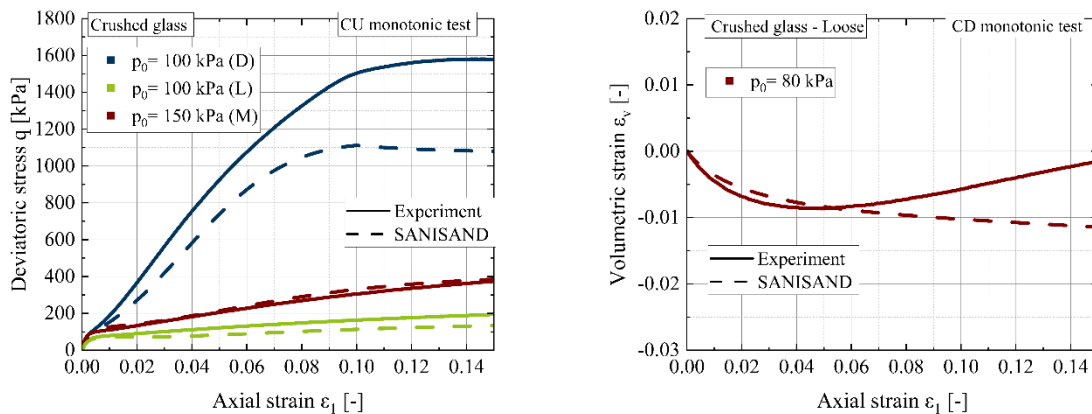
Exploring waste settlements and biodegradation across scales and processes

Cristhian F. Andrade, Julia Gebert, Anne-Catherine Dieudonné & Timo Heimovaara

Faculty of Civil Engineering and Geosciences, Delft university of Technology, Netherlands

c.f.andradecorona@tudelft.nl

***Keywords***: municipal solid waste, biodegradation, density, mass loss

Abstract

Landfills are highly heterogeneous systems that experience a wide range of environmental (thermo-bio-chemo-hydraulic) processes. For instance, it is difficult to identify which mechanism(s) govern their dynamic behavior. It is well known that biodegradation is responsible for the long-term settlement response in municipal solid waste (Fei & Zekkos, 2013). However, the process from mass loss to collapse of the waste structure is not clearly understood. This poster explores the potential of using a bio-physico-chemical modeling framework (Andrade et al, 2023) applied to waste to understand the link between organic matter degradation and settlement (Figure 1).

Our model calculates the evolution of gas production, concentration of various chemical components, and state parameters due to degradation. Waste heterogeneity can be captured by executing scenarios with multiple initial conditions. Consequently, mass loss and volume change can be quantified as a result of gas venting and leachate leaving the system. The governing mass loss mechanism is Methanogenesis in systems that are O2 limited. In the future, model mass loss and volume change should be compared and calibrated to measured settlements at the landfill. Similarly, to quantify the link between mass loss and settlement.

References

[1] Andrade, C. F., Dieudonné A.C., Gebert, J., Heimovaara, T. Mechanisms governing carbon and nitrogen pathways during enhanced waste degradation in landfill simulator reactors. 19th International symposium on waste management and sustainable landfilling.

[2] Fei, X., & Zekkos, D. (2013). Factors Influencing Long-Term Settlement of Municipal Solid Waste in Laboratory Bioreactor Landfill Simulators. Journal of Hazardous, Toxic, and Radioactive Waste, 17(4), 259–271. https://doi.org/10.1061/(asce)hz.2153-5515.0000167

Figures
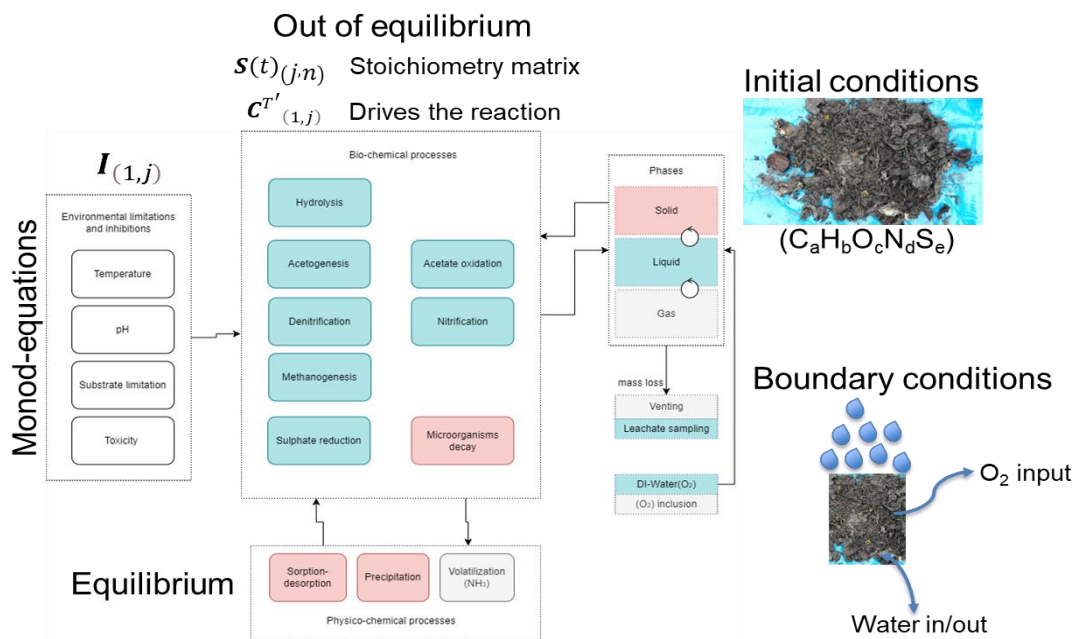
Figure 1: Bio-physico-chemical mechanisms included in the model, and step-wise approach for model integration.

Hysteresis within unsaturated granular assemblies: DEM-LBM coupling

N. Younes [1,2,3], O. Millet [1], A. Wautier [2], R. Wan[3], F. Nicot [4]*

[1]Lasie, UMR CNRS 7356, University of La Rochelle, La Rochelle, France

[2]Aix-Marseille University, INRAE, UMR RECOVER, Aix-en-Provence, France

[3]Department of Civil Engineering, Schulich School of Engineering, University of Calgary, Calgary, Canada

4 University of Savoie Mont-Blanc, ISTerre, Chambéry, France

nabil.younes@ucalgary.ca

Keywords: DEM-LBM Coupling, SWCC, capillary stress, hysteresis.

Abstract

In this work, we have combined the Lattice Boltzmann Method (LBM) with the Discrete Element Method (DEM) to thoroughly investigate how materials behave under unsaturated conditions. Regarding the LBM, a GPU phase-field-based model is adopted to solve both Allen-Cahn and Navier-Stokes equations to capture the formation of capillary interfaces between air and water. Concerning the DEM, the open-source YADE is used, accounting for contacts between rigid spherical grains [1]. The pivotal aspect of the integration between these models henges on the integration of capillary forces computed via LBM into the DEM calculation cycles.

Multiple validations are conducted on small granular assemblies, e.g., doublets and triplets of particles. Firstly, the formation of capillary bridges between two-particle configurations (doublets) and the comparison of their geometries with the Young-Laplace solution within the pendular regime are examined [2]. This scheme goes further to compute the capillary forces resulting from isolated and coalesced capillary bridges in two- and three-spherical-particle configurations, doublets and triplets, respectively, hence illustrating the transition from the pendular regime to the funicular regime, as shown in Figure (1). Our findings align well with available experimental data in the literature [3].

These studies are further extended to a sample made of thousands of spherical particles under unsaturated conditions subjected to both evaporation and condensation processes at the Representative Elementary Volume (REV) scale [4]. The proposed coupling has proven its capabilities to capture the hysteresis of both mean capillary stress and suction during evaporation and condensation. Regarding the mean capillary stress, it increases with the degree of saturation up to a certain threshold beyond which, it drops to reach zero at fully saturation, and the suction decreases continuously and reaches zero at fully saturation, as depicted in Figure (2). Furthermore, it is highlighted that both the suction and the mean capillary stress are higher during evaporation compared to condensation [5].

The DEM-LBM model has proven its capabilities in capturing multiple physical phenomena of unsaturated soils. It highly believed that the devised model holds significant potential for the thorough study of instabilities at the REV scale, paving the way for its broader application in more complicated systems, including earthen dikes.

References

[1] V. Šmilauer et al. (2021), Yade Documentation 3rd ed. The Yade Project.

[2] Younes, N., Millet, O., Benseghier, 2023. A relevant phase-field-based Lattice-Boltzmann method for water-air capillary interfaces. In preparation.

[3] Younes, N., Benseghier, Z., Millet, O., Wautier, A., Nicot, F., Wan, R., 2022. Phase-field Lattice Boltzmann model for liquid bridges and coalescence in wet granular media. Powder Technology.

[4] Younes, N., Wautier, A., Wan, R., Millet, O., Nicot, F., Bouchard, R., 2023. DEM-LBM coupling for partially saturated granular assemblies. Computers and Geotechnics.

[5] Younes, N., Wautier, A., Wan, R., Millet, O., Nicot, F., 2023. On the hysteresis phenomenon of unsaturated granular assemblies using DEM-LBM coupling. In preparation.
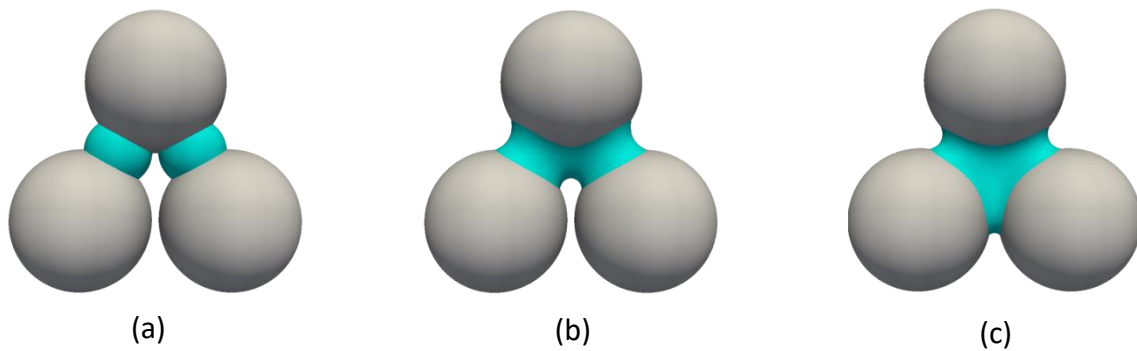
Figures

(a)   (b)   (c)

Figure 1: *(a) Initialization phase, (b) transition phase, and (c) equilibrium state.*

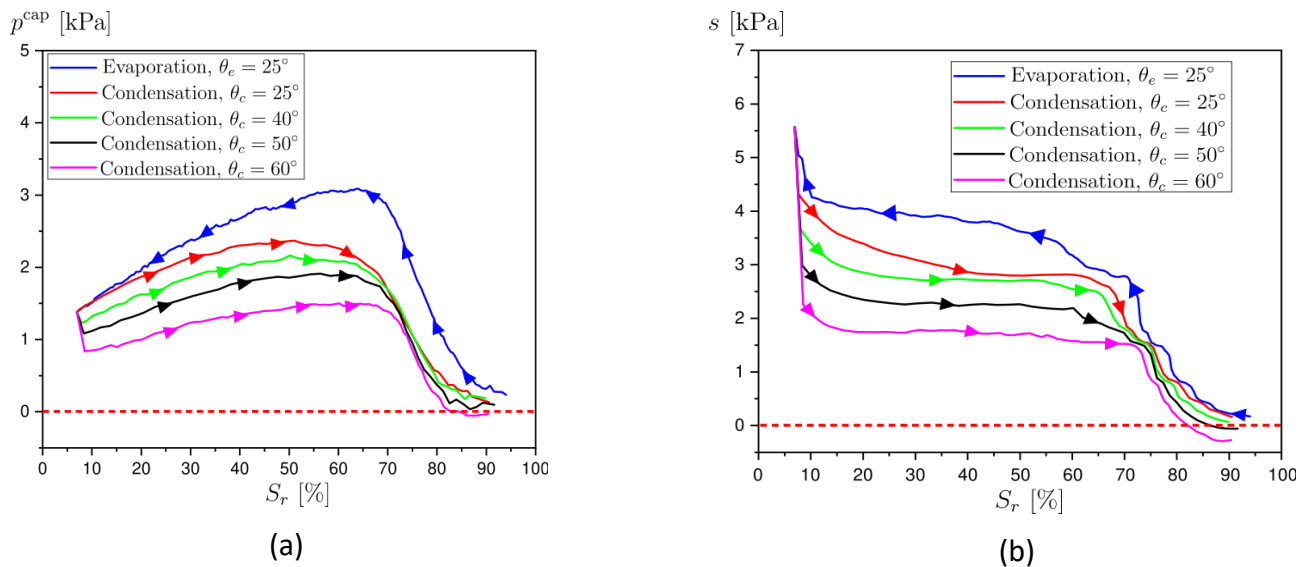(a)   (b)

Figure 2: *Evolution of (a) the mean capillary stress p^{cap} [kPa] and (b) suction s [kPa] in terms of degrees of saturation S_r [%] during condensation and evaporation processes for several wetting angles θ.*

ALERT Geomaterials

The Alliance of Laboratories in Europe for Education, Research and Technology